# Septin 9 (SEPT9) negatively regulates ubiquitin-dependent downregulation of epidermal growth factor receptor (EGFR)

**Inaugural-Dissertation**

to

obtain the academic degree

Doctor rerum naturalium (Dr. rer. nat.)

submitted to the Department of Biology, Chemistry and Pharmacy

of the

Freie Universität Berlin

by

Katrin Diesenberg

born in

Preetz, Germany

2015

Thesis prepared from September 2009 until July 2015


Thesis prepared at : Institute of Chemistry and Biochemistry,
Membrane Biochemistry, Freie Universität Berlin
(2009 – August 2012)

and

Leibniz Institut für Molekulare Pharmakologie (FMP),
Berlin-Buch (from September 2012)

Supervisor: Prof. Dr. Michael Krauß
Prof. Dr. Volker Haucke


1st reviewer: Prof. Dr. Michael Krauß
2st reviewer: Prof. Dr. Volker Haucke

Date of defense: 08.12.2015

## Acknowledgments

I would like to thank Prof. Dr. Michael Krauß for the excellent supervision and guidance through my PhD studies. Your expertise and patience was a great help in questions of science and lab tasks. I would also like to thank Prof. Dr. Volker Haucke for his supervision. Both of you helped me to overcome a multitude of experimental problems.

I would like to greatly acknowledge the contribution of our collaborations with Dr. Eberhard Krause (mass-spectrometry) and Dr. Peter Schmieder (NMR spectroscopy).

Many thanks go to all present and past members of the 'AG Haucke/Krauß/Schmoranzer' for providing a great and productive working atmosphere. The scientific (and non-scientific!) conversations significantly increased my stamina and my happiness factor:

Jelena Bacetic, Katharina Branz, Caroline Bruns, Gala Claßen, Marielle Eichhorn-Grünig, Fabian Feutlinske, Uwe Fink, Niclas Gimber, Claudia Gehring, Claudia Gras, Isabelle Grass, Kira Gromova, Sabine Hahn, Burkhard Jakob, Maria Jäpel, Lisa Jerndal, Natalie Kaempf, Christina Kath, Peter Koch, Gaga Kochlamazashvili, Natalia Kononenko, Seong Joo Koo, Ludwig Krabben, Marijn Kuijpers, André Lampe, Wen-Ting Lo, Delia Löwe, Tania López Hernández, Martin Lehmann, Gregor Lichtner, Andrea Marat, Tanja Maritzen, Julia Mössinger, Maria Mühlbauer, Arndt Pechstein, Jasmin Podufall, York Posor, Dmytro Puchkov, Yijian Rao, Christine Rückert, Linda Sawade, Hannah Schachtner, Jan Schmoranzer, Irene Schütz, Kyungyeun Song, Tolga Soykan, Wiebke Stahlschmidt, Susanne Thomsen, Lena von Oertzen, Anela Vukoja, Ingeborg Walther, Anna Wawrzyniak, Mirjana Weimershaus, Marnix Wieffer, Susanne Wojtke and Silke Zillman.

I also want to express my gratitude to my parents for ongoing support in everything I decide to do. You provided me with the privileg to direct my life according to my own will.

Many thanks also go to my brother and friends, who endured my moaning and grumbling about failed experiments and joined me in the non-scientific part of my life.

Lastly I would also like to thank the Deutsche Forschungsgemeinschaft (DFG) for financial support within the SFB958.

Affidavit

I declare that my PhD thesis entitled 'Septin 9 (SEPT9) negatively regulates ubiquitin-dependent downregulation of epidermal growth factor receptor (EGFR)' has been written independently and with no other sources and aids than quoted.

Berlin, 05.08.2015

Katrin Diesenberg

# Table of Contents

**I.Abstract.....5**

**II.Zusammenfassung.....7**

**1 Introduction.....9**

1.1 Receptor tyrosine kinases (RTKs).....9

1.1.1 The EGFR signaling interactome.....11

1.1.2 Internalization.....13

1.1.3 Endosomal trafficking.....15

1.1.3.1 The E3 ligase Cbl ubiquitylates EGFR.....15

1.1.3.2 Ubiquitylated EGFR is sorted for lysosomal degradation.....18

1.1.3.3 Unubiquitylated receptor is recycled to the plasma membrane.....20

1.1.4 'Crosstalk' between EGF-induced pathways.....20

1.1.5 The adaptor protein CIN85.....21

1.2 Septin GTPases.....24

1.2.1 Nomenclature and structure of septins.....24

1.2.2 Biological functions of septin GTPases in mammals.....27

1.2.3 Septins in human pathologies.....29

1.3 Septin 9.....31

1.3.1 Biological role of SEPT9 in mammals.....32

1.3.2 SEPT9 in disease.....33

1.4 Breast Cancer.....34

1.5 Aims of this study.....36

**2 Material and Methods.....37**

2.1 Materials.....37

2.1.1 Chemicals and disposables.....37

2.1.2 Solutions and media.....38

2.1.3 DNA Oligonucleotides.....40

2.1.4 Small interfering RNA oligonucleotides.....40

2.1.5 Synthetic peptides.....41

2.1.6 Bacterial strains.....41

2.1.7 Eukaryotic cell lines....41
2.1.8 Plasmids....41
2.1.9 Enzymes....43
2.1.10 Antibodies....43
2.1.11 Software and internet resources....45
2.2 Molecular biological methods....46
2.2.1 Primers for cloning....46
2.2.2 Polymerase chain reaction and site-directed mutagenesis....46
2.2.3 Preparative and analytical agarose gel electrophoresis....47
2.2.4 Purification of DNA from agarose gels and PCRs....47
2.2.5 Restriction digests....47
2.2.6 Dephosphorylation of vector DNA....48
2.2.7 Ligation of DNA fragments into linearized vectors....48
2.2.8 Preparation of chemically competent E. coli....48
2.2.9 Transformation of chemically competent E. coli....48
2.2.10 Glycerol stocks....49
2.2.11 Over night cultures of E. coli....49
2.2.12 Purification of plasmid DNA from E. coli cultures....49
2.2.13 UV spectroscopy for determining nucleic acid concentrations....49
2.2.14 Sequencing....50
2.3 Biochemical methods....51
2.3.1 Protein determination (Bradford assay)....51
2.3.2 SDS polyacrylamide gel electrophoresis (SDS-PAGE)....51
2.3.3 Immunoblotting....52
2.3.4 Densitometric Analysis of Western Blots....53
2.3.5 Preparation of protein extracts from eukaryotic cells....53
2.3.6 Immunoprecipitation....53
2.3.7 Expression of recombinant proteins in E. coli....53
2.3.8 Purification of GST- and His6 -fusion proteins expressed in E. coli....54
2.3.9 GST-Pulldown assay....55
2.3.10 In vitro binding assay....55
2.3.11 Purification of denatured protein from inclusion bodies....55
2.3.12 Affinity purification of polyclonal antibodies from rabbit serum....56
2.3.13 Cytosol membrane fractionation....58
2.3.14 EGFR degradation....58

2.3.15 NMR spectroscopy....59
2.3.16 125I-EGF uptake....60
2.3.17 125I-EGF recycling....60
2.3.18 EGFR downstream signaling....61
2.3.19 EGFR ubiquitylation....61
2.3.20 Analysis of EGFR interactome by SILAC-based mass spectrometry....62
2.4 Cell biological methods....64
2.4.1 Mammalian cell culture....64
2.4.2 Long-term storage of mammalian cells....64
2.4.3 Transfection of plasmid DNA....64
2.4.4 Small interfering RNA treatments and rescue experiments....64
2.4.5 Immunofluorescence....65
2.4.6 EGF uptake....66
2.4.7 Surface binding of EGF....66
2.4.8 Fluorescence microscopy....66
2.4.9 Image analysis and quantification....67
2.5 Statistics....67
**3 Results....68**
3.1 SEPT9 controls EGFR degradation....68
3.1.1 Depletion of SEPT9 in fibroblasts decreases surface levels of EGFR....68
3.1.2 SEPT9 regulates sorting of EGFR between lysosomal and recycling pathways....70
3.1.3 SEPT9 stabilizes heterooligomeric septin filaments....73
3.2 SEPT9 forms a complex with the adaptor protein CIN85....74
3.2.1 The N-terminus of SEPT9 is important for stabilizing EGFRs....74
3.2.2 SEPT9 associates with all three SH3 domains of CIN85....75
3.2.3 CIN85 binds to a PR-rich motif located in the N-terminus of SEPT9....77
3.3 CIN85 recruits SEPT9 to activated EGFR at the cell surface....80
3.3.1 SEPT9-containing complexes are recruited to activated EGFR at the plasma membrane....80
3.3.2 SEPT9 localizes to activated EGFR exclusively at the plasma membrane....85
3.3.3 EGF stimulation induces SEPT9 association with membranes....87
3.3.4 SEPT9 impairs ERK signaling....88
3.4 SEPT9 regulates Cbl-dependent ubiquitylation of EGF receptors....89

3.4.1 SEPT9 and the E3 ligase Cbl occupy the same binding site on CIN85.....89
3.4.2 SEPT9 competes with Cbl for binding to CIN85.....91
3.4.3 SEPT9 regulates Cbl-b-mediated downregulation of EGFR.....92
3.5 Identification of novel SEPT9 interaction partners.....95
3.5.1 Proteomic analysis of the SEPT9_v3 interactome.....95
3.5.2 Implications of SEPT9 in membrane trafficking – preliminary data.....97
**4 Discussion.....98**
4.1 CIN85 recruits SEPT9-containing complexes to sites of activated EGFR at the plasma membrane.....98
4.2 SEPT9 regulates Cbl-b-dependent ubiquitylation of EGF receptors.....99
4.3 Septin complexes form diffusion barriers.....103
4.4 Putative isoform-specific effects of SEPT9.....104
4.5 A putative role of septin complexes in EGFR trafficking.....107
4.6 Conclusions and Outlook.....108
4.6.1 Trafficking of other RTKs.....108
4.6.2 Biological role of SEPT9 in cancer.....110
4.6.3 Putative complex formation of CIN85/CD2AP with other septin isoforms. .113
**5 Bibliography.....115**
**6 Appendix.....139**

# I. Abstract

Septins constitute a family of GTP-binding proteins that are involved in a broad range of cellular processes including membrane trafficking, cell division and motility. By associating with membranes they form diffusion barriers to create distinct cellular domains, which serve as scaffolds to recruit proteins to these specific compartments. 13 different isoforms have been identified in mammals, several of which have been implicated in disease, but the molecular mechanisms underlying pathogenesis are poorly understood. In this study, we elucidate a role of septin 9 (SEPT9) in the ubiquitin-dependent downregulation of the EGF receptor (EGFR), one of the best-studied members of receptor tyrosine kinases (RTK). This receptor responds to epidermal growth factor (EGF) and transduces signaling events to regulate cell survival and proliferation. Activated receptor is internalized and then either recycled back to the plasma membrane, or ubiquitylated to target the receptor for degradation.

In this study, we show that depletion of SEPT9 in Hela cells decreases surface levels of epidermal growth factor receptors (EGFRs) to nearly 50% by enhancing receptor degradation. EGFR internalization is unaffected by SEPT9, independent of the mode of endocytosis. A PxxxPR consensus motif located within the N-terminal domain of SEPT9 (aa 125-130 of SEPT9_v3) supports its association with all three SH3 domains of the adaptor protein CIN85 (also known as SH3KBP1). A CIN85–SEPT9 complex is localized exclusively at the plasma membrane, where SEPT9 is recruited to EGF-engaged receptors in a CIN85-dependent manner. Furthermore, we show that CIN85 recruits septin complexes, most probably a SEPT2/6/7/9 complex, to sites of activated EGFR. Biochemical fractionation experiments reveal a ligand-induced recruitment of these septin complexes from the cytosol to membrane. We further characterize the CIN85-SEPT9 interaction by a structural approach and show that SEPT9 and Cbl, the E3 ubiquitin ligase responsible for EGFR ubiquitylation, share the same binding surface on the SH3 A domain of CIN85. We demonstrate that SEPT9 negatively regulates EGFR degradation by preventing the association of Cbl with CIN85, resulting in reduced EGFR ubiquitylation. Our proteomic analysis of the EGFR interactome at the plasma membrane restricts this effect to the isoform b-Cbl, whereas the second isoform c-Cbl is recruited in a SEPT9-independent manner. We also identify two migration-associated proteins, the class II PI3 kinase PI3KC2β and the Rho-GEF VAV3, to be slightly enriched at activated EGFR upon

SEPT9 depletion. Taken together, these observations identify a novel role for septins in stabilizing the EGF receptor by protecting them from degradation. In addition, we apply a proteomic approach to identify potential novel interactors of SEPT9 including regulators of actin and tubulin polymerization, components of the COPII-coat and several E3 ubiquitin ligases. In line with the latter finding, we show an upregulation of the ubiquitin-binding protein p62 upon loss of SEPT9. In conclusion, SEPT9 might be implicated also in other ubiquitin-dependent processes such as autophagy.

# II. Zusammenfassung

Septine bezeichnen eine Familie von GTP-bindenen Proteinen, die an einer Vielzahl von biologischen Prozessen beteiligt sind wie beispielsweise Zellteilung, Zellmotilität und Membrantransport. Die Assoziierung mit Membranen ermöglicht ihnen die Bildung von Diffusionsbarrieren, die klar abgegrenzte zelluläre Domänen definieren. Durch Assemblierung in oligomere Filamente bilden Septine zudem Gerüste aus, die andere Proteine zu diesen Kompartimenten rekrutieren. In Säugetieren wurden bislang 13 verschiedene Isoformen identifiziert. Einige Isoformen sind in Krankheiten impliziert, allerdings sind die molekularen Mechanismen der Pathogenese weitgehend unverstanden.

In dieser Studie implizieren wir septin 9 (SEPT9) in die Ubiquitin-abhängige Herabregulierung des EGF Rezeptors (EGFR), einer der am besten studierten Rezeptoren der Familie der Rezeptor Tyrosin Kinasen (RTK). Wir zeigen, dass die Depletion von SEPT9 in Hela Zellen die Oberflächenkonzentration von EGFR durch Beschleunigung des Rezeptorabbaus auf nahezu 50% reduziert. Dabei wird die Internalisierung des Rezeptors nicht von SEPT9 beeinflusst, unabhängig von dem Modus der Endozytose. Biochemische Experimente belegen, dass ein PxxxPR Konsensus Motif in der N-terminalen Region von SEPT9 (aa 125-130 von SEPT9_v3) verantwortlich ist für die Interaktion mit allen drei SH3-Domänen des Adapterproteins CIN85, auch bekannt unter dem Namen SH3KBP1. Ein Komplex bestehend aus CIN85 und SEPT9 ist ausschließlich an der Plasmamembran zu finden, wo SEPT9, in Abhängigkeit von CIN85, zu EGF-gebundenen Rezeptoren rekrutiert wird. Des Weiteren zeigen wir, dass CIN85 ganze Septin-Komplexe, wahrscheinlich SEPT2/6/7/9, zu aktiviertem EGFR rekrutiert. Biochemische Fraktionierungs-Experimente weisen darauf hin, dass die Ligandenstimulierung eine Rekrutierung dieser Septin-Filamente aus dem Zytosol an Membrandomänen zur Folge hat. Um die Funktion von SEPT9 während der Stabilisierung von EGFR mechanistisch zu verstehen, wurden stukturelle Analysen der CIN85/SEPT9 Interaktion durchgeführt. Diese Experimente belegen eindrücklich, dass SEPT9 an die gleiche Oberfläche in der SH3 A-Domäne von CIN85 bindet wie Cbl, eine Ubiquitin-Ligase, die für die EGFR-Ubiquitylierung verantwortlich ist. Wir demonstrieren ferner, dass SEPT9 den EGFR-Abbau negativ reguliert, indem es die Assozierung von Cbl mit CIN85 verhindert. Dies führt zu einer Hemmung der EGFR-Ubiquitylierung. Unsere proteomische Analyse des EGFR Interaktoms an der Plasmamembran begrenzt diesen Effekt auf die Isoform b-Cbl,

während c-Cbl unabhängig von SEPT9 an den Rezeptor rekrutiert werden kann. Die Depletion von SEPT9 erlaubt daneben die Detektion erhöhter Mengen der PI3 Kinase PI3KC2β und dem Rho-GEF VAV3, die mit dem EGFR assoziieren. Zusammengefasst identifizieren unsere Beobachtungen eine neue Rolle für Septin GTPasen für den Schutz des EGFR vor lysosomalen Abbau, sowie für die Modulation der durch EGF initiierten Signalkaskaden.

Zusätzlich identifizieren wir mittels einer proteomischen Methode potentielle neue Interaktionspartner von SEPT9 wie zum Beispiel Regulatoren der Aktin- und Tubulin-Polymerisation, Komponenten von COPII-Vesikeln und mehrere E3 Ubiquitin Ligasen. In Übereinstimmung mit Letztgenanntem können wir in Abwesenheit von SEPT9 eine Erhöhung des Ubiquitin-bindenden Proteins p62 detektieren. Diese Resultate weisen auf eine potentielle Funktion von SEPT9 auch in anderen Ubiquitin-abhängigen Prozessen hin, beispielsweise für den Prozess der Autophagie.

# 1 Introduction

Cells rely on the ability to continously respond to their environment. For instance, several physiological processes, such as cell division and differentiation, are regulated by external stimuli, which in many cases trigger changes in gene expression. Most of the extracellular signal molecules lack the ability to enter the cell, and therefore the nucleus, directly. They rather function as ligands for receptors, which are exposed at the cells surface, and transduce the signal to the intracellular space.

The precise regulation of signal transduction in a spatial and temporal manner is highly dependend on the receptor composition in the plasma membrane. Therefore, a dynamic interplay of endo- and exocytosis regulates the receptor composition, as well as their concentration, in the plasma membrane.

## 1.1 Receptor tyrosine kinases (RTKs)

Cell surface receptors can be classified into distinct families based on the mechanisms they use to transduce the signal. They include for example cytokine receptors, G protein-coupled receptors (GPCRs), Wnt receptors and receptor tyrosine kinases (RTKs). The superfamily of RTKs comprises 58 different members, which can be classified into 20 subfamilies including human epidermal growth factor receptors (HERs), fibroblast growth factor receptor (FGFRs), platelet derived growth factor receptors (PDGFRs), vascular endothelial growth factor receptors (VEGFRs), hepatocyte growth factor receptors (HGFRs), ephrin receptors (Ephs) and the insulin receptor (Lemmon & Schlessinger 2010). Stimulation with their respective ligand induces signaling events to regulate critical cellular processes such as proliferation, differentiation, cell survival, cell migration and cell-cycle control. All RTKs share a common architecture, consisting of three distinct domains: an extracellular ligand binding domain, a single transmembrane α-helix, and a cytosolic part that includes an intrinsic tyrosine kinase domain. The HER family consists of four members, HER1-4. Without stimulation these receptors are found as monomers with the intrinsic kinase domain remaining inactive (Clayton et al. 2005; Gadella & Jovin 1995). More than 20 different ligands can bind to HER1-4 (Fig. 1.1; Olayioye et al. 2000; Lemmon et al. 2014). These ligands can be grouped into different classes according to their receptor specificity.

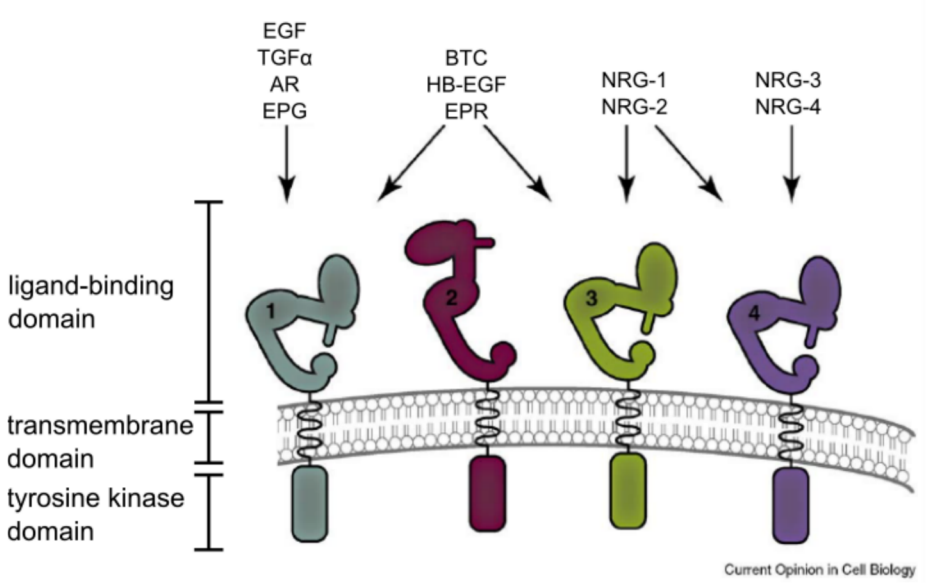


**Fig. 1.1: Structure of the HER family members HER1-4.**

All four receptors of the HER family consist of an extracellukar ligand-binding domain, a transmembrane domain and a cytoplasmic tail that includes a tyrosine kinase domain. Without stimulation, HER1/3/4 are found in a monomeric closed conformation, which disables the formation of homo- and heterodimers. Ligand binding induces a conformational change of the extracellular domain, thereby exposing a binding surface needed for homo- or heterodimerization. HER2 depicts an exception and is found constitutively in an open conformation. No HER2 ligand has been identified so far. A selection of ligands for the respective receptors is shown above their structure. HER1 is commonly known as EGFR. EGF: epidermal growth factor; TGFα: transforming growth factor α; AR: amphiregulin; EPG: epigen; BTC: β-cellulin: HB-EGF: heparin-binding EGF; EPR: epiregulin; NRG: neuregulin. Modified from (Hynes & MacDonald 2009).

In the focus of this study, epidermal growth factor (EGF) binds specifically to HER1, also known as EGFR. Ligand binding induces a conformational change in the extracellular domain, which allows the formation of homo- and/or heterodimers with other HER family members (Dawson et al. 2007; Ferguson et al. 2003). In contrast to its family members, no ligand for HER2 has been identified to date. The activation of this receptor is rather regulated by heterodimerization with other members of the HER family (Graus-Porta et al. 1997; Garrett et al. 2003).

Ligand binding and subsequent dimerization activates the cytoplasmic kinase domain of the receptor (Clayton et al. 2005; Gadella & Jovin 1995). In turn, intermolecular cross-phosphorylation modifies several tyrosine residues in the cytoplasmic tails (Honegger et al. 1989). These residues serve as docking sites for Src-homology 2 domain (SH2) or phosphotyrosine-binding (PTB) domains of multiple adaptor proteins, which control **signal transduction**, **internalization** and **intracellular sorting events**. The following chapters will focus on EGFR, the best studied member of the HER family.

### 1.1.1 The EGFR signaling interactome

Binding of the growth factor EGF activates several signaling pathways including Ras/MAP kinase signaling to control cell division and motility, AKT signaling to control apoptosis and angiogenesis, PLCγ-mediated signaling to regulate differentiation and apoptosis and the JAK/STAT pathway to regulate proliferation and cell survival (Lurje & Lenz 2009). This chapter will give an overview of MAPK and AKT-mediated signaling as the best-studied EGF-induced pathways (Fig. 1.2).

MAP kinases describe a group of several Ser/Thr kinases. Extracellular signal-regulated kinase (ERK) is the most studied MAPK activated by EGF. ERK signaling is initiated at the plasma membrane by binding of the signaling adaptor Grb-2 to the activated receptor. It encodes two SH3 domains and one SH2-domain, which associates with a phospho-tyrosine-based motif in EGFR (Jiang et al. 2003; Goh et al. 2010).

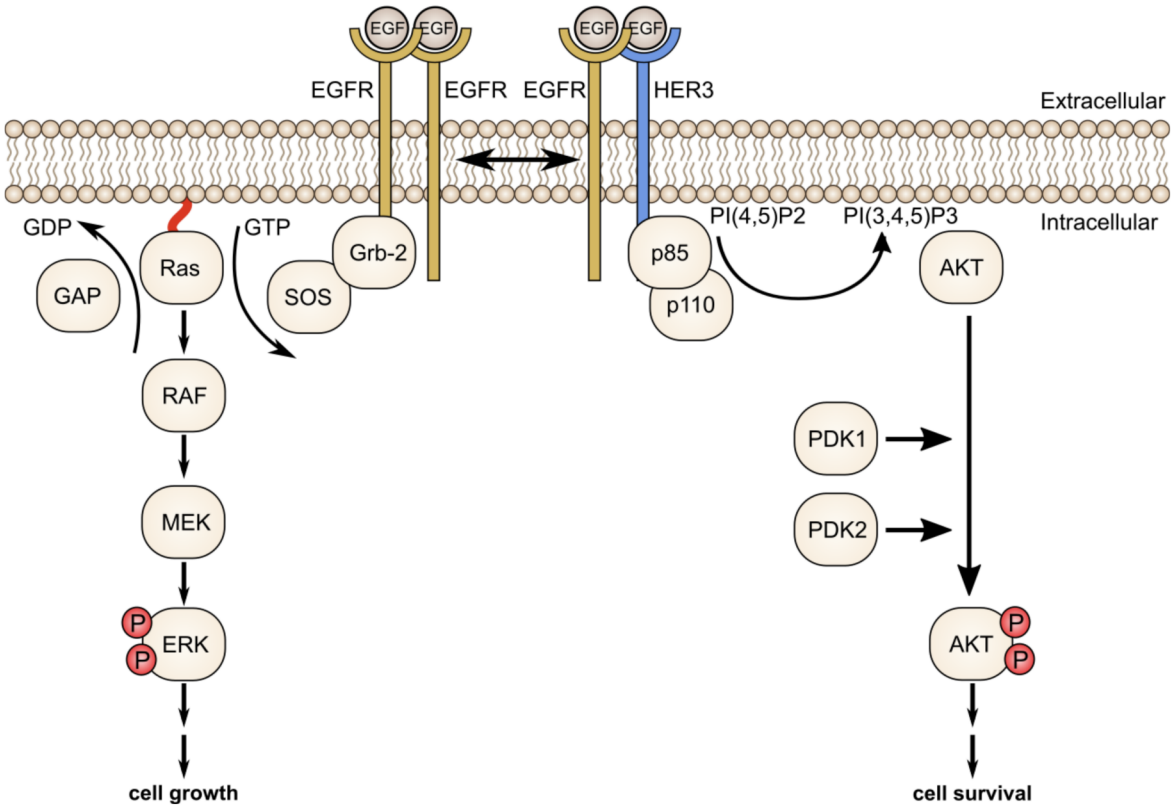


**Fig. 1.2: Major signaling pathways activated by EGF**

EGF activates Ras/MAPK (left side) and the phosphatidylinositol 3-kinase (PI3K)-AKT signaling (right side). See text for details. ERK: extracellular signal-regulated kinase; Grb2: growth factor receptor-bound protein 2; MEK: MAPK/ERK kinase; mTOR: mammalian target of rapamycin; SOS: son of sevenless. Modified from (Sharma et al. 2007).

A central mediator of signal transduction in this pathway is ascribed to the small GTPase Ras (Lowenstein et al. 1992). The two SH3-domains of Grb-2 recruit the Ras GEF son of sevenless (SOS) to membrane-bound Ras (Chardin et al. 1993). SOS mediates GDP release and reloading with GTP, thereby generating the 'active' form of Ras. Ras-GTP activates a cascade of protein kinases (Hallberg et al. 1994; Vojtek et al. 1993; Koide et al. 1993; Seger et al. 1992; Matsuda et al. 1992), which finally phosphorylates and activates ERK. Phosphorylated ERK (P-ERK) translocates into the nucleus to initiate target gene expression (Lenormand et al. 1993; Lidke et al. 2010).

Contrasting the MAPK pathway, phosphatidylinositol 3-kinase (PI3K)-AKT signaling is initiated by the modification of phosphoinositides (PIs). These phospholipids consist of a glycerophospholipid with an inositol ring as a headgroup that can be reversibly phosphorylated at positions 3, 4 and 5 by PI kinases and phosphatases (Di Paolo & De Camilli 2006). The resulting seven different PI-species are enriched in the membrane of distinct cellular compartments, for example PI(4,5)P2 in the plasma membrane (Vanhaesebroeck et al. 1997). Signaling is initiated by the recruitment of a PI3 kinase (PI3K) to activated receptor. PI3K can be grouped in three different classes (Vanhaesebroeck et al. 2010). Class I and III have well-studied roles during the endocytosis of EGFR. Class I PI3 kinases form heterodimers, consisting of a regulatory (p85) and a catalytical subunit (p110). p85 is recruited to EGFR/HER3 heterodimers, since only this coreceptor contains a binding site for the SH2-domain of p85 (Soltoff et al. 1994; Buck et al. 2006). When associated with the receptor, p85 activates the kinase activity of the catalytical subunit p110, which phosphorylates plasma membrane-associated PI(4,5)P2 to PI(3,4,5)P3 (Ueki et al. 2000).

PI(3,4)P2 is an alternative phospholipid that has been implicated in AKT signaling. This PI might be produced by PI3KC2β, an ubiquitously expressed isoform of class II PI3K (El Sheikh et al. 2003). Several studies suggest that PI(3)P and PI(3,4)P2 are the preferred *in vivo* products of PI3KC2β (Virbasius et al. 1996; Domin et al. 1997; Crljen et al. 2002; Maffucci et al. 2003; Posor et al. 2013). Accordingly, PI3KC2β is recruited to activated EGFR (Wheeler & Domin 2001; Wheeler & Domin 2006) and has been shown to produce PI(3)P (Banfic et al. 2009) and PI(3,4)P2 (Haucke lab, unpublished observations) upon EGF stimulation.

AKT, also known as protein kinase B (PKB), encodes a Pleckstrin homology (PH) domain that binds to either PI(3,4,5)P3 or PI(3,4)P2 (Franke et al. 1997; Klippel et al.

1997; Frech et al. 1997). This interaction leads to a partial activation of AKT (Stokoe et al. 1997). Full activation requires phosphorylation of two regulatory residues by the Ser/Thr kinases PDK1 and PDK2. PDK1 phosphorylates AKT at Thr-308 (Alessi et al. 1997). Phosphorylation at Ser-473 by PDK2 fully activates the kinase (Sarbassov et al. 2005). Phosphorylated AKT (P-AKT) dissociates from the plasma membrane and phosphorylates a multitude of target proteins, which promote cell survival.

### *1.1.2 Internalization*

Endocytosis is used by the cell to remove activated receptors from the cell surface in order to fine-tune signal transduction. In general, cargo can be endocytosed by different processes including phagocytosis, macropinocytosis, caveolar-type endocytosis and clathrin-mediated endocytosis (CME) (Doherty & McMahon 2009). In case of EGFR two different internalization routes have been described, CME and clathrin-independent endocytosis (CIE). Which of the pathways is predominantly used depends on the EGF concentration applied. At low doses of ~1.5 ng/ml EGF the receptor is internalized mainly by CME, whereas higher doses (> 20 ng/ml EGF) trigger an increasing contribution of CIE (Lund et al. 1990; Yamazaki et al. 2002; Sigismund et al. 2005; Orth & McNiven 2006a; Sigismund et al. 2008).

CME is driven by a complex machinery of proteins. The formation of an endocytic vesicle requires adaptors to recruit cargo to the forming pit, effectors to induce and assist membrane curvature formation and a membrane scission machinery (Fig. 1.3; Conner & Schmid 2003; McMahon & Boucrot 2011). Internalization through CME is initiated by the recruitment of adaptor protein 2 (AP-2) and clathrin to PI(4,5)P2 enriched membrane domains (Sorkin et al. 1996; Rohde et al. 2002). These adaptors serve as two central interaction hubs for the endocytic protein network due to their multitude of endocytic interaction partners. The triskelion-shaped clathrin molecules polymerize to hexagons and pentagons, thereby forming a coat around the nascent pit (Näthke et al. 1992; Dannhauser & Ungewickell 2012; Ybe et al. 1999). The GTPase dynamin is recruited to the neck of the clathrin coated pit and mediates membrane scission upon GTP hydrolysis, which releases a coated vesicle (Mettlen et al. 2009; Hill et al. 2001). These vesicles undergo uncoating for further endosomal progression and recycling of the coat components (Heuser & Steer 1989; Massol et al. 2006; Schmid et al. 1984).

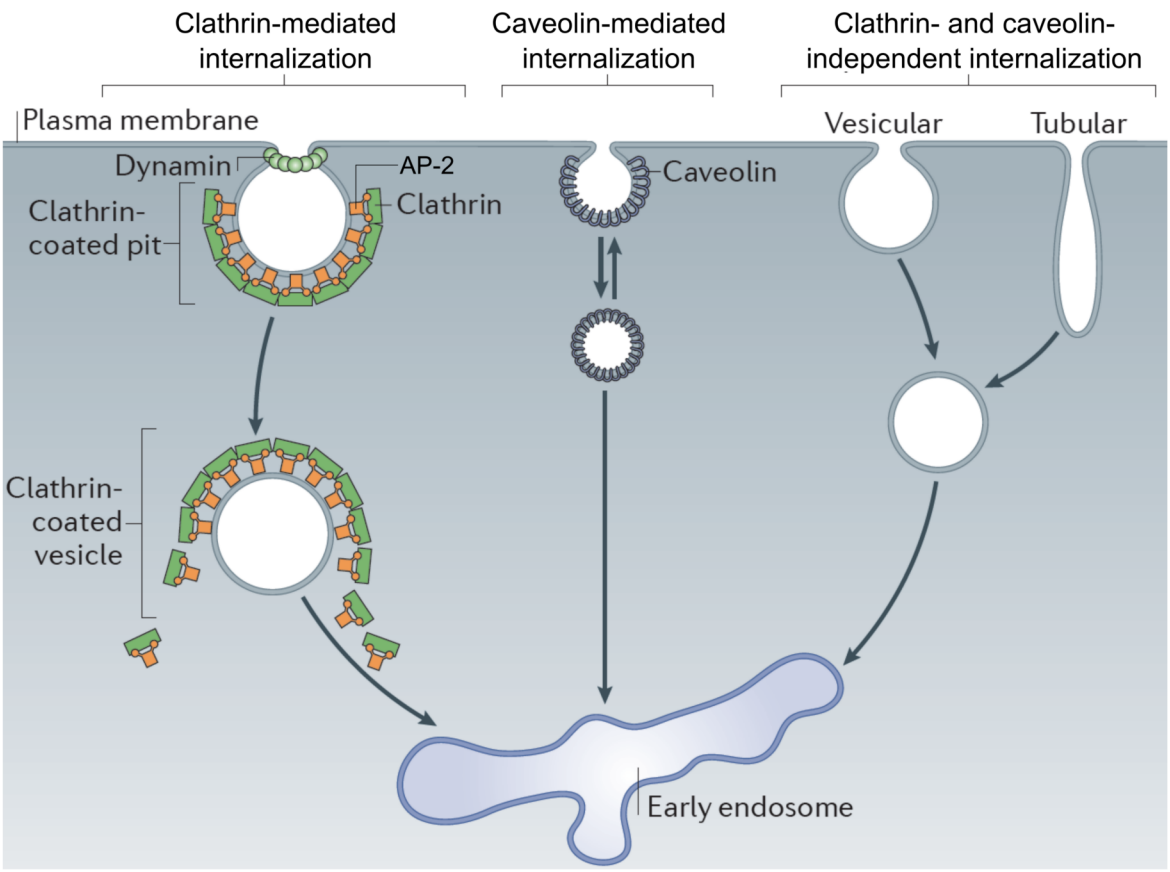


**Fig. 1.3: EGFR internalization**

EGFR can be internalized through clathrin-mediated endocytosis (CME; left), caveolin-mediated internalization (middle) or clathrin- and caveolin-independent internalization pathways (right). For CME, a vesicle is formed by the recruitment of several adaptor proteins, which drive membrane deformation and cargo recognition. AP-2 and clathrin form central binding hubs for the multitude of endocytic adaptors. Clathrin polymerizes to a coat assembling aroung the nascent pit. Membrane scission is catalyzed by the GTPase dynamin. See text for additional details. Modified from (McMahon & Boucrot 2011).

On the contrary, CIE is not a specific pathway, but rather a collection of several mechanisms that might participate during the internalization of RTKs. In comparison to the well-characterized CME, these mechanisms remain poorly understood. The most prominent clathrin-independent endocytosis is mediated by the coat protein caveolin. This type of internalization was shown for EGFR (Couet et al. 1997; Sigismund et al. 2005) and also other RTKs (Sehat et al. 2008; Salani et al. 2010). Caveolin builds small, flask shaped endocytic structures termed caveolae (Kirkham & Parton 2005; Hommelgaard et al. 2005). Dynamin is either constitutively or transiently recruited to the neck of caveolae and a burst of actin polymerization forms an actin tail, which drives the inward movement of the caveolae into the cell (Pol et al. 2000; Mundy et al. 2002; Muriel et al. 2011).

Other mechanisms of internalization can be roughly summarized as macropinocytosis-like endocytosis, which is actin dependent and partially also dynamin-dependent (Haigler et al. 1979; Barbieri et al. 2000; Yamazaki et al. 2002; Orth & McNiven 2006b; Valdez et al. 2007). For instance, stimulation with several growth factors including EGF, HGF and PDGF, induce the formation of circular dorsal ruffles. These highly dynamic membrane structures were shown to selectively sequester and internalize RTKs (Orth & McNiven 2006a; Buccione et al. 2004).

### *1.1.3 Endosomal trafficking*

An overview of the intracellular trafficking routes of EGFR is given in Fig. 1.4. Newly formed vesicles fuse with early endosomes (EE) shortly upon internalisation. The EE constitutes a central sorting station for activated receptors. In summary, internalized receptors are either sorted for recycling back to the plasma membrane or for degradation towards lysosomes. Recycling can occur through two kinetically and mechanistically distinct mechanisms, a slow and a fast route. The major regulatory signal that determines the fate of the receptor upon activation is the degree of its ubiquitylation. The ubiquitin moiety is recognized by the endosomal sorting complexes required for transport (ESCRT) leading to sorting into multivesicular bodies (MVBs) and subsequent degradation in the lysosome. Regulation of the balance between these routes also controls the surface level of EGFR.

#### 1.1.3.1 The E3 ligase Cbl ubiquitylates EGFR

The general ubiquitylation process throughout the cell involves three consecutive steps (Schulman & Harper 2009; Ye & Rape 2009): First, ubiquitin is attached to an ubiquitin-activating enzyme (E1) in an ATP-dependent manner. This ubiquitin molecule is transferred to a cysteine residue of an ubiquitin-conjugating enzyme (E2). The ubiquitin-protein ligase (E3) then catalyzes the transfer of ubiquitin to the amino-group of the side chain of a lysine residue in the target protein. For several proteins, a conjugation of ubiquitin to the N-terminal amino-group is described (Breitschopf et al. 1998; Reinstein et al. 2000). Target specificity is determined by the E3 ligase. These enzymes can be sorted into three main groups: monomeric HECT-type, monomeric RING-type and multimeric RING-type E3 ligases (Ashizawa et al. 2012).

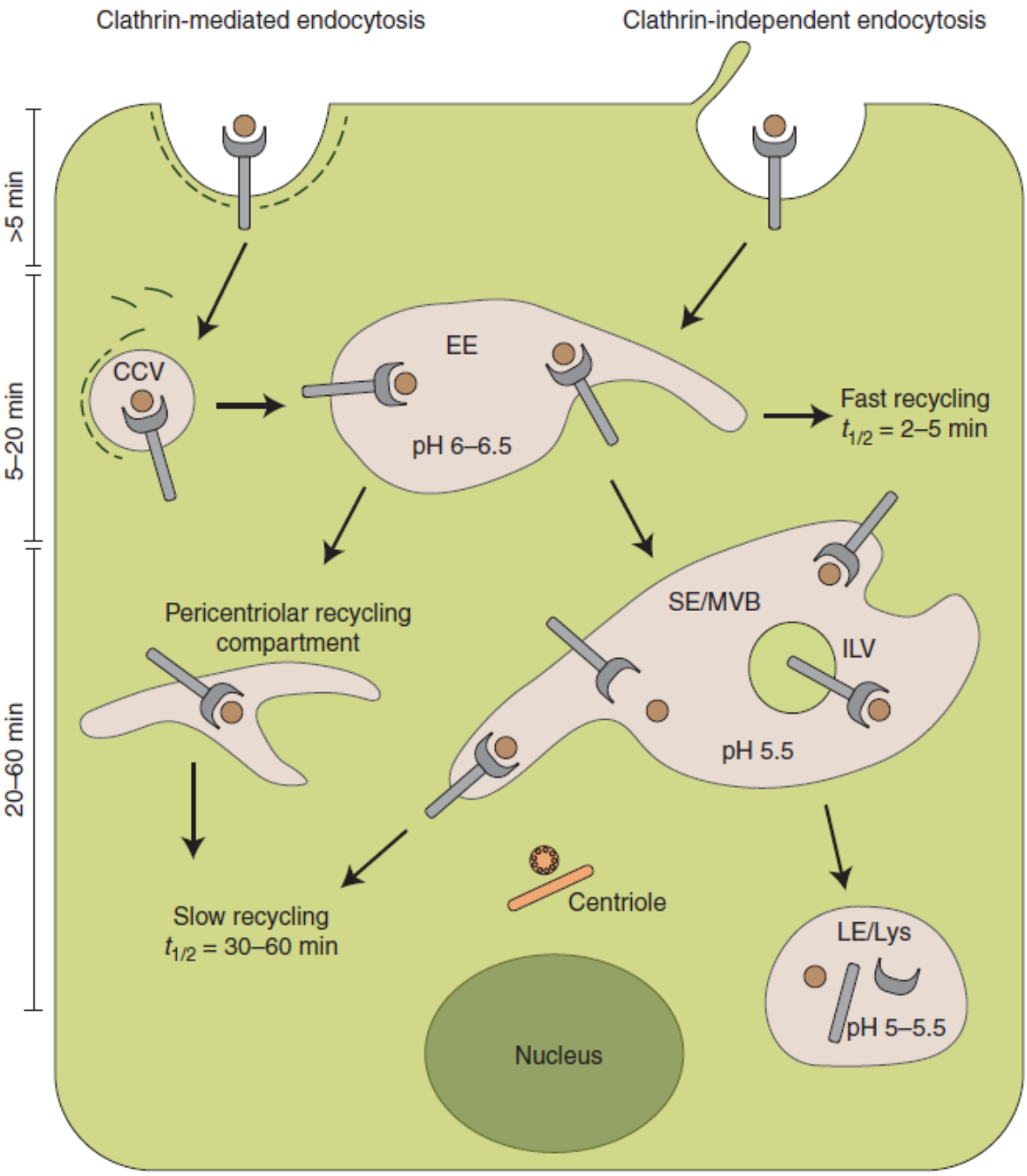


**Fig. 1.4: Trafficking of RTKs. Taken from (Goh & Sorkin 2013)**

Newly formed vesicles fuse with the early endosomal compartment (EE) shortly upon internalization. The EGFR is either recycled back to the plasma membrane or sorted into multivesicular bodies (MVBs) for degradation. Recycling can occur though two different routes. Fast recycling describes a pathway from the EE directly to the plasmam membrane. A second, slower route is targeted by sorting into the recycling compartment. If not recycled, the receptor accumulates in intraluminal vesicles (ILV) of the MVB and is further progressed to late endosomes (LE), at later stages to lysosomes (Lys) for subsequent degradation. The receptor can also be 'rescued' from degradation by sorting from the MVB to the recycling compartment. CCV: Clathrin coated vesicle; SE: sorting endosome.

The ubiquitylation process can also proceed leading to the formation of polyubiquitin-chains. Ubiquitin contains seven lysine residues (K6, K11, K27, K29, K33, K48 and K63), all of which can be used to attach another ubiquitin molecule. Importantly, the residue number used to extend the chain determines the regulatory function (Adhikari & Chen 2009). K48-linked polyubiquitin-chains display the most common linkage found in the cell and provide a targeting signal for proteasomal degradation. K63-linked chains are implicated in different cellular processes such as DNA repair and vesicle trafficking. Polyubiquitylation through K11 is known to mediate endoplasmic reticulum-associated degradation (ERAD; Xu et al. 2009).

The major E3 ligase responsible for ligand-induced ubiquitylation of the EGF receptor is the monomeric RING-type ligase casitas B-lineage lymphoma (Cbl) (Levkowitz et al. 1999; Grøvdal et al. 2004). Three homologs have been characterized in mammals. Cbl-b and c-Cbl are ubiquitiously expressed and share mostly similar functions. Cbl-c, a shorter variant, is expressed mainly in epithelial cells and is presumably dispensable for EGFR ubiquitylation (Griffiths et al. 2003). The long isoforms encode a PTB domain, which binds to a phospho-tyrosine-based motif in EGFR, a RING finger domain, which associates with E2 enzymes, a proline-rich region, which interacts with SH2- and SH3-domains and a C-terminal ubiquitin-associated (UBA) domain that contains a leucine-zipper motif (Thien & Langdon 2001). Cbl associates with activated EGFR shortly upon EGF stimulation and gets tyrosine phosphorylated at a site flanking the RING finger domain (Fukazawa et al. 1996). This modification activates ligase activity leading to the attachment of several ubiquitin molecules to at least six distinct lysine residues of the receptors cytoplasmic tail (Huang et al. 2006; Dou et al. 2012; Tong et al. 2014). Several of these sites are polyubiquitylated, primarily linked through Lys63, indicating that the EGFR gets multi-monoubiquitylated, as well as polyubiquitylated.

Cbl displays a target for several regulatory mechanisms. For instance, Src-homology-2-containing phosphatase-1 (SHP1) dephosphorylates Cbl, thereby inhibiting its ligase activity (Uddin et al. 1996). Another negative feedback loop involves targeting of Cbl for proteasomal degradation through ubiquitylation by Itch, a HECT-type E3 ligase (Magnifico et al. 2003; Azakir & Angers 2009).

#### 1.1.3.2 Ubiquitylated EGFR is sorted for lysosomal degradation

Endosomal progression is regulated by multiple factors, but key roles are assigned to PIs, small GTPases of the Rab family (Zerial & McBride 2001) and the ESCRT complex. Rab5 has been shown to be recruited to the endocytic vesicle already during internalization where it facilitates uncoating of clathrin-coated vesicles (Semerdjieva et al. 2008), as well as fusion with early endosomes (Rubino et al. 2000). The latter step is driven by Rab5-dependent formation of PI(3)P, a PI defining the identity of early endosomes (Gillooly et al. 2000). Active Rab5 encompasses a multitude of effectors including class I PI 3-kinase (PI3K), which generates PI(3,4,5)P3 from PI(4,5)P2 at the plasma membrane. PI 5-phosphatases and 4-phosphatases, also Rab5 effectors, mediate dephosphorylation of PI(3,4,5)P3 to PI(3)P (Shin et al. 2005). An alternative synthesis route for PI(3)P is achieved through the recruitment of a class III PI3K, hVps34, which uses PI as a substrate (Volinia et al. 1995). Rab5 then recruits early endosome antigen-1 (EEA1), which additionally binds through its FYVE domain to PI(3)P and provides a tethering function to promote fusion with EE (Mills et al. 2001).

The EE compartment comprises a heterogenous morphology and consists of vesicular and tubular membranes (Miller et al. 1986). Ligand-bound EGFR reaches this compartment 2 - 5 min upon stimulation. The mildly acidic pH (6.0-6.5) is not sufficient to cause dissociation of EGFR-ligand complexes (Sorkin et al. 1988). As a consequence, the receptor remains dimerized, active and associated to Cbl. Of note, also Grb-2 remains associated with active EGFR and continues to initiate MAPK signaling (Fukazawa et al. 1996; Oksvold et al. 2001; Xue & Lucocq 1998).

The receptor can be further progressed into either the recycling compartment or multivesicular bodies (MVBs) located in the perinuclear region of the cell. Sorting into the degradational pathway is regulated by the ESCRT complex, which consists of four different heterooligomeric protein complexes (Babst 2011). ESCRT-0,-I and -II complexes contain proteins harbouring ubiquitin interacting motifs (UIMs), which bind ubiquitylated receptor. Lys63-linked ubiquitin chains and monoubiquitin are recognized by UIMs in a similar manner (Varadan et al. 2004). Sorting into MVBs is initiated by the recruitment of the UIM-containing ESCRT-0 component Hrs, which binds to PI(3)P on EEs through its FYVE domain (Petiot et al. 2003; Raiborg et al. 2002). EEs mature into sorting endosomes by gradually losing endosomal components and are characterized by an enrichment of late endosomal proteins such as Rab7 (Rink et al. 2005). During this process, ubiquitylated

receptor is handed from the ESCRT-0 to ESCRT-I and then -II complex (Lu et al. 2003). In detail, Hrs binds and sequesters ubiquitylated cargo (Raiborg et al. 2002; Urbé et al. 2003), whereas ESCRT-I in concert with ESCRT-II initiates inward membrane invagination in order to generate intraluminal vesicles (ILVs). The avidity of the weak ubiquitin-UIM interactions is promoted by the presence of multiple ubiquitylated sites in the receptor. This ubiquitin-based platform allows for simultaneous interactions with multiple UIMs of ESCRT components, thereby increasing the efficiency of sorting into ILVs (Ren & Hurley 2010). ESCRT-II initiates the assembly of the ESCRT-III complex, which drives further maturation and scission of ILVs (Urbé et al. 2003). During this step, the ESCRT-III subunits Vps2 and Vps24 form helical tubular structures, which presumably assemble within the neck of a forming ILV (Muzioł et al. 2006; Ghazi-Tabatabai et al. 2008). The ATPase Vps4 recognizes Vps2 and binds to these helical structures (Stuchell-Brereton et al. 2007). ATP hydrolysis causes disassembly of ESCRT-III, which induces fission of cargo-containing ILVs (Wollert et al. 2009). It is assumed that the receptor has to be deubiquitylated before ILVs are pinched of (Alwan et al. 2003; Luhtala & Odorizzi 2004). The activation of signaling pathways is abrogated latest at this step, since ILVs are not connected to the outer membrane of the MVB (Longva et al. 2002). Receptor degradation is initiated by fusion of MVBs with primary lysosomes (Bright et al. 2005; Schaik et al. 1989; Bright et al. 1997). Further maturation decreases the pH to 5 - 5.5 and activates lysosomal proteases leading to rapid proteolysis of EGFR, which still locates to ILVs.

Although the receptor gets degraded exclusively through the lysosome (Futter et al. 1996), proteasomal degradation also affects EGFR trafficking indirectly by regulating the decay of multiple sorting factors (Longva et al. 2002; Melikova et al. 2006). For instance, the E3 ligase Tsg101-associated ligase (TAL) polyubiquitylates the ESCRT-I subunit Tsg101, leading to its proteasomal degradation (McDonald & Martin-Serrano 2008). As already mentioned above, the E3 ligase Itch mediates proteasomal degradation of Cbl. On the contrary, also deubiquitylating enzymes (DUBs) can be recruited along the degradational route. For example, UBPY and AMSH associate with endosomes and regulate ubiquitylation of ESCRT-0 subunits (Komada 2008).

#### 1.1.3.3 Unubiquitylated receptor is recycled to the plasma membrane

Unubiquitylated receptor can be rapidly recycled from the EE ('fast recycling') or further progressed into the recycling compartment ('slow recycling'). Of note, the recycling routes described here were examined for the transferrin receptor (TfR), which enters the cell exclusively by CME (Warren et al. 1997; Motley et al. 2003). It is assumed that the EGF receptor uses the same recycling routes and can be sorted out by sensing its ubiquitylation.

The mechanism underlying fast recycling is only poorly understood. Important regulators of this pathway are Rab4 and Rab35 (van der Sluijs et al. 1992; Kouranti et al. 2006; Sato et al. 2008). The second recycling route is characterized by slower kinetics and includes sorting through recycling endosomes. Transport to this compartment originates at the EE and also from the tubular extensions of MVBs. For the latter route, EGFR needs to be deubiquitylated prior to being sorted into ILVs (Eden et al. 2012). Morphologically, the recycling compartment is defined as a tubular compartment that is largely devoid of fluid. A central regulator of this pathway is Rab11 (Pasqualato et al. 2004; Ullrich et al. 1996; Ren et al. 1998). The detailed sorting mechanism is only poorly understood, but several regulators were associated to this pathway. For instance, EHD3 associates with two Rab effectors, rabenosyn 5 and Rab11FIP2, and is therefore considered to connect the Rab5-positive EE with the Rab11-positive recycling compartment (Galperin et al. 2002; Cai et al. 2013). Rab11 also participates in the vesicular transport to the plasma membrane (Ward et al. 2005; Takahashi et al. 2012). Here, it mediates tethering of recycling endosomes with the plasma membrane in concert with the SNARE complex (Leung et al. 1998; Prekeris et al. 1998).

### *1.1.4 'Crosstalk' between EGF-induced pathways*

Growing evidence supports a model by which internalization, signaling and ubiquitylation induced by EGF do not represent autonomous pathways, but rather show several interdependencies. Importantly, ubiquitylation is largely dispensable for the internalization (Huang et al. 2006; Sigismund et al. 2008; Ahmad et al. 2014). However, the mode of internalization is coupled to the degree of ubiquitylation, whereby Cbl recruitment is controlled by the ligand concentration in a threshold-dependent manner. Therefore, EGFR ubiquitylation was correlated with CIE, rather than CME (Sigismund et al. 2013). As a consequence, at low EGF doses sorting into the recycling

routes is favoured over the degradational pathway.

Internalization plays a critical role for sustained signal transduction (Vieira et al. 1996). In some cases, signaling adaptors were shown to affect also ubiquitylation (Ettenberg et al. 1999; Goh et al. 2010; Huang & Sorkin 2005). This connection is mediated by the interaction between Cbl with different signaling adaptors, including p85, Shc1 and Grb-2 (Fukazawa et al. 1996; Jiang et al. 2003).

### *1.1.5 The adaptor protein CIN85*

The E3 ligase Cbl displays one of the central regulatory hubs during EGFR downregulation, since multiple interactors inhibit or enhance its activity (Schmidt & Dikic 2005). One member of these enhancers is Cbl-interacting protein of 85kDa (CIN85), which is recruited to the plasma membrane already in complex with Cbl (Petrelli et al. 2002; Dikic 2003; Szymkiewicz et al. 2002). The domain structure and a selection of its interactors are depicted in Fig. 1.5. CIN85, also known as SH3KBP1, encodes three SH3-domains located at the N-terminus, a proline-rich middle domain and a C-terminal coiled-coil region, which mediates homooligomerization, as well as heterooligomerization with CD2AP, a close homolog (Borinstein et al. 2000).

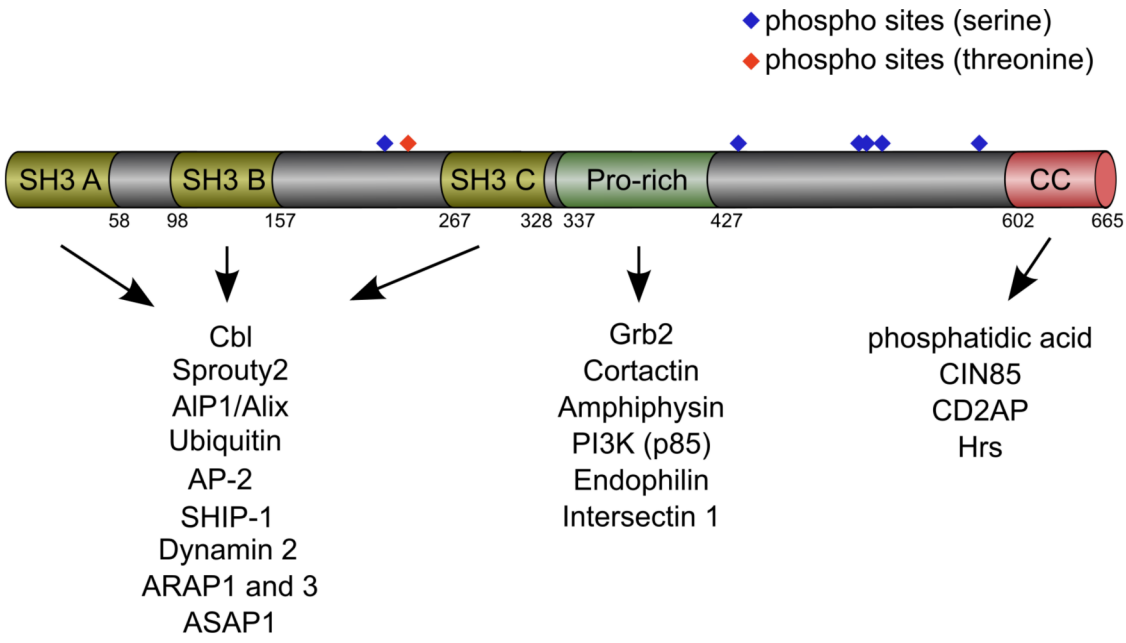


**Fig. 1.5: Domain structure and a selected interactome of CIN85.**

CIN85, also known as SH3KBP1, encodes three SH3 domains, a Pro-rich domain and a coiled-coil region (CC). It interacts with a multitude of endocytic adaptors. A selection of those interactions is depicted below the domains they associate with.

Three additional isoforms exist, which are N-terminally truncated, lacking one, two or all three SH3-domains (Take et al. 2000; Watanabe et al. 2000; Mayevska et al. 2006). However, functional implications of these truncated versions have not been studied so far. The SH3-domains mediate binding to the atypical proline-arginine based motif PxxxPR (Kowanetz et al. 2003). This motif is indispensable for binding of Cbl to CIN85. The positively charged C-terminus mediates association with membranes containing phosphatidic acid (Zhang et al. 2009).

Upon EGF stimulation, CIN85 is recruited to the plasma membrane in complex with Cbl (Fig. 1.6). EGF-induced phosphorylation of Cbl not only activates ubiquitin ligase activity, but also enhances its interaction with CIN85, whereby CIN85 further assists the activation of ligase activity (Szymkiewicz et al. 2002). Furthermore, CIN85 also associates with multiple adaptor proteins implicated in internalisation (endophilin, intersectin) (Petrelli et al. 2002; Nikolaienko et al. 2009), degradative sorting (Alix, Sprouty 2, Hrs) (Schmidt et al. 2004; Kurakin et al. 2003; Haglund et al. 2005; Rønning et al. 2011) and signaling (Grb2, p85) (Gout et al. 2000; Borinstein et al. 2000; Borthwick et al. 2004). By binding and sequestering the regulatory PI3K subunit p85, CIN85 can attenuate PI3K activity. The recruitment of endophilin to the forming pit is thought to occur in a CIN85-dependent manner. However, whether CIN85 is really involved in endocytosis is still under debate (Rønning et al. 2011; Ahmad et al. 2014).

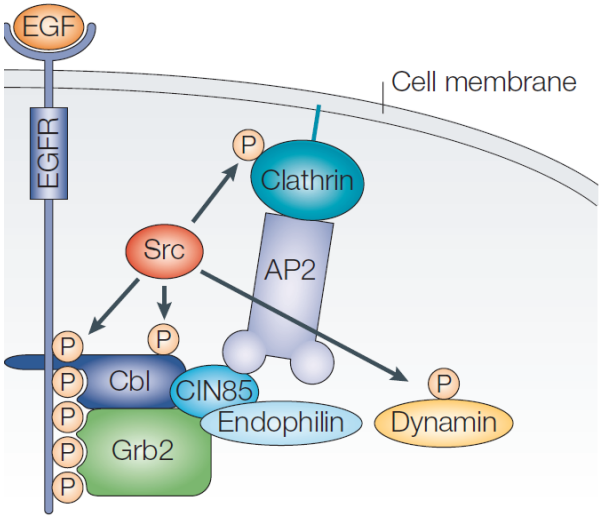


**Fig. 1.6: CIN85 recruitment to activated EGFR in complex with Cbl.**

Upon EGF stimulation, CIN85 gets recruited to activated receptor in complex with Cbl. Furthermore, it interacts with several endocytic adaptors implicated in internalization and signaling. See text for details. Taken from (Schmidt & Dikic 2005).

An important feature of CIN85 is its ability to simultaneously bind to multiple interaction partners via its three SH3 domains. CIN85 clusters its effectors, thereby acting as a molecular scaffold.

CIN85 remains associated with Cbl at activated EGFRs during endosomal sorting (Haglund et al. 2005). This localisation depends on its tyrosine phosphorylation by Src-kinases (Schroeder et al. 2012). Based on its interaction with dynamin 2 during the formation of MVBs, CIN85 has been suggested to contribute to degradative trafficking of EGFR (Schroeder et al. 2010a). The mechanistical details of this function and whether the interactions with two ESCRT-components, Alix and Hrs, play a role here, are not fully understood (Schmidt et al. 2004; Rønning et al. 2011). At later stages of endocytosis, CIN85 itself becomes a target of Cbl activity. Multi-ubiquitylation at several lysine residues in the C-terminus targets the protein for degradation in the lysosome (Verdier et al. 2002; Haglund et al. 2002).

The CIN85/Cbl complex has also been implicated in the endocytosis of other RTKs, such as c-Met, PDGFR, c-Kit and VEGFR (Petrelli et al. 2002; Kobayashi et al. 2004). Entry of the bacterial pathogen Listeria, which hijacks the target cell through binding to c-Met, is inhibited by down-regulation of CIN85 (Veiga & Cossart 2005).

Furthermore, CIN85 is implicated in various other biological processes. For instance, it is involved in cytoskeletal rearrangements at focal adhesions, thereby being implicated in the regulation of cell adhesion (Schmidt et al. 2003). This function is mediated by its interaction with the adaptor protein AIP1.

## 1.2 Septin GTPases

### *1.2.1 Nomenclature and structure of septins*

Mammalian septins constitute a family of guanine-nucleotide-binding proteins comprising 13 isoforms that are differentially expressed in a cell- and tissue-specific manner. They belong to the GTPase superclass of P-loop NTPases, which also includes the myosin/kinesin superfamily of cytoskeleton motors and the Ras superfamily of GTPases (Leipe et al. 2002). All septins share a conserved GTP-interacting motif (Weirich et al. 2008). Based on sequence similarity the different isoforms can be classified into the SEPT2, SEPT3, SEPT6 or SEPT7 subgroups, as depicted in Fig. 1.7 (Kinoshita 2003). Of note SEPT13, which had initially been identified as a distinct isoform, later turned out to be a pseudogene of SEPT7.

All isoforms contain a central GTP binding domain (G-domain) and N- and C-terminal extensions of variable length and architecture. In comparison to other GTP-binding domains, the G-domain contains a conserved sequence termed septin unique element (SUE) located at the C-terminus. GTP hydrolysis is mediated by a threonine residue located in the switch I region of all but the SEPT6 subgroup (Sirajuddin et al. 2009). All isoforms except the SEPT3 subgroup members encode C-terminal coiled-coil domains that have been implicated in interactions with non-septin binding partners. Septins are expressed from fungi to mammals, with a high variation in the number of individual genes found in different organisms (e.g. two in *C. elegans*, seven in *S. cerevisiae*, five in *D. melanogaster*).

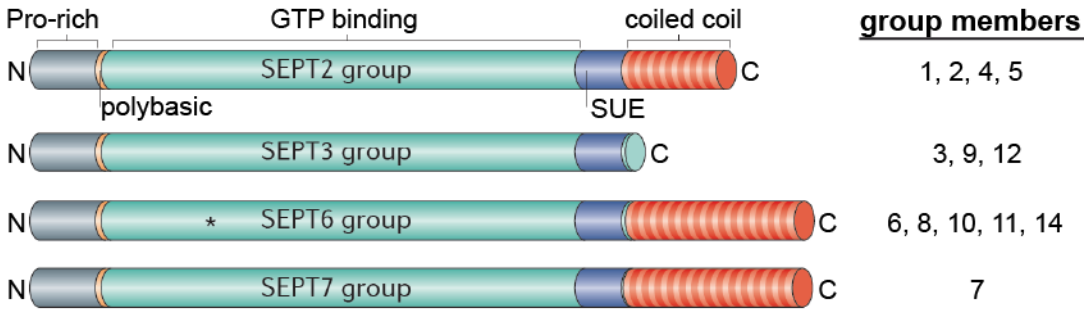


**Fig. 1.7: Domain structure of septin GTPases.**

Septins share a central GTP-binding domain (G-domain), but vary in their N- and C-terminal extensions. The G-domain of septins, in comparison to other GTPases, contains a septin unique element (SUE). The asterisk indicates that members from the SEPT6 group cannot hydrolyze GTP to GDP.
Modified from (Mostowy & Cossart 2012).

A characteristic feature of septins is their ability to form oligomeric complexes, which in turn can assemble into higher ordered structures such as filaments and rings. The best described septin complex consists of alternating SEPT2/6/7/9-units (Low & Macara 2006; Estey et al. 2011). Fig. 1.8 depicts the structure of the basic octameric unit of this complex and illustrates that septin-septin interactions are based on two different interfaces. The G-interface is formed by oligomerization of two neighbouring G-domains, whereas the interaction between the N- and C-terminal extensions determines the NC-interface. In the SEPT2/6/7/9-octamer, SEPT9 occupies the terminal positions by the formation of a G-interface with SEPT7. The inclusion of SEPT9 regulates filament elongation or abrogation (M. S. Kim et al. 2011). This specific function of SEPT9 is described in further detail in chapter 1.3.

Filament extension is facilitated by SEPT9-dimerization through NC-interfaces, which builds a link to the neighboring octamer. Individual members of the same subgroup can substitute for each other in the SEPT2/6/7 complex except SEPT7, which constitutes the sole member of its subgroup (Sellin et al. 2011). As a consequence, loss of SEPT7 influences total levels of multiple other septin isoforms (Kremer et al. 2005; Tooley et al. 2009). A structural analysis of the SEPT2/6/7-complex revealed that only SEPT6 is GTP-bound, whereas SEPT2 and SEPT7 are bound to GDP (Sirajuddin et al. 2007). The nucleotide state of SEPT9 in the octameric complex has not been specified yet.

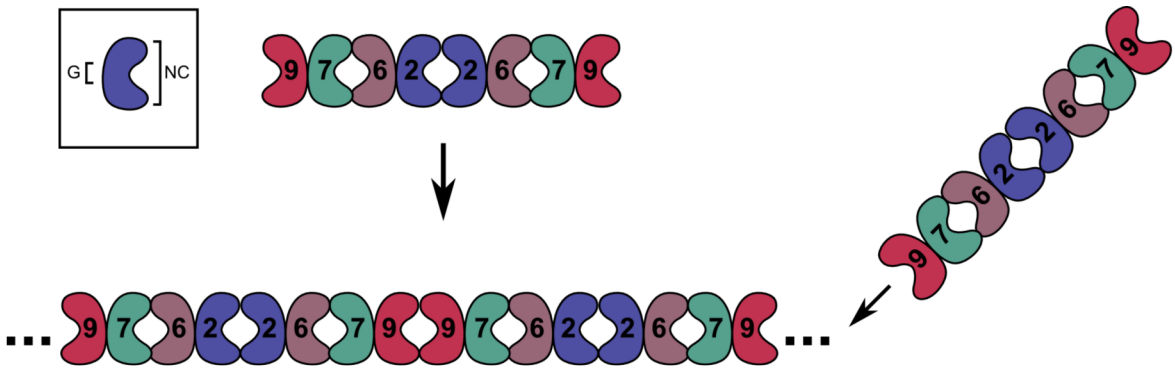


**Fig. 1.8: Arrangement and filament assembly of the SEPT2/6/7/9 complex.**

Septin monomers are represented by a 'bean'-like structure with the G-domain (G) in the middle, which is extended by the N- and C-terminal domains (NC). The basic octameric unit is shown on the top. Dimerization of SEPT9 allows filament assembly (bottom). Modified from (Estey et al. 2011).

How single septin molecules cycle between their filamentous and monomeric states is only poorly understood. In particular, it is unclear to date if and how the intrinsic GTPase activity is correlated with filament assembly. The excess of GDP bound in filaments indicates that GTP hydrolysis is controlling assembly, rather than disassembly (Sirajuddin et al. 2007; Sheffield et al. 2003a). A structural analysis of SEPT2 revealed that the GDP- and the GTP-bound forms exhibit distinct conformations not only of the switch regions in the G-domain, but also of the N-terminal region (Sirajuddin et al. 2009). This supports the hypothesis that the nucleotide binding state controls complex formation by affecting both, the G-interface and the NC-interface. Furthermore, septins might exhibit different functions depending on their nucleotide binding state. In comparison to other GTPases, the intrinsic GTP hydrolysis of septins occurs only at a slow rate and varies strongly between different isoforms (Weirich et al. 2008; Zent & Wittinghofer 2014). Turnover rates of septins within their respective filaments is at least 2–3 times slower compared to actin and tubulin, but significantly more rapid than intermediate filament subunits (Hu et al. 2008).

An alternative model for the rearrangement and assembly of septin subunits claims that complex formation is rather mediated by post-translational modifications and/or association with non-septin binding partners (McMurray & Thorner 2009). Posttranslational modifications of septins include Ser/Thr phosphorylation by cell-cycle dependent kinases (She et al. 2004; Yu et al. 2009). Sumoylation (Ho et al. 2011) and acetylation of septins (Mitchell et al. 2011) have so far been characterized exclusively in yeast, but might also occur in mammalian cells. Interestingly, several studies correlated septin filament stability with Rho signaling events and suggested that septins are downstream effectors of Rho GTPases (Ito et al. 2005; Nagata & Inagaki 2005; Sadian et al. 2013). Hypothetically, septin binding partners could also act as surrogate GAPs or GEFs. However, no interaction partner was so far shown to directly modulate GTPase activity *in vitro*. Apparently, only a few direct interaction partners were identified to date. For instance, Borg proteins, downstream effectors of the Rho GTPase Cdc42, interact with the SEPT2/6/7 complex and might regulate assembly and disassembly of septin filaments (Joberty et al. 2001; Sheffield et al. 2003b).

### 1.2.2 Biological functions of septin GTPases in mammals

Septins form part of the cytoskeleton and are stabilized by actin stress fibers (Kinoshita et al. 1997; Kinoshita et al. 2002; Mostowy & Cossart 2012). This connection is partially interdependent, since septin complexes are also able to stabilize actin structures at specific subcellular domains such as focal adhesions (Dolat et al. 2014). Septins associate with microtubules and presumably regulate their interaction with microtubule-associated proteins (MAPs), such as MAP4, and microtubule motor proteins (Kremer et al. 2005; Kremer et al. 2007; Hu et al. 2008). However, the extent of septin colocalization with microtubules varies depending on the septin isoform under study, the cell type and the cell cycle phase (Surka et al. 2002; Kim et al. 2004; Robertson et al. 2004; Fujishima et al. 2007).

Furthermore, septins promote and maintain cell asymmetry by imposing rigidity to the cell membrane, thereby affecting the formation especially of protrusive membrane structures. A substantial feature of septins is their ability to form diffusion barriers by associating with membranes. Septins bind to membrane surfaces enriched in negatively charged phospholipids, such as phosphoinositides (PI) (Tanaka-Takiguchi et al. 2009). Distinct septin isoforms show a preference to PI(4,5)P2, which is predominantly found in the plasma membrane (Zhang et al. 1999; Bertin et al. 2010). The mechanism underlying the formation of diffusion barriers is based on the ability of septins to rigidify membrane, which inhibits lateral diffusion rates of membrane proteins, such as receptors, and membrane-associated proteins. As a consequence, a local diffusion 'block' enables the cell to regulate protein concentrations in a spatial and temporal manner (Hall & Russell 2012). The diffusion barriers serve to define distinct cellular compartments and/or domains during a multitude of cellular processes, including membrane trafficking, signal transduction, cell division and motility and development (Caudron & Barral 2009). In addition, septin complexes also serve as scaffolds to recruit proteins to these membrane subdomains. Fig. 1.9 illustrates several examples, where septin filaments serve as diffusion barriers:

Septins regulate cell motility in several cell types. For instance, a septin barrier assembles during spermiogenesis at the annulus of spermatozoa (panel a; Toure et al. 2011; Kuo et al. 2015) or at the cortex of amoeboid T lymphocytes (panel d,e; Tooley et al. 2009). Here, they preserve the morphology and polarisation of the cell, which is essentiell for cell migration. In addition, septin barriers often stabilize protrusions by assembling at their base. For example, they can be found at primary cilia, an antenna-like protrusion,

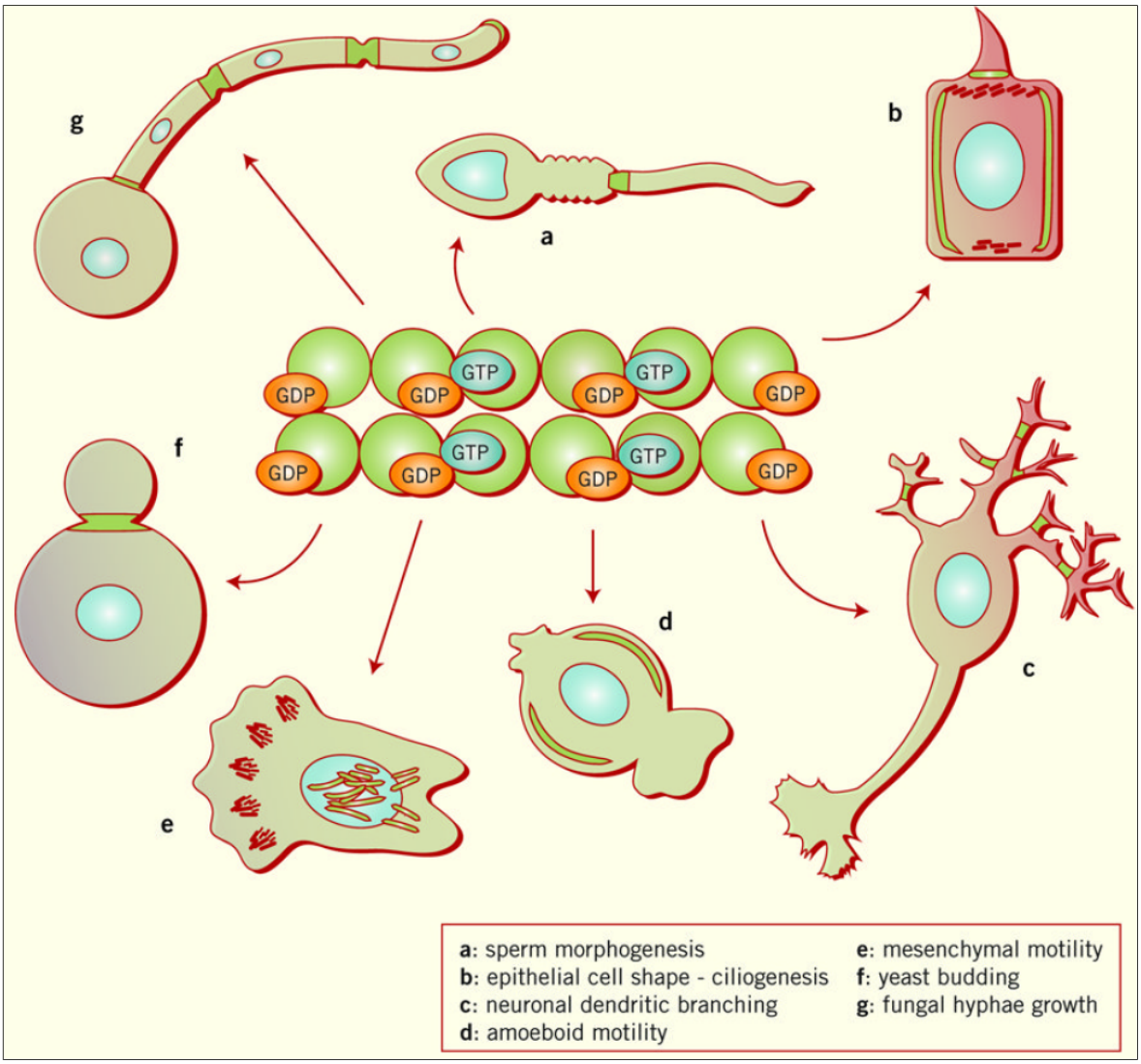


**Fig. 1.9: Septins in several biological processes.**

Septins can act as scaffolds and/or diffusion barriers in a multitude of cellular processes. This function is conserved from fungi to mammals. The cellular localisation of septin diffusion barriers are indicated in green. See text for details. Taken from (Spiliotis & Gladfelter 2012).

which enhances the efficiency of signal transduction by concentrating signaling receptors in its membrane. These receptors were shown to be retained in the cilium by the SEPT2-based diffusion barrier located at its base (panel b; Chih et al. 2012; Hu et al. 2010). Panel c exemplifies septin localization in post-mitotic cells like neurons. Here, septin diffusion barriers stabilize the base of dendritic protrusions and branching points and thereby assist the accurate formation and growth of dendritic spines and dendrites (Vega & Hsu 2003; Xie et al. 2007; Tada et al. 2007; Shinoda et al. 2010; Li et al. 2011).

Septin-based diffusion barriers are highly conserved through species, since they were also identified in multiple fungal organisms (Gladfelter 2010). In filamentous fungi, septins assemble into cortical bars at cell-cell-contacts of long multicellular, tubular extensions termed hyphae (panel g; Wightman et al. 2004; Juvvadi et al. 2013). These bars conserve the asymmetric morphology of hyphae, which is essential for both growth and reproduction. In budding yeast, an hourglass-shaped septin ring assembles at the bud neck and is essential to seperate mother and daughter cell (panel f; Longtine & Bi 2003; Oh & Bi 2011).

Septin function in mediating cell division is also present in mammalian cells, where different isoforms assemble at different stages of mitosis. SEPT2, SEPT7, SEPT9 and SEPT12 have been shown to localize to the midbody, where they mediate midbody abscission (Kouranti et al. 2006; Estey et al. 2010; M. S. Kim et al. 2011; Menon et al. 2014). In addition, SEPT2 localizes to the microtubule spindle apparatus (Spiliotis et al. 2005) and SEPT7 to the kinetochore (Zhu et al. 2008). Here, they regulate chromosome congression and segregation.

Furthermore, several septin GTPases are implicated in membrane trafficking events by associating with components of the SNARE complex. For instance, SEPT5 inhibits exocytosis by interacting with syntaxin 1A and thereby competes with α-SNAP for binding to the SNARE complex (Beites et al. 2005; Tokhtaeva et al. 2015). In podocytes, SEPT7 regulates glucose transporter trafficking by associating with VAMP2 on transport vesicles (Wasik et al. 2012).

### *1.2.3 Septins in human pathologies*

Given the fundamental importance of the processes septins are involved in, it is not surprising that certain isoforms have been correlated with the development of certain diseases including neurodegeneration and tumorigenesis. Several neurodegenerative disorders, such as Parkinson's and Alzheimer's disease, are marked by the formation of protein aggregates in the brain. Some septin isoforms like the neuron-specific SEPT4 were found in these aggregates (Ihara et al. 2003; Ihara et al. 2007). Accordingly, the E3 ligase parkin, a key player in the pathogenesis of Parkinson, was shown to ubiquitylate SEPT5, thereby regulating its degradation (Zhang et al. 2000). In addition, alterations in septin expression were associated with several other neurodegenerative diseases, such as Down syndrome (Sitz et al. 2008) and schizophrenia (Wesseling et al. 2014).

Furthermore, several members of the septin family were found associated with tumorigenesis, in particular leukemia. Here, genetic fusions of the histone methyltransferase MLL plays a central role in the pathogenesis of approximately 10% of human leukemias. SEPT2/5/6/9/11 were found as fusion partners of MLL (Cerveira et al. 2011) with MLL-SEPT6 being the most common fusion in acute myeloid leukemia (AML) (Meyer et al. 2009).

However, further studies are needed to clarify, whether septin malfunction directly paticipates in the pathogenesis of leukemia or neurodegenerative disorders. In particular, whether the underlying molecular mechanisms derive from a cytokinetic defect or are rather mediated by complex formation with non-septin binding partners needs to be addressed.

## 1.3 Septin 9

Septin 9, also known as MLL septin-like fusion protein (MSF), represents the longest isoform among septins. The gene gives rise to eight different transcript variants generated by extensive alternative splicing of the N-terminal domain, which are depicted in Fig. 1.10. Please note that v5 and v6 are produced by alternative splicing, but result in an identical amino-acid sequence (isoform e). The isoforms can be roughly subdivided into long (v1, v2, v3, v8) and short transcripts (v4, v5 and v6, v9). However, all transcript variants retain an intact G-domain. The N-terminus of the longest variant v1 consists of an acidic stretch at the beginning followed by a proline-rich sequence right in front of the G-domain.

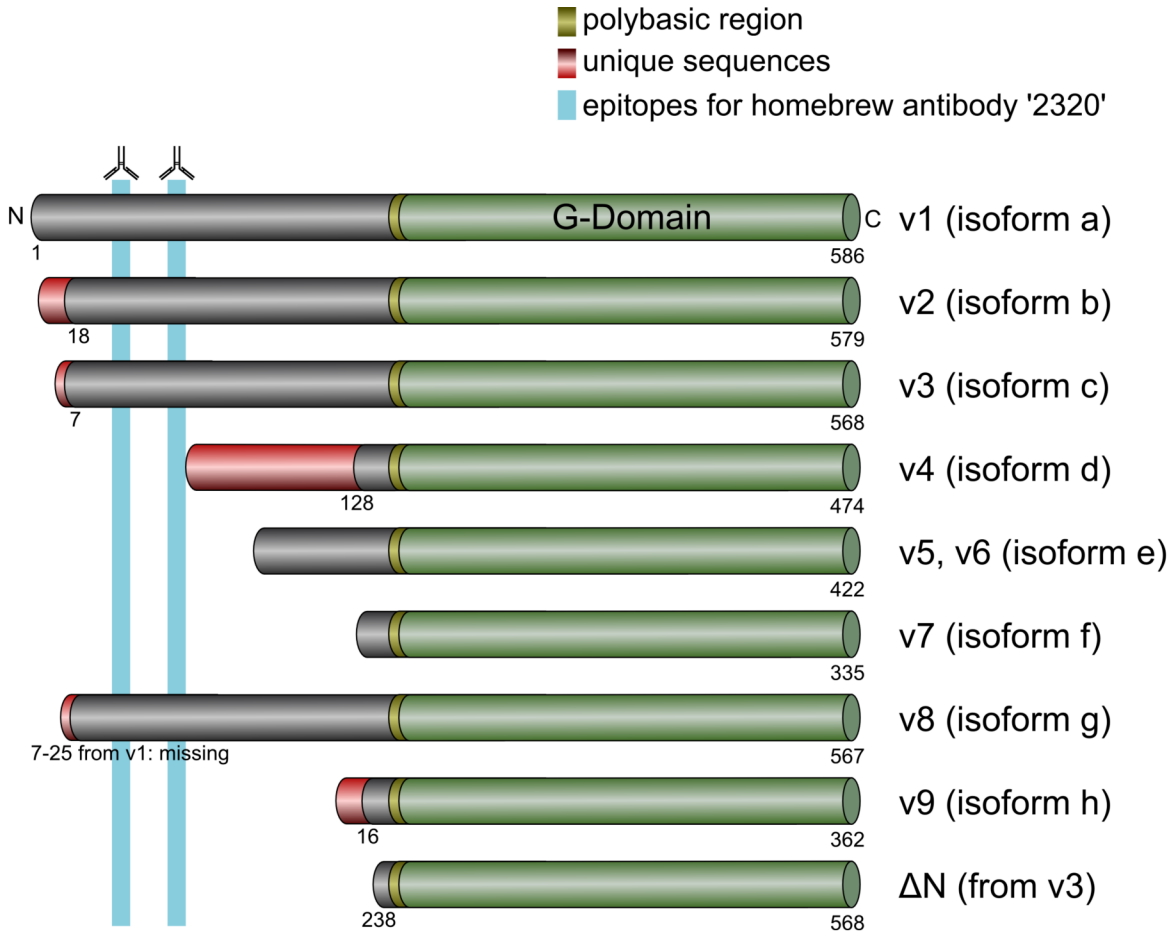


**Fig. 1.10: Domain structure of human SEPT9 isoforms.**

The numbers indicate the respective amino acid. Note: Overexpression experiments in this study were performed with SEPT9_v3 and a N-terminally truncated mutant (ΔN). Our polyclonal, home-brew antibody detects two stretches located in the N-terminus of the long isoforms 1, 2, 3 and 8 (blue).

SEPT9 is expressed ubiquitiously with the highest expression in lymphoid cell populations, but distinct tissues and cells generate selected sets of splice variants (Scott et al. 2005).

Up to now, two different SEPT9-containing septin complexes have been described. As already noted in chapter 1.2.1, SEPT9 forms part of the SEPT2/6/7/9-complex, where SEPT9 occupies the terminal positions and regulates filament elongation or abrogation (M. S. Kim et al. 2011). This function depends on the lenght of the transcript variant incorporated. Long transcripts show the ability to homo-dimerize, thereby allowing filament elongation, whereas the incorporation of short isoforms promote filament abrogation. The second known SEPT9-containing complex consists of SEPT7/9/11 and was identified in rat embryonic fibroblasts (REF52 cells) (Nagata et al. 2004). A possible implication and presence of this complex in other cell types remains elusive. Also, it remains unclear if this complex would also incorporate a member of the SEPT2 subgroup.

### *1.3.1 Biological role of SEPT9 in mammals*

During mitosis SEPT9 mediates the abscission of the midbody in the late telophase (Estey et al. 2010; Kechad et al. 2012). In line with this function, depletion of SEPT9 has been shown to cause cell cycle arrest and the accumulation of binucleated cells (Surka et al. 2002). Homozygous deletion of SEPT9 in mice results in embryonic lethality around day 10 of gestation (Füchtbauer et al. 2011). However, mice homozygous for a conditional allele develop normally. Murine embryonic fibroblasts (MEFs) prepared from these animals show cytokinetic defects such as abnormal, fragmented and multiple nuclei. Additionally, shorter SEPT7 fibers were detected in these cells, consistent with a role of SEPT9 in modulating SEPT2/6/7-filament stability (M. S. Kim et al. 2011). Conditional SEPT9 knock-out mice specific for T-cells revealed an implication in T-cell development and in the homeostasis of CD8+ T-cells (Lassen et al. 2013).

Several specific functions of SEPT9 are based on the interplay with cytoskeletal components such as actin (Kechad et al. 2012; Dolat et al. 2014). SEPT9 does not bind to actin directly, but rather takes part in actin remodeling events by associating with regulators of actin polymerisation. In epithelial cells, SEPT9 was shown to function as an actin-crosslinker during the maturation of focal adhesions, most likely by binding to the actin bundling protein α-actinin-1 (Dolat et al. 2014). In this context, knockdown of SEPT9 decreases migration, a phenotype that could also be observed in MEFs obtained

from SEPT9$^{cond/cond}$ mice (Füchtbauer et al. 2011). These findings strengthen a role of SEPT9 in cell motility.

Another actin-dependent role of septins was identified during receptor-mediated entry of the bacterium *Listeria*, where they contribute important functions during anti-bacterial autophagy (Mostowy & Cossart 2011c). This pathogen invades cells by hijacking the receptor tyrosine kinase c-Met, to which it binds and together with which it gets endocytosed in a clathrin-dependent manner (Veiga & Cossart 2005). Upon internalisation the pathogen is trapped in cage-like structures containing F-actin, SEPT2 and SEPT9. These septin cages assist the compartmentalization of the invading bacterium and target the pathogen for degradation through autophagy (Mostowy & Cossart 2011a).

As already mentioned, septin filament assembly was connected to the small GTPase Rho, a regulator of actin polymerization. In this context, SEPT9_v2 associates with two modulators of Rho activity, septin-associated Rho guanine nucleotide exchange factor (SA-RhoGEF) (Nagata & Inagaki 2005) and Rhotekin (Ito et al. 2005). These interactions indicate that SEPT9 regulates septin filament assembly through modulation of Rho activity.

SEPT9_v1 also localizes to the nuclear envelope, where it associates with the transcription factor hypoxia-inducible factor 1α (HIF1α) (Amir et al. 2006), a key regulator of the hypoxia response pathway (Gardner & Corn 2008). SEPT9_v1 is required for the association between HIF1α and importin-α to promote efficient nuclear translocation (Golan & Mabjeesh 2013). Furthermore, this transcript variant regulates the activity and stability of the MAPK c-Jun- N-terminal kinase (JNK), which is important in the cellular stress response, cell proliferation and cell survival (Gonzalez et al. 2009).

### *1.3.2 SEPT9 in disease*

Point mutations in SEPT9_v3 (R88W, S93F) or a duplication of the *sept9* gene were linked to symptoms of Hereditary Neuralgic Amyotrophy (HNA) (Kuhlenbäumer et al. 2005; Laccone et al. 2008; Landsverk et al. 2009; Ueda et al. 2010). This autosomal-dominant neuropathy is characterized by episodes of a sudden onset of severe pain in the shoulder girdle and/or the upper limb (Wang Ip et al. 2006). Additionally, patients suffer from amyotrophy in the affected regions. So far, it is unclear how the mutations contribute to the development of these symptoms, since only a few studies addressed their functional consequence. On the cellular level, septin filaments containing these SEPT9 mutations are

resistent to disruption initiated by Rho/Rhotekin signaling (Sudo et al. 2007). Moreover, SEPT9 binds and bundles microtubules and thereby promotes asymmetric neurite outgrowth. This function is inhibited by the point mutation R88W, which locates in the microtubule binding motif (Bai et al. 2013).

Furthermore, several cancer types were associated to misregulation of SEPT9 expression levels. These are described in detail in the next chapter.

## 1.4 Breast Cancer

SEPT9 is upregulated in a multitude of human carcinomas including head and neck, ovarian, endometrial, kidney, pancreatic and breast cancer (Scott et al. 2005; Peterson et al. 2011). Hypermethylated *sept9* DNA has been established as a potential biomarker for early diagnosis of colorectal cancer (Warren et al. 2011; Potter et al. 2014; Tóth et al. 2014). This hypermethylation presumably misregulates the expression levels of distinct SEPT9 transcript variants. In particular SEPT9_v1 is downregulated (Tóth et al. 2011).

A critical role of SEPT9 also emerges in breast cancer. This type of cancer can be subdivided into four groups according to gene expression profiles (Abramson et al. 2014). The first three groups are either positive for the estrogen receptor (ER), positive for the progesterone receptor (PR) or exhibit amplification of HER2. The fourth group, triple-negative breast cancer (TNBC), is a heterogenous group that summarizes approximately 15% of breast cancers, which are negative for the biomarkers of the residual groups. Recent studies observed an overexpression of the long isoforms SEPT9_v1 and _v3 in breast tumor samples and during breast tumorigenesis (Gonzalez et al. 2007; Connolly et al. 2011; Connolly et al. 2014). Despite the role of SEPT9 in cytokinesis, the overexpression of SEPT9 during tumorigenesis is presumably not simply a proliferation-associated phenomenon, since the SEPT9 expression level revealed no striking correlation with proliferation rates (Scott et al. 2005). A significant increase in SEPT9 copy number is observed in HER2-positive and ER-positive carcinomas, as well as in a TNBC subgroup termed basal-like (BL) carcinoma (Connolly et al. 2014). Of note, the latter one shows a strong association to misregulation of EGFR (Olayioye et al. 2000; Normanno et al. 2006). This receptor and its downstream pathways were shown to regulate epithelial-mesenchymal transition (EMT), a process by which cells undergo a morphological change from polarized epithelial cells to mesenchymal fibroblast-like cells. This switch promotes

tumor progression as it allows for cancer cell invasion (Radisky 2005; Thiery 2002).

Importantly, in several cases misregulation of EGFR trafficking pathways as observed in breast cancer were associated to overexpression of CIN85 (Nam et al. 2007; Samoylenko et al. 2012). Here, it modulates Cbl activity and contributes to cancer cell invasiveness.

In the last decades an increasing number of targeted therapies improved the survival rates for patients with ER-, PR- and HER2-positive cancer types significantly. However, systemic cytotoxic chemotherapy is still in widespread use for TNBC and survival rates are low. Better biomarkers to further characterization of the different subtypes and novel molecular targets for therapeutic strategies are needed to improve the treatment.

## 1.5 Aims of this study

During the past decade septin GTPases have received increasing attention, due to their implication in a multitude of biological processes. Their complexity and versatility is illustrated by their unique ability to form dozens of different heterooligomeric complexes. Interestingly, in particular membrane trafficking events have been shown to be regulated by septins. In this study, we set out to explore a possible connection between septin GTPases and trafficking of receptor tyrosine kinases. We focus on an interaction between SEPT9 and the adaptor protein CIN85 and investigate the physiological role of this complex. We further address the question, whether SEPT9 functions in its monomeric form or is rather incorporated in a heterooligomeric septin complex. In addition, we apply an unbiased approach to identify novel interaction partners of SEPT9 to expand the cellular processes this isoform might be involved in.

# 2 Material and Methods

## 2.1 Materials

### *2.1.1 Chemicals and disposables*

The supplier for reagents used in specific applications is mentioned in the respective methods section. Disposables were obtained from Sarstedt, Greiner, and Whatman.

**Table 2.1: Chemicals**

| Chemical | Supplier |
|---|---|
| Acidic Acid | Carl Roth GmbH |
| Agarose | Biozym |
| Coffee | Eduscho |
| DAPI | Sigma-Aldrich |
| DMSO | Sigma-Aldrich and Carl Roth GmbH |
| DNA loading dye, 6x | Fermentas |
| ECL Western Blotting Detection Reagent | GE Healthcare |
| EGF, human recombinant | Peprotech |
| Ethanol | Carl Roth GmbH |
| Ethidium bromide | Carl Roth GmbH |
| GeneRuler 1 kb ladder and 50 bp ladder | Fermentas |
| HEPES | Carl Roth GmbH |
| Isopropanol | Carl Roth GmbH |
| Lipofectamine 2000 Reagent | Invitrogen |
| Methanol | Carl Roth GmbH |
| Nitrocellulose Transfer Membrane PROTRAN 0.2µm | Whatman |
| Nucleotides for PCR cloning | Invitrogen |
| Oligofectamine Reagent | Invitrogen |
| Phosphatase Inhibitor Cocktail 2 + 3 | Sigma-Aldrich |
| Prestained Molecular Weight Marker for SDS gels | Page Ruler, Fermentas |
| Protease Inhibitor Cocktail | Sigma-Aldrich |
| Protein A/G PLUS-Agarose Beads | Santa Cruz Biotechnology |
| SDS ultra pure | Carl Roth GmbH |
| Tris | Carl Roth GmbH |
| Triton-X-100 | Sigma-Aldrich |

### 2.1.2 Solutions and media

All solutions and buffers were prepared with ultrapure water (resistance of 18 MΩ, ddH2O) and pH was adjusted using NaOH or HCl. Buffers for specific protocols are described in the respective methods section.

**Table 2.2: Buffers and solutions used for molecular biology experiments**

| **Molecular Biology** | |
|---|---|
| 10x TBE | 890 mM Tris<br>890 mM Boric acid<br>20 mM EDTA |
| LB Medium | 1.0 % (w/v) yeast extract<br>0.5 % (w/v) Trypton<br>0.5 % (w/v) NaCl<br>pH 7.4 |
| 2xYT medium | 1.0 % (w/v) yeast extract<br>1.6 % (w/v) Trypton<br>0.5 % (w/v) NaCl<br>pH 7.4 |
| Ampicillin stock 500x | 50 mg/ml in ddH2O<br>sterile filtered |
| Kanamycin stock 200x | 10 mg/ml in ddH2O<br>sterile filtered |
| Ethidium bromide stock 3000x | 10 mg/ml in ddH2O |
| Glycerol stock buffer | 10 mM Tris pH 8<br>50 mM $MgSO_4$<br>50% glycerol<br>autoclaved |

**Table 2.3: Buffers and solutions for biochemistry experiments**

| **Biochemistry** | |
|---|---|
| 10x TBS<br>200 mM Tris<br>1.4 M NaCl<br>pH 7.6 | 10x SDS running buffer<br>246 mM Tris<br>1.92 M Glycine<br>10% SDS |
| 4x SDS stacking gel buffer<br>0.4% SDS<br>0.5 M Tris<br>pH 6.8 | 4x SDS separating gel buffer<br>0.4% SDS<br>1.5 M Tris<br>pH 8.8 |
| Ponceau stain<br>0,3% Ponceau S<br>3% Acetic acid | Ponceau destain<br>1% Acetic acid |

**Biochemistry**

Lysis buffer A
20 mM Hepes pH 7.4
100 mM KCl
2 mM $MgCl_2$
1% Triton X-100
*add freshly:*
0.3% protease inhibitor cocktail
1 mM PMSF

6x SDS-PAGE sample buffer
375 mM Tris
60 % glycerol (v/v)
30 % β-mercaptoethanol (v/v)
18 % SDS (w/v)
Bromophenol blue (to deep blue color)
pH 6.8

Coomassie stain
0.5 g/l Coomassie G250
10 % Acetic acid
25 % Methanol

Coomassie destain
10 % Acetic acid
25 % Methanol

Immunoblot blocking solution
3 % milk powder
in 1x TBS

Immunoblot antibody dilution solution
3 % Bovine serum albumin
0.02 % $NaN_3$
1x TBS

Immunoblot stripping buffer
25 mM Glycin
1% SDS (w/v)
pH 2.2

2x Bradford reagent
140 g/l Coomassie G250
200 ml 85 % $H_3PO_4$
100 ml Ethanol
(filtered)

TSM buffer
100 mM Tris pH 9.5
100 mM NaCl
5 mM $MgCl_2$

NBT stock solution
50 mg/ml nitro blue tetrazolium
in 70% DMF

BCIP stock solution
20mg/ml 5-bromo-4-chloro-3-indolyl phosphate, p-toluidine salt

AP developing solution
165 µg/ml BCIP
305 µg/ml NBT
in TSM buffer

**Table 2.4: Buffers and solutions used for cell biology experiments**

**Cell biology**

10× PBS
1.37 M NaCl
27 mM KCl
43 mM $Na_2HPO_4$
14 mM $NaH_2PO_4$
pH 7.4
autoclaved

DMEM
Dulbecco's modified eagles medium
4.5 g/l or 1 g/l glucose
*Additives:*
10 % fetal calf serum (heat-inactivated)
100 U/ml Penicillin
0.1 mg/ml Streptomycin
for 1 g/l glucose: 2mM L-glutamin

PFA fixing solution
4 % PFA
4 % Sucrose
1× PBS
pH 7.4

1 M $Na_xH_xPO_4$ stock solution
1 M $Na_2HPO_4$
1 M $NaH_2PO_4$
titrate $Na_2HPO_4$ (~60 ml) to $NaH_2PO_4$ (~400ml)
until pH = 7.4

**Cell biology**

PBS + $Mg^{2+}$
1× PBS + 10 mM $MgCl_2$

Trypsin / EDTA
200 mg/ml Versene (EDTA)
170 000 U trypsin/ml

IF wash buffer w. detergent
0.1 % Triton-X-100
150 mM NaCl
3.3 mM $Na_xH_xPO_4$
pH 7.4

IF wash buffer w/o detergent
120 mM $Na_xH_xPO_4$
pH 7.4

Goat serum dilution buffer (GSDB)
3.3 % goat serum
0.1 % Triton-X-100
150 mM NaCl
6.6 mM $Na_xH_xPO_4$, pH 7.4

### 2.1.3 DNA Oligonucleotides

Synthetic DNA oligonucleotides used as primers for polymerase chain reactions (PCRs) were purchased from MWG-Biotech or BioTez Berlin-Buch GmbH, respectively, as a lyophilized powder and dissolved in $ddH_2O$ to a concentration of 100 µM.

### 2.1.4 Small interfering RNA oligonucleotides

Synthetic RNA oligonucleotides for RNA interference were obtained from MWG-Biotech as a lyophilized powder and dissolved to a concentration of 100 µM in RNAse-free siMAX buffer supplied by the manufacturer. All small interfering RNA (siRNA) sequences used in this study were synthesized with a 3'-TT-overhang and are listed in the following table and were directed against the human mRNA sequence. Please note that for the depletion of SEPT9, siRNA #1 was used in all experiments except where explicitly stated otherwise.

**Table 2.5: siRNAs used in this study**

| target mRNA | siRNA sequence (5' - 3') |
|---|---|
| SEPT9 #1 | GGA GGA GGU CAA CAU CAA C |
| SEPT9 #2 | AGA CCA UCG AGA UCA AGU C |
| CIN85 | GGC ACA GAA UGA UGA UGA A |
| SEPT7 | CUU GCA GCU GUG ACU UAU A |
| control | AUC GUU GAC UUA CAA GAG A |

### 2.1.5 Synthetic peptides

Peptides derived from SEPT9 were synthesized from Dr. R. Volkmer at the Charité, Berlin.

**Table 2.6: synthetic peptides**

| peptide | aa sequence (N- to C-terminus) | MW (g/mol) |
|---|---|---|
| SEPT9 PxxxPR | $NH_2$ -EVLGHKTPEPA**PR**RTE-COOH | 1817 |
| SEPT9 PxxxAA | $NH_2$ -EVLGHKTPEPA**AA**RTE-COOH | 1706 |

### 2.1.6 Bacterial strains

For cloning and amplification of plasmid DNA the E. coli TOP10 strain (Invitrogen) was used. It features high transformation efficiency and is suited for plasmid propagation.

Recombinant proteins were expressed in the E. coli BL21-Codon Plus strain (Stratagene) that is designed for high-level expression of proteins. This strain contains multiple copies of rare tRNA genes that can limit the translation efficiency of heterologous proteins in E. coli.

### 2.1.7 Eukaryotic cell lines

For all cell biological experiments, HeLa cells (clone HeLa M) were used as a model system of mammalian cells that were derived from a cervix carcinoma in 1951. A small subset of experiments was also carried out in A431 cells (epidermoid carcinoma).

### 2.1.8 Plasmids

An overview of the general plasmid backbones used here is provided in Table 2.7. The '-MK' plasmids are based on pcDNA3.1(+) with the sequence between the NdeI (within CMV promoter) and EcoRV (beginning of polylinker) sites having been exchanged for the corresponding sequence from pcHA2. The respective tag is placed between the KpnI and BamHI sites. Table 2.8 provides an overview of all expression plasmids used in this study. cDNA clones were used for cloning of human SEPT9_v3 (BC021102; isoform c) and human CIN85_v1 (BC015806).

**Table 2.7: expression vectors**

| plasmid | expr. system | tag (pos.) | resistance | source |
|---|---|---|---|---|
| pGEX 4T-1 | prokaryotic | GST (N) | Amp | Amersham - Pharmacia |
| pGEX 5T-2 | prokaryotic | GST (N) | Amp | Amersham - Pharmacia |
| pET-28a(+) | prokaryotic | $His_6$ (N) | Kan | Novagen |
| pcDNA3.1 (+) | eukaryotic | - | Amp | Invitrogen |
| pcHA-MK | eukaryotic | HA (N) | Amp | custom made from pcDNA3.1 (+) |
| pcmRFP-MK | eukaryotic | mRFP (N) | Amp | custom made from pcDNA3.1 (+) |

**Table 2.8: Expression plasmids.** *FL* = full-length, *wt* = wild-type.

| construct | backbone | amino acids | mutation | comment |
|---|---|---|---|---|
| GST-CIN85 SH3 A | pGEX 4T-1 | 1-69 | wt | used for Pulldown exp. |
| GST-CIN85 SH3 A | pGEX 4T-1 | 1-58 | wt | used for NMR exp. |
| GST-CIN85 SH3 B | pGEX 4T-1 | 96-163 | wt | |
| GST-CIN85 SH3 C | pGEX 4T-1 | 256-333 | wt | |
| GST-CIN85 SH3 A-C | pGEX 4T-1 | 1-333 | wt | |
| GST-CIN85 SH3 A-C | pET-28a(+) | 1-333 | wt | |
| GST-CIN85 CT | pGEX 4T-1 | 334-end | wt | C-terminus incl. Pro-rich domain |
| mRFP-CIN85 FL | pcmRFP-MK | FL | wt | |
| His-EGFP | pET-28a(+) | | wt | used as negative control |
| GST-SEPT9 FL | pGEX 5X-2 | FL | wt | |
| GST-SEPT9 FL | pGEX 5X-2 | FL | PR26/27AA | |
| GST-SEPT9 FL | pGEX 5X-2 | FL | PR129/30AA | |
| GST-SEPT9 FL | pGEX 5X-2 | FL | PR219/220AA | |
| GST-SEPT9 NT | pGEX 5X-2 | 1-220 | wt | |
| GST-SEPT9 ΔN | pGEX 5X-2 | 238-end | wt | |
| SEPT9 | pcDNA3.1 | FL | si-resistent against #1 and #2 | |
| HA-SEPT9 ΔN | pcHA-MK | 238-end | wt | |
| EGFP-Rab5 Q79L | pcDNA3 | FL | Q79L | GTPase defective mutant |
| Rab11-GFP | | FL | wt | |
| EGFP-Vps4A | | FL | E228Q | Gift from H. G. Kräusslich |

### 2.1.9 Enzymes

Restriction endonucleases (RENs), Vent polymerase, alkaline phosphatase (AP) and calf intestinal phosphatase (CIP) were purchased from New England Biolabs/Thermo Scientic. Taq DNA polymerase and T4 DNA ligase were from Fermentas.

### 2.1.10 Antibodies

All commercially available primary antibodies used in this study are listed in the following tables. Antibodies were stored at 4°C or -20°C according to the recommendation by the company. For storage at -20°C glycerol was added to 50%, if not already present.

**Table 2.9: List of antibodies used for immunofluorescence experiments**

| antigen | clone | host | company | catalog # | Dilution for IF |
|---|---|---|---|---|---|
| β1-Integrin | | mouse | EMD Millipore | MAB1981 | |
| EEA1 | | mouse | BD Transduction | 610456 | |
| EGFR | R-1 | mouse | Santa Cruz | sc-101 | 1:200 |
| HA | HA.11 | mouse | Babco/Convance | | 1:400 |
| LAMP-1 | | mouse | BD Pharmingen | 555801 | |
| Paxillin | | mouse | BD Transduction | 611436 | |

**Table 2.10: List of antibodies used for biochemistry experiments. WB = Western Blot**

| antigen | clone | host | company | catalog # |
|---|---|---|---|---|
| β-Actin | AC-15 | mouse | Sigma-Aldrich | A1987 |
| Clathrin heavy chain | TD-1 | mouse | homebrew; hybridoma cell line | - |
| Dynamin 1/2 | 41 | mouse | BD Bioscience | 610245 |
| c-Cbl | 17 | mouse | BD Transduction | 610441 |
| EGFR | | rabbit | Cell signaling | 4267 |
| Tubulin | B-5-1-2 | mouse | Sigma-Aldrich | T5168 |
| Ubiquitin | P4D1 | mouse | Cell signaling | 3936 |
| SEPT6 | | rabbit | Sigma-Aldrich | HPA005665 |
| SEPT2 | | rabbit | Sigma-Aldrich | HPA018481 |
| Grb-2 | 81 | mouse | BD Transduction | 610112 |
| AKT1/2/3 | | rabbit | Cell signaling | 9272 |
| Phospho-AKT (S473) | D9E | rabbit | Cell signaling | 4060 |
| ERK1/2 | | rabbit | Abcam | ab17942 |
| phospho-ERK1/2 | MAPK-YT | mouse | Sigma-Aldrich | M8159 |
| → recognizes diphosphorylated ERK1 (T202 + Y204) and ERK2 (T185 + Y187) | | | | |

| antigen | clone | host | company | catalog # | Dilution for WB |
|---|---|---|---|---|---|
| $His_6$ | | mouse | EMD Millipore | 70796-3 | |
| CIN85 | 179.1.E1 | mouse | Upstate | 05-731 | 1:250 - 1:500 |
| SEPT9 | 2C6 | mouse | Abnova | H00010801-M01 | 1:250 - 1:500 |

**Table 2.11: homebrew antibodies generated for this study**

| antigen | No. | injected epitope | affinity-purified on | Appli-cation |
|---|---|---|---|---|
| SEPT9 | 2320 | NH2 -CSTQKFQDLGVKNSEP- CONH2<br>NH2 -CTELSIDISSKQVEN- CONH2 | GST-SEPT9_v3 (aa1-220) | WB<br>IF |
| CIN85 | 6665 | $His_6$- CIN85 (aa429-end) | GST-CIN85 (aa334-end) | IF |
| CIN85 | 2318 | NH2 -CLQMEVNDIKKALQSK- COOH<br>NH2 -CKQLLSELDEEKKIRL- CONH2 | GST-CIN85 (aa 600-end) | IP |
| CIN85 | 2319 | NH2 -CLQMEVNDIKKALQSK- COOH<br>NH2 -CKQLLSELDEEKKIRL- CONH2 | GST-CIN85 (aa 600-end) | IP |
| SEPT7 | | NH2 -CYEFPETDDEEENKLV- COOH | Injected peptide | WB |

Polyclonal antibodies against SEPT7, SEPT9 and CIN85 were raised in rabbits and are summarized in Table 2.11. All antisera were affinity-purified and tested for specificity. A detailed protocol for affinity-purification is described in chapter 2.3.12. The epitope for the SEPT9 antibody was designed such that the resulting antibody detects all long isoforms of SEPT9 (v1, v2, v3 and v8) that contain the PR-motif located at position 129/130 of isoform v3. This antibody was used throughout the whole study for immunofluorescence and immunoblotting except for the coimmunoprecipitation experiment in Fig. 3.6 B. Here, the SEPT9 antibody from Abnova was used. To allow for parallel detection of endogenous CIN85 and SEPT9 our SEPT9-specific antibody '2320' was directly coupled to Atto565 using the Lightning LinkTM Rapid Conjugation System (Innova Biosciences, #351-0010) according to the manufacturer's instructions.

All fluorescent secondary antibodies modified with AlexaFluor dyes were obtained from Molecular Probes (Invitrogen) and were used at a dilution of 1:200. Horse radish peroxidase- (HRP) and alkaline phosphatase (AP)-coupled antibodies were obtained from Dianova and were used at a dilution of 1:5000 – 1:2500.

### 2.1.11 Software and internet resources

| | |
|---|---|
| Fiji | - microscopy analysis |
| Volocity | - microscopy analysis |
| NCBI (www.ncbi.nlm.nih.gov) | - literature research |
| | - DNA and protein sequences |
| | - BLAST |
| BioEdit | - handling of sequencing data |
| CloneManager | - DNA and protein sequence handling |
| | - alignments |
| Expasy (www.expasy.org) | - protein parameters |
| Minimotif Miner (http://mnm.engr.uconn.edu/MNM/) | |
| | - identification of putative binding motif |

## 2.2 Molecular biological methods

### *2.2.1 Primers for cloning*

Primers were designed such that the salt-adjusted melting temperature, calculated using the MWG online tool, lies at approximately 60°C and that, if possible, the last nucleotide is a G or C.

### *2.2.2 Polymerase chain reaction and site-directed mutagenesis*

The polymerase chain reaction (PCR) allows the exponential amplification of a specific DNA sequence from a given template (Saiki et al. 1988). In a repeated cycle of template DNA denaturation, annealing of specific oligonucleotides for priming of DNA synthesis and elongation of DNA strands, the newly synthesized DNA serves as template in the following cycles and thus leads to an exponential DNA amplification. PCRs were used for amplification of protein coding sequences from plasmid DNA for subsequent cloning into expression vectors and for screening of E. coli colonies after transformation of ligation reactions (colony-PCR).

Standard PCRs were performed in a volume of 50 µl containing 1x polymerase reaction buffer, 200 µM of each dNTP, 10 µM of each primer, 10-50 ng of plasmid DNA and 2 units of Vent polymerase. The following program was then run in a thermocycler:

| | | |
|---|---|---|
| Initial Denaturation | 95°C | 1 min |
| Denaturation | 95°C | 30 sec |
| Primer annealing | 60°C | 30 sec |
| Elongation | 72°C | 1 min/kbp |
| Final elongation | 72°C | 5 min |
| | 4°C | ∞ |

Steps 2 to 4 were repeated in 30 cycles.

For the generation of point mutations, a mutagenic reverse and forward primer annealing to the region containing the targeted nucleotides were used in combination with a forward and a reverse primer that anneal to the start and end of the cDNA of interest, respectively, so that two individual amplificates would result, a 5'- and a 3'-fragment. The mutagenic primers were designed such that the 5'- and 3'-fragments would share an overlapping sequence (that contains the mutated nucleotides) and that this overlap has a

salt-adjusted melting temperature of 60°C. These PCRs were done with only 20 cycles. The 5'- and 3'-fragments were then fused together by PCR using equimolar amounts of both fragments, the non-mutagenic outer forward and reverse primers used to generate these fragments in the first place, and Vent DNA polymerase. Initial mutagenic PCRs and the Fusion PCR were always carried out in quick succession and UV-exposure of 5'- and 3'-fragments was minimalized or, in difficult cases, avoided entirely.

### *2.2.3 Preparative and analytical agarose gel electrophoresis*

Agarose was dissolved in 1× TBE buffer to a concentration of 0.7 % to 2 % (w/v) by heating. The gel was cast and covered with 1× TBE buffer, DNA samples in 1× DNA loading dye were applied and separated at 90-110 V for 20 to 45 min. The gel was stained in a water bath containing 3 µg/ml ethidium bromide (EtBr) for at least 15 min and DNA was visualized with UV light. In case DNA was destined for further preparative use, UV-exposure was reduced to an absolute minimum.

### *2.2.4 Purification of DNA from agarose gels and PCRs*

For purification of DNA from agarose gels and restriction digests of PCR products the respective kits from Machery-Nagel were used according to the manufacturer's instructions. The DNA band of interest was excised from an agarose gel and dissolved in binding buffer, whereas binding buffer was directly added to restriction digests. The DNA was then reversibly bound to a silica membrane and washed with non-aqueous washing buffer. Pure DNA was eluted using 50 µl of water.

### *2.2.5 Restriction digests*

Restriction digests were performed using Thermo Scientific FastDigest enzymes. 200 ng (restriction analysis) or 2 µg (preparative restriction digests) of vector DNA were incubated in a total volume of 50 µl with 1 µl of FastDigest enzyme per µg DNA for 30 to 60 min at 37°C. Digested vector DNA was separated on agarose gels and purified. PCR products were digested in a total volume of 100 µl with 1.5 µl FastDigest enzyme for 3-4 h at 37°C. Digested PCR product was purified with a PCR purification kit from Machery-Nagel.

### 2.2.6 Dephosphorylation of vector DNA

Linearized vector DNA was dephosphorylated by adding 10 units of CIP directly to the completed restriction digest reaction and incubating 3 min at 37°C. CIP hydrolyzes the 5'-phosphates from linear DNA molecules, thereby preventing spontaneous recircularization of linearized vectors and reducing the number of false positive colonies after transformation of ligation reactions.

### 2.2.7 Ligation of DNA fragments into linearized vectors

The concentration of the DNA fragment (insert) and the linearized vector were compared on an agarose gel. Assuming a linear increase of ethidium bromide fluorescence with the size of the DNA molecule, the insert was used in a 5- to 10-fold molar excess over vector DNA. Ligation reactions were performed in a volume of 10 µl containing 1× ligase buffer and 1 unit of T4 DNA ligase. Reactions were incubated at 16°C for 6 h - overnight and 5 µl of a ligation reaction were transformed into chemically competent E. coli.

### 2.2.8 Preparation of chemically competent E. coli

For preparation of chemically competent bacteria, a 50 ml LB culture of the E. coli strain of interest was started from a fresh plate or from a glycerol stock validated to give highly competent bacteria. This culture was grown at 37°C and 250 rpm until the optical density at 600 nm (OD 600) reached 0.4. Bacteria were harvested in sterile centrifuge tubes by centrifuging for 10 min at 4000 rpm and 4°C. The pellet was resuspended in 10 ml ice-cold and sterile 0.1 M $CaCl_2$ solution and incubated on ice for at least 15 to 30 min. Bacteria were then sedimented for 10 min at 4000 rpm and 4°C and the pellet was resuspended in 2 ml 0.1 M $CaCl_2$ solution. Glycerol was added to a final concentration of 10 % and 50 µl aliquots were prepared, snap-frozen in liquid nitrogen and stored at -80°C.

### 2.2.9 Transformation of chemically competent E. coli

Chemically competent E. coli of the TOP10 strain were transformed following a heat shock protocol. 50 µl of $CaCl_2$ chemically competent cells were thawed on ice, DNA was added (5 µl of ligation reactions, 5 ng of plasmid DNA) and cells were left on ice for 30 min. The heat shock was carried out by incubating 90 sec at 42°C followed by 2 min on ice. 500 µl of LB medium without antibiotics was added. E. coli were allowed to recover 30-60 min at 37°C. Before spreading, the bacteria were pelleted by briefly accelerating to

maximal speed in a microcentrifuge, resuspended in about 150 µl of LB medium and then transferred to a LB agar plate containing the selective antibiotic for selection. For bacteria transformed with plasmid DNA, only 200 µl of the bacteria in 500 µl LB were plated.

### *2.2.10 Glycerol stocks*

For long-term storage of E. coli clones containing a desired construct 750 µl of an overnight culture were mixed with 750 µl of glycerol stock buffer and stored at -80°C.

### *2.2.11 Over night cultures of E. coli*

Clones found to be positive by colony-PCR screening (or colonies resulting from the transformation of plasmid DNA) or cells from a glycerol stock were picked with a sterile pipette tip and grown overnight at 37°C shaking at 200 rpm in 5 ml (for "mini-prep") or 100 ml (for "midi-prep") LB-medium containing the appropriate antibiotic.

### *2.2.12 Purification of plasmid DNA from E. coli cultures*

Small scale plasmid DNA preparations (mini-prep) from 6 ml of E. coli overnight cultures were carried out using the Nucleospin Plasmid kit from Macherey-Nagel according to the manufacturer's instructions. Following alkaline lysis of the cells, precipitated genomic DNA and protein are removed by centrifugation. The plasmid DNA is then bound to a silica membrane and washed to remove contaminants. DNA was eluted in 50 µl of water. For larger amounts and a higher purity, plasmid DNA was purified from 100 ml E. coli overnight cultures using the Nucleobond Midi kit from Macherey-Nagel according to the manufacturer's instructions. With this system, plasmid DNA is first purified on a silica membrane of higher DNA binding capacity and then precipitated using isopropanol. The precipitate is washed with ethanol and finally resuspended to a concentration of 1 mg/ml in water.

### *2.2.13 UV spectroscopy for determining nucleic acid concentrations*

The concentration of DNA preparations was determined using a photometer. 1-3 µl DNA were diluted in a total of 90 µl ddH2O in a UV-transmitting plastic cuvette. The extinction at 260 nm ($E_{260nm}$) was measured and the concentration was calculated according to Lambert-Beer's law, assuming an extinction coefficient $\varepsilon_{dsDNA}$ of 50 ml/µg x cm (d: lightpath in the solution = 1 cm):

$$c = \frac{E_{260\,nm}}{d \cdot \varepsilon_{dsDNA}} \cdot dilution = \frac{E_{260\,nm}}{1\,cm \cdot 50 \frac{ml}{\mu g \cdot cm}} \cdot 50$$

The quality of the DNA preparation was judged satisfactory if the coefficient of extinction at 260 nm (absorption maximum of dsDNA) over 280 nm (strong protein absorption based on aromatic residues) was between 1.8 and 2.2.

The concentration of RNA preparations was determined identically, assuming an extinction coefficient $\varepsilon_{RNA}$ of 40 ml/µg x cm.

### *2.2.14 Sequencing*

0.5 - 1 µg of purified plasmid DNA (mini-prep) were air dried at 60°C and sent for sequencing (Sanger method) to MWG Biotech or BioTez Berlin-Buch. Sequencing results were analyzed with the open source software CloneManager and BioEdit.

## 2.3 Biochemical methods

### *2.3.1 Protein determination (Bradford assay)*

For determining the protein concentration of cell extracts and purified protein solutions, 1µl of the sample was diluted in 500 µl water and 500 µl 2× Bradford reagent was added. The mixture was then incubated 5 min at room temperature and $OD_{595nm}$ was determined with a photometer blanked against 1× Bradford reagent and 1µl buffer. Only extinction values between 0.1 and 0.5 were considered reliable. The protein concentration was calculated from a standard curve covering the range of 1 µg to 10 µg BSA.

### *2.3.2 SDS polyacrylamide gel electrophoresis (SDS-PAGE)*

Sodium dodecysulfate (SDS) polyacrylamide gel elctrophoresis (PAGE) is a method for separating proteins based on their molecular mass. SDS ($H_3C$-$(CH_2)_{11}$-$SO_4^{2-}$ complexed with $Na^+$) is an ionic detergent that disrupts the non-covalent interactions stabilizing the protein's secondary and tertiary structure. It associates with the protein in a ratio of about 1 SDS molecule per 2 amino acids and thereby completely masks the protein's native charge with its triply negatively charged head group and generates a constant protein mass to charge ratio. Therefore, proteins are separated depending on their molecular weight only.

The polyacrylamide gel is formed by radical polymerization of an acrylamide / N, N'-methylenebisacrylamide (AA/BA) mixture. The decay of the radical initiator ammonium peroxodisulfate (APS) is catalyzed by tetraethylenediamine (TEMED), producing $SO^{4-}$- radicals which then attack the carbon-carbon double bond in acrylamide molecules and initiate the formation of a chain. N, N'-methylenebisacrylamide serves as a linker of polyacrylamide chains and thus generates a gel-like network.

SDS-PAGEs were carried out according to Laemmli (Laemmli 1970), using Tris-glycine based buffers and a 3 % stacking and 8 % to 12 % separating gel. In the pH 6.8 stacking gel, glycine molecules are only partly ionized and migrate slowly. Together with $Cl^-$ ions at the front, glycine leads to a modulation of electric field intensity (stronger at the rear, weaker at the front) over the protein stack and thus allows isotachophoresis: all protein molecules of one species assemble at the same position in the protein stack, finally resulting in sharp protein bands. The effect of glycine as the slow terminating ion is lost upon entry into the pH 8.8 separating gel and proteins are separated according to their mass.

SDS-PAGEs were run at 15 to 20 mA per gel. After electrophoresis, gels were either processed for immunoblotting or proteins were visualized by staining with Coomassie. Coomassie stain was shortly heated in the microwave and the gel was stained for 10 min. Background staining was removed by repeatedly washing with Coomassie destain. Protein gels for MS/MS analysis were stained and destained at RT using fresh and filtered buffers.

### *2.3.3 Immunoblotting*

Immunoblotting or "Western Blotting" is a highly sensitive method for detecting specific proteins after separation by SDS-PAGE. The proteins, still associated with SDS and thus negatively charged, are transferred from the gel onto a nitrocellulose membrane in an electrical field by semi-dry electroblotting using the Fastblot device from Biometra. Therefore, Whatman filter and membrane were pre-wetted in blotting buffer and assembled on a semi-dry blotting device in the order Whatman / membrane / gel / Whatman (bottom to top). Electrotransfer was performed at 1 mA/ $cm^2$ (50 mA per gel).

The transferred protein was reversibly stained with Ponceau stain for 5 min at room temperature and destained with 1% acetic acid. After washing once in TBS, the highly protein-adsorptive membrane was blocked against unspecific antibody binding using 3% milk powder in TBS for one hour at room temperature. A specific primary antibody diluted in antibody dilution solution was then incubated on the membrane for 2 hours at room temperature or, preferably, overnight at 4°C. The antibody was recycled and the membrane was washed 3 times for 10 min at room temperature in TBS. Secondary HRP-coupled antibodies that specifically recognize immunoglobulins of the species the first antibody was raised in were used to detect the protein of interest. The secondary antibody was incubated on the membrane diluted 1:5,000 – 1:2,500 in 3 % milk powder in TBS for one hour at room temperature. Unspecific secondary antibody binding was reduced by washing 3 times for 10 min at room temperature in TBS. Signal was detected by adding enhanced chemiluminescence reagent (ECL reagent, Amersham Biosciences) to the membrane and exposing to an X-ray film. The ECL reagent serves as a substrate for HRP that catalyzes a luminescent reaction of luminol with hydrogen peroxide. The produced chemiluminescent signal is then used to blacken a X-Ray film (Hyperfilm ECL 18 x 24cm from GE Healthcare).

### 2.3.4 Densitometric Analysis of Western Blots

Quantification from Western Blots was performed using the Western Blot plugin from ImageJ/Fiji from black&white scans (600 dpi).

### 2.3.5 Preparation of protein extracts from eukaryotic cells

Total protein extracts from eukaryotic cells were prepared using lysis buffer A. It contains 1% of the non-ionic detergent TritonX-100, which disrupts membranes and solubilizes integral and membrane associated proteins. Cells grown on plastic dishes were transferred to ice and washed two times with ice-cold PBS. PBS was aspirated completely and lysis buffer A was added (100 µl for a confluent 6-well-dish). Cells were harvested using a cell scraper, vortexed and lysed for 30 min on ice. Lysates were clarified by centrifuging at 13,000 rpm and 4°C in a tabletop microcentrifuge. If extracts were to be used for further binding studies, aggregated protein was removed by ultracentrifugation at 65,000 rpm and 4°C in TLA-110 or TLA-100.2 rotors.

### 2.3.6 Immunoprecipitation

3 - 10 µg of antibody were coupled to 30 - 50 µl washed Protein A/G PLUS Agarose Beads (Santa Cruz) in lysis buffer A over night at 4°C under rotating agitation. On the next day, tissue extracts were prepared as described above and, if several extracts were compared, adjusted to the same concentration. A small aliquot of the lysates was saved as an input control and kept on ice during incubation times. Beads were washed 1x with lysis buffer A and incubated with extracts for 1-4 h at 4° C under rotating agitation. Beads were washed three times with 1 ml lysis buffer A and once with 1 ml lysis buffer A without detergent. Bound proteins were eluted by adding 20 µl 2x SDS sample buffer and boiling for 3 min at 95°C. Input samples were boiled in parallel with 2x SDS sample buffer. Eluates were transfered to new Eppendorf tubes using a Hamilton pipette and 1x SDS sample buffer ad. 90 µl was added to the beads. Leftover proteins were eluted again by boiling for 3 min and the eluates were pooled. Samples were stored at -20°C or directly analyzed by SDS-PAGE and immunoblotting.

### 2.3.7 Expression of recombinant proteins in E. coli

Overnight cultures of the E. coli BL21 strain transformed with pET-28a or pGEX expression constructs were diluted 1:10 to 500 ml 2x YT medium containing the

appropriate antibiotic and grown to an $OD_{600}$ of 0.7 to 0.8. At this point, cultures enter the log phase and rapidly proliferate. Expression of recombinant proteins was then induced by adding isopropyl thiogalactoside (IPTG) to a concentration of 0.5 mM. Induced cultures were incubated for 3 hours at 30°C shaking at 200 rpm. Alternatively, expression was carried out at 16°C overnight. Bacteria were harvested by centrifugation at 4000x g for 15 min. The pellet was resuspended in 30 ml PBS, splitted to 3 aliquots and stored -20°C.

### *2.3.8 Purification of GST- and $His_6$ -fusion proteins expressed in E. coli*

In order to obtain purified recombinant proteins for in vitro experiments, Glutathione S-Transferase- (GST, a 27 kDa protein) or 6x Histidine-tagged ($His_6$) proteins are bound to an affinity gel. Using the so-called batch protocol, GST can be bound to glutathione immobilized on beads, whereas $His_6$-tags bind to Nickel ions ($Ni^{2+}$) that in turn are linked to agarose beads via the chelator nitrilotriacetic acid (Ni-NTA beads). All steps were performed on ice. E. coli BL 21 pellets were thawed and diluted to 30 ml with washing buffer (PBS for GST-tagged proteins and TBS for $His_6$-tagged proteins). 125 units benzonase (a DNase/RNase), a spatula tip of lysozyme (a bacterial cell wall degrading enzyme from chicken egg white) and PMSF to 1 mM were added. After incubating for 15 min, cells were sonicated two times for one minute (50% duty cycle, 70% power). The mixture was incubated for 15 min and then centrifuged for 15 min at 35,000x g to pellet the cell debris. 500 µl of the respective binding resin (GST bind resin from Novagen; Ni-NTA beads from Sigma-Aldrich) were washed in 30 ml PBS. Beads were generally sedimented by centrifuging 2 min at 3000x g. Supernatants containing the expressed recombinant protein were then added to the washed binding resin and incubated under rotating agitation at 4°C for 1 h. Beads were washed 3 times in washing buffer, transferred to a 2 ml Eppendorf tube and resuspended in 1 ml washing buffer. For $His_6$-fusion proteins, 10 mM imidazole was added during binding and washing to minimize unspecific background binding to the resin. They were eluted in 500 µl of 300 mM imidazole in TBS for 30 min under rotating agitation at 4°C. The beads were pelleted by spinning 1 min at 13,000 rpm and the supernatant was cleared by a second centrifugation step under the same conditions. Protein concentration of GST only was determined by Bradford assay.

Concentrations of the fusion proteins were determined relative to GST by SDS-PAGE following Coomassie staining. Proteins were stored at 4°C.

### 2.3.9 GST-Pulldown assay

Protein extracts were prepared as described in 2.3.5. A small aliquot was saved as an input control and kept on ice during incubation times. 50-70 µg of purified bead-bound GST-tagged proteins were pipetted into Eppendorf tubes, shortly centrifuged and residual buffer was aspirated to avoid dilution of the extracts. Same amounts of lysates were added to the GST-tagged proteins and incubated for 2 h at 4°C under rotating agitation, washed three times with 1 ml lysis buffer A and once with 1 ml lysis buffer A without Triton X-100. Bound proteins were eluted by the addition of 20 µl 2x SDS sample buffer and boiling the samples for 3 min at 95°C. The input sample was boiled in parallel with 2x SDS sample buffer. Eluates were transferred to new Eppendorf tubes using a Hamilton pipette and 1x SDS sample buffer ad. 90 µl was added to the beads. Leftover proteins were eluted again by boiling for 3 min and the eluates were pooled. Samples were stored at -20°C or directly analyzed by SDS-PAGE and immunoblotting.

### 2.3.10 In vitro binding assay

Eluted $His_6$-tagged proteins were cleared from possible precipitates right before the experiment by ultracentrifugation at 180,000 x g. 115 pmol of GST-tagged proteins were incubated with equimolar amounts of $His_6$-tagged proteins for 30 min at 4°C under rotating agitation. Beads were washed and proteins were eluted as described for the pulldown assay but 10 mM imidazole was added during binding and washing.

### 2.3.11 Purification of denatured protein from inclusion bodies

For the purification of large amounts of natively unfolded $His_6$-CIN85 (aa 429 - end), 5 l of culture were expressed in E. coli BL21 at 37°C for 4 h. Cell pellets from 1 l of culture were resuspended in 30 ml resuspension buffer (20 mM Tris pH 8.0, 500 mM NaCl) and cells were lysed using 500 units benzonase (20 µl of 25 U/µl working stock) and a big tip-of-a-spatula of lysozyme in the presence of 1 mM PMSF on ice for 15 min. Lysis was completed by sonicating 2 times for 2 min (50 % duty cycle, 70 % power). Debris was removed by centrifuging at 9,000× g for 15 min at 4°C and the pellet was washed four times by resuspending vigorously in 20 ml washing buffer (20 mM Tris pH 8.0, 500 mM NaCl, 0.05% Triton X-100, 0.05% Chaps) and sedimenting as described above. After the last wash, the pellet was resuspended in 15 ml denaturing buffer (8 M urea, 20 mM Tris pH 8.0, 500 mM NaCl). Undissolved inclusion bodies were

removed by ultra-centrifugation for 30 min at 125,000× g and 4°C in a Ti70 rotor. A determination of the protein concentration by measuring absorption at 280 nm was skipped at this point, since the protein fragment has no aromatic residues. The cleared inclusion body solution was filtered through a 0.45 µm membrane and imidazole was added to 10 mM. A 1 ml HisTrap FF column (GE Healthcare) was equilibrated in column wash buffer (6 M urea, 20 mM Tris pH 8.0, 500 mM NaCl, 10 mM imidazole; degased) using an Akta prime and protein was bound at a flow rate of 0.1 ml/min over night, since the protein solution was very viscous. The column was washed with column wash buffer at 0.3 ml/min until absolutely no more protein was detected in the eluate, followed by washing with about 15 ml of intermediate wash buffer (4 M urea, 20 mM Tris pH 8.0, 500 mM NaCl, 10 mM imidazole; degased) to prevent precipitation of urea. Bound protein was eluted with elution buffer (4 M urea, 300 mM imidazole, 20 mM Tris pH 8.0, 500 mM NaCl; degased) in 1.5 ml fractions, with total protein eluting within 7-12 ml (or 13-17 ml, depending on the volume of the tubing system). The eluate was concentrated to 9 ml using a Millipore centrifugal filter device (MWCO 30kDa) and dialyzed against 20 mM Tris pH 8.0, 150 mM NaCl, 10 mM imidazole in 1 l for 1 h.

### *2.3.12 Affinity purification of polyclonal antibodies from rabbit serum*

**Table 2.12: List of homebrew polyclonal antibodies**

| antigen | No. | affinity-purified on | Expression |
|---|---|---|---|
| SEPT9 | 2320 | GST-SEPT9_v3 (aa1-220) | 4h at 30°C |
| CIN85 | 6665 | GST-CIN85 (aa334-end) | 4h at 30°C |
| CIN85 | 2318 +2319 | GST-CIN85 (aa 600-end) | 4h at 30°C |

Polyclonal antibodies listed in table 2.12 were raised in rabbits at Eurogentec S.A., Belgium. Specific antibodies were affinity purified from serum using a native protein fragment, which is bigger compared to the fragment used for immunization. GST-fused fusion proteins were purified as described above, but with an additional high-salt wash with 1 M NaCl in PBS after binding of the proteins to the beads. To prevent elution of the antigen together with the bound antibody, the GST fusion proteins were crosslinked to the resin using Bis[sulfosuccinimidyl] suberate (BS3; Thermo Scientific), a water-soluble amine-to-amine crosslinker. Therefore, a 100 mM stock solution of BS3 was prepared freshly in PBS, a 10x to 50x molar excess of BS3 was added to the fusion protein and

incubated for 30 min at 4°C under rotating agitation. Beads were washed with PBS and crosslinking was repeated once under the same conditions. Beads were washed twice with PBS and a small aliquot was analyzed by SDS-PAGE and Coomassie staining to control the crosslinking efficiency.

A porous filter disc was pushed to the bottom of a 10 ml PE-column and the resin was transferred to the column. It was equilibrated by washing three times alternatingly with washing buffer A (10 ml 0.1 M sodium acetate, 500 mM NaCl pH 5.3) and washing buffer B (10 ml 0.1 M $NaHCO_3$, 500 mM NaCl pH 8.3), followed by one wash with 10 ml TBS to adjust pH 7.4. For pre-elution of the column, 10 ml acid elution buffer (0.2 M glycine / HCl pH 2.2) were added and allowed to flow through. The column was washed with 30 ml TBS. Rabbit sera were prepared for binding by heat inactivating 5-12 ml at 56°C for 30 min and centrifuging for 30 min at 4000x g to remove cell debris. The outlet of the column was closed with a cap and parafilm and the cleared serum was added to the beads. The top of the column was sealed using the lid and parafilm and incubated slowly rotating at 4°C overnight. The next day, the beads were left to settle on ice and the serum was allowed to flow through.

The column was then washed with 20 ml washing buffer C (10 mM Tris pH 7.5), 10 ml washing buffer D (0.1 M Na tetraborate, 500 mM NaCl, 0.1% Tween-20), 15 ml washing buffer C and 40 ml washing buffer E (10 mM Tris pH 7.5, 500 mM NaCl). For elution, 2 ml Eppendorf tubes were prepared for the acid elution with 180 µl 2 M Tris (pH 11.25) and for the alkaline elution with 200 µl 10x PBS and 200 µl 1 M HCl. The antibody was first eluted with 15 ml acid elution buffer (0.2 M glycine / HCl pH 2.2) by collecting 2 ml-fractions into the prepared Eppendorf tubes. The column was washed with 2 ml 15 mM Tris pH 8.8 and eluted with 6 ml 2 M Tris pH 11.25 by collecting 2 ml-fractions. Absorption at 280 nm was measured for every second fraction. 15 µl of all fractions containing significant amounts of protein were analyzed by SDS-PAGE and Coomassie-staining. Additionally, an aliquot of the column after elution was also analyzed to control elution efficiency. Antibody content was identified by the presence of light chains (~25 kDa) and heavy chains (~55 kDa) of the IgG antibody. In all cases, antibody was eluted under acid conditions. In case significant antibody amounts were still bound to the column, elution was repeated.

Antibody containing fractions were pooled, concentrated using an Amicon Centrifugal Filter Device (Millipore, MWCO 50 kDa) and dialyzed oN at 4°C against

PBS. 0.02 % $NaN_3$ and 50% Glycerol was added for storage at -20°C. Antibody concentration was roughly calculated by dividing absorption at 280 nm through the factor 1.4 and controlled again by Coomassie staining.

Specificity was tested by 'stripe test': 1 mg of control and knockdown cell lysates were blotted using a 1-well-comb. Stripes with a width of ~2 mm were cut and decorated with different dilutions of the antibody (usually 1:100 to 1:5000), which were detected by alkaline phosphatase (AP). Therefore, stripes were decorated with AP-coupled secondary antibody diluted 1:1000 to 1:10,000 in immunoblot blocking solution for 1 h at room temperature. Stripes were washed 2x with TBS and 1x with TSM to adjust the optimal pH for the AP. Alkaline phosphatase catalyses the removal of a phosphate group from BCIP, generating a product that oxidizes and dimerizes to dibromodichloro indigo. The reducing equivalents produced during the dimerization reaction reduce NBT to an insoluble purple dye, diformazan. Stripes were incubated at RT with AP developing solution until a strong band was visible on the stripe. The reaction was stopped by washing with water. Stripes were dried and aligned with the protein marker using a stroke, which was painted with a pen at the bottom of the blot before cutting.

### *2.3.13 Cytosol membrane fractionation*

HeLa cells were starved for 3h in serum-free medium, cooled down on ice and treated with the indicated concentrations of EGF for 60 min at 13°C to prevent internalization. Cells were scraped in 20 mM HEPES pH 7.4, 100 mM KCl, 2 mM $MgCl_2$ and cracked using a cell cracker device (HGM, Heidelberg, Germany) following three freeze-thaw cycles in liquid nitrogen. Nuclei and cell debris were discarded by a centrifugation at 1,000 x g for 5 min. Cytosol and membrane was separated by an ultracentrifugation for 1 h at 440,000 x g. The membrane pellet was dissolved in hot SDS-PAGE sample buffer and thoroughly homogenized. Equal amounts of both fractions were analyzed by immunoblotting.

### *2.3.14 EGFR degradation*

HeLa cells were starved for 4h in serum-free media and incubated for the indicated time points with 500 ng/ml EGF in presence of 10 µg/ml cycloheximide. For harvesting, cells were placed on ice, washed once with ice-cold PBS and scraped in extract buffer. Lysates were centrifuged for 5 min at 13,000 x g and supernatants were subjected to

Western blot analysis. EGFR-levels were quantified, corrected for a loading control (actin or tubulin) and each time course was normalized to time point zero.

### *2.3.15 NMR spectroscopy*

NMR studies were performed in collaboration with Dr. Peter Schmieder, FMP Berlin. $^{15}$N-labeled $His_6$-CIN85 SH3 A (aa1-58, subcloned into pET28a) was purified in 20 mM Tris pH 8, 50 mM NaCl and subjected to thrombin cleavage over night at 4°C. The $His_6$-tag was removed by gel filtration on a Superdex 75 (GE Healthcare). Purified SH3 A was dialyzed over night into a buffer containing 50 mM cacodylate pH 7.4. A reference assignment of the resonances of the $^{1}$H, $^{15}$N-HSQC of the protein was kindly provided by others (Ceregido et al., 2013). Since the protein construct used here slightly differed from the one documented previously, we performed measurements to confirm the assignment of the protein resonances. A sample of 600 µL of 15N-labeled 120  M SH3-A was used in a 5 mm NMR tube at a temperature of 298 K. Experiments were performed on a AV600 Bruker spectrometer (600 MHz 1H frequency) using a QXI probe equipped with a self-shielding z-gradient.

Three 3D experiments were performed: a $^{15}$N-NOESY-HSQC using 16 scans, a data size of 512($^{1}$H) x 64($^{15}$N) x 80($^{1}$H) complex points, $t_{H,max}$ = 51.2 ms, $t_{N,max}$ = 21.2 ms, tH,max(i) = 9.6 ms, a $^{15}$N-TOCSY-HSQC using 8 scans, a data size of 512($^{1}$H) x 64($^{15}$N) x 80($^{1}$H) complex points, $t_{H,max}$ = 51.2 ms, $t_{N,max}$ = 21.2 ms, $t_{H,max}$(i) = 9.6 ms and a HNHA using 8 scans, a  data size of 512($^{1}$H) x 48($^{15}$N) x 46($^{1}$H) complex points, $t_{H,max}$ = 51.2 ms, $t_{N,max}$ = 15.9 ms, $t_{H,max}$(i) = 10.6 ms.

NMR experiments to study the interaction with a SEPT9-derived peptide were performed on a AV600 Bruker spectrometer (600 MHz 1H frequency) using a TCI cryoprobe equipped with a self-shielding z-gradient. For the titration the peptide was added from a stock solution of 5 mM or 50 mM for the higher concentrations to avoid dilution of the sample. Five $^{1}$H,$^{15}$N-HSQCs were recorded using 4 scans, a data size of 512($^{1}$H)*128($^{15}$N) complex points and a $t_{H,max}$ = 51.2 ms and $t_{N,max}$ = 42.5 ms. The protein:peptide ratio was 1:0, 1:0.5, 1:1, 1:2 and 1:10. No attempt was made to completely saturate the protein. Differences in chemical shift were calculated from the peak positions in the individual spectra using the formula shift = $\mathrm{sqrt}[(\Delta\delta(^{1}H))^2 + (\Delta\delta(^{15}N)/10)^2]$, where $\Delta\delta$ is the difference in chemical shift in the respective dimensions.

All spectra were recorded and processed using topspin 3.1. (Bruker Biospin, Karlsruhe, Germany). The processed data were first converted to UCSF-format (Goddard and Kneller, SPARKY 3. University of California, San Francisco) and subsequently transferred to CCPN (Vranken et al., 2005) for assignment. A molecular model was created using the X-ray structure B2Z8 by replacing the amino acid side chains and minimizing the energy using Sybyl.

### 2.3.16 $^{125}$I-EGF uptake

$^{125}$I-EGF uptake was performed as previously described (Kornilova et al. 1996). HeLa cells were seeded in 24-well plates and starved for 4 h in serum-free medium containing 0.1 % BSA and 20 mM HEPES pH 7.4. Cells were stimulated with $^{125}$I-EGF in starvation medium at 37°C and washed twice on ice with PBS. Surface-bound $^{125}$I-EGF was removed by an acid wash with 0.2 M acetic acid, 0.5 M NaCl, pH 2.5 for 5 min on ice. Cells were dried at room temperature for 5 min and lysed with 1 N NaOH for 60 min.

$^{125}$I-EGF released by acid wash and the remaining $^{125}$I-EGF in the cell lysate was quantified using a scintillation counter (HIDEX 300SL). Non-specific binding was measured for each time point in the presence of a 300-fold excess of cold EGF and was subtracted from all values. The ratio of internalized to surface-bound EGF was plotted as a ratio of time.

### 2.3.17 $^{125}$I-EGF recycling

$^{125}$I-EGF recycling was performed as previously described (Kornilova et al. 1996). HeLa cells were seeded in 24-well plates and starved for 4 h in serum-free medium containing 0.1 % BSA and 20 mM HEPES pH 7.4. Cells were stimulated with 20 ng/ml $^{125}$I-EGF in 300 µl starvation medium for 15 min at 37°C and washed twice on ice with PBS. $^{125}$I-EGF remaining on the cell surface was removed by a mild acid wash (0.2 M sodium acetate, 0.5 M NaCl, pH 4.5) on ice for 3 min. To allow for endosomal progression of EGF-bound receptors cells were washed twice with pre-warmed starvation medium and further incubated in 300 µl starvation medium containing 4 µg/ml EGF for 40 min at 37°C. Cells were placed on ice and medium was collected. After washing cells twice with PBS, surface-bound EGF was removed by an acid wash (0.2 M acetic acid, 0.5 M NaCl, pH 2.5) for 2 min on ice. The acid wash was collected and radioactivity was measured. Cells were dried at room temperature for 30 min and lysed in 1 mM NaOH for 30 min under gentle

agitation. Lysates were collected by scraping and pipetting up and down. Medium and cell lysate were subjected to a TCA-precipitation over night at 4°C. TCA-precipitation was performed in a finale volume of 1 ml by adding 650 µl 0.75 % BSA (in PBS) and 50 µl 100% TCA to 300 µl sample to reach final concentrations of 5 % TCA and 0.5 % BSA. TCA-precipitated (intact EGF) and TCA-soluble (degraded EGF) $^{125}$I were separated by a centrifugation at 14,000 rpm for 5 min. The pellet was dissolved in 1 M NaOH, and both fractions were analyzed in a γ-counter (Wallac 1470 Wizard). Non-specific counts were measured for each time point in the presence of a 300-fold excess of unlabelled EGF and were subtracted from all values. Recycling and degradation was calculated as % of total internalized radioactivity, which was calculated as the sum of measured radioactivity per well.

### *2.3.18 EGFR downstream signaling*

Phosphorylation of AKT at Ser473 was measured using [pSer473] Akt1/2 ELISA kit (Enzo Life Sciences, #ADI-900-162). HeLa cells were starved over night in medium containing 0.1% FCS and stimulated for 5 min at 37°C with EGF. Cells were placed on ice, washed twice with PBS and lysed on ice in 20 mM Tris pH 7.4, 500 mM NaCl, 10 mM EDTA, 1% Triton X-100, 20 mM NaF, 20 mM glycerophosphate, 1 mM PMSF, protease inhibitor cocktail (Sigma), phosphatase inhibitor cocktails (Sigma, #P0044 and #P5726). Lysates were centrifuged for 5 min at 13,000 x g and supernatants were used for the ELISA assay at final concentrations of 40 µg/ml according to the manufacturer's instructions. Total level of [pSer473] AKT1/2 were determined using a standard curve, which was processed in parallel for each experiment. Values were normalized to control cells under starved conditions. Additionally, lysates were subjected to immunoblot analysis to control total AKT1/2/3-level.

### *2.3.19 EGFR ubiquitylation*

HeLa cells were starved for 3 h in serum-free medium, cooled down on ice and treated with 100 ng/ml EGF for 30 min at 13°C to prevent internalization. Cells were lysed in RIPA buffer (50 mM Tris pH 7.4, 150 mM NaCl, 1 mM EDTA, 0.1 % SDS, 1 % Triton-X 100, 1% sodium deoxycholate, 1mM PMSF, protease inhibitor cocktail (Sigma) and phosphatase inhibitor cocktails (Sigma, #P0044 and #P5726). 1 mg of lysates were ultracentrifuged for 15 min at 180,000 x g and incubated with 3µg EGFR-antibody

(sc-101) immobilized on protein A/G PLUS-agarose (both Santa Cruz Biotechnology) for 2 h at 4°C on a rotating wheel. Upon 4 washing steps with 1 ml RIPA buffer, bound proteins were eluted with SDS-PAGE sample buffer and analyzed by immunoblotting. Since ubiquitylation is unstable, samples were not stored frozen but analyzed immediately after elution by immunoblotting using specific antibodies against ubiquitin and EGFR. To compensate the decrease in EGFR level in SEPT9 knockdown samples, a 1.6-fold volume of the IP-sample was loaded on the gel compared to the control condition. For quantification, the amounts of ubiquitin were corrected for the amount of immunoprecipitated EGFR, which was determined from parallel gels. Western Blots for these experiments were detected with the FUSION-FX7 Advance Imaging System from PeqLab.

### *2.3.20 Analysis of EGFR interactome by SILAC-based mass spectrometry*

We identified endocytic adaptors, which associate with EGFR at the plasma membrane using a proteomic approach based on stable isotope labeling with amino acids in cell culture (SILAC). HeLa cells were kept in medium containing either heavy isotopes of arginine and lysine or light isotopes, respectively, for 8 days in total. Labeling efficiency was tested beforehand by analyzing one arbitrary band from a coomassie-stained protein gel. Both labeled and unlabeled cells were transfected with siRNA (described in detail in chapter 2.4.4) and each condition was splitted to one 10 cm tissue culture dish. Cells were washed two times with PBS and starved for 3 h in HBSS (including $MgCl_2$, $CaCl_2$). Cells were precooled on ice for 10 min and stimulation with 500 ng/ml human EGF (Peprotech) in HBSS at 9°C for 30 min. Culture dishes were transferred to ice and HBSS was aspirated completely. Cells were harvested using a cell scraper in 500 µl lysis buffer A (containing protease and phosphatase inhibitors), vortexed and lysed for 30 min on ice. Lysates were clarified by ultracentrifugation at 65,000 rpm at 4°C in TLA-100.2 rotors. ~2.5 mg of each lysate was subjected to affinity-purification of EGFR using 5 µg antibody (sc-101 from Santa Cruz Biotechnology) for 1 h. The detailed protocol for immunoprecipitation is described in chapter 2.3.6. 6.6% of the eluates were analyzed by immunoblotting using EGFR-specific antibodies in order to quantify the amount of affinity-purified EGFR. Eluates with equal amounts of EGFR from control cells containing heavy isotopes (H) and from SEPT9 knockdown cells containing light isotopes (L) were mixed and analyzed by LC-MS/MS (performed in collaboration with Eberhard Krause; Leibniz Institute for

Molecular Pharmacology, Berlin). The reverse experiment with SEPT9 knockdown cells being labeled was performed in parallel. The detected proteins were defined as an interactor of EGFR if the respective protein was accordingly described in the literature. The experiment was repeated one time and the normalized ratio L/H (or H/L for the reverse experiment) were merged. Only interactors, which showed a consistent effect in both forward and reverse experiment, were analyzed.

## 2.4 Cell biological methods

### *2.4.1 Mammalian cell culture*

HeLa M and A431 cells were cultured in a humidified incubator at 37°C and 5 % $CO_2$. As general culture medium, Dulbecco's Modified Eagles Medium (DMEM + Glutamax, purchased from Lonza), 10% heat-inactivated fetal calf serum (FCS), and 50 units/ml penicillin and 50 µg/ml streptomycin was used. HeLa M cells were cultured in DMEM containing 1 g/l glucose, whereas A431 cells were kept in DMEM with 4.5 g/l glucose. Cells were passaged every 2 to 4 days and seeded to a new culture dish at a dilution of 1:10 to 1:20. For detaching, cells were washed with PBS and trypsinized with one volume of trypsin-EDTA (1 ml for a 10 cm dish, Gibco) for 5 min at 37°C and resuspended in 10 volumes of culture medium with FCS to inactivate the trypsin. Freshly thawed cells were passaged at least once before use in an experiment. Cells were abandoned beyond passage 35 to 40.

### *2.4.2 Long-term storage of mammalian cells*

Eukaryotic cell lines were stored in freezing medium (90% FCS, 10% DMSO) in liquid nitrogen. Cells were grown on a 10 cm tissue culture dish to a confluency of around 90% and disattached by a trypsin/EDTA treatment. Cells were resuspended in 9 ml serum-containing medium and pelleted at 300 x g for 5 minutes. Cells were resuspended in 2-3 ml freezing medium. 1 ml aliquots were frozen at -80°C and transferred to liquid nitrogen 1 week to one year after freezing.

### *2.4.3 Transfection of plasmid DNA*

HeLa cells were seeded one day prior to transfection to a density of 100% on the next day. Plasmid DNA was transfected using lipofectamine 2000 (Invitrogen) or JetPrime (Polyplus transfections) according to the manufacturer's instructions. Cells were transfected for 4 h, allowed to recover for 1-2 h in fresh medium and split to coverslips.

### *2.4.4 Small interfering RNA treatments and rescue experiments*

HeLa cells were seeded on day 0 and transfected at a confluency of ~50% with siRNAs using oligofectamine (Invitrogen) according to the manufacturer's instructions on

day 1. Briefly, one 6-well was transfected with 2 µl 100 µM siRNA and 2 µl oligofectamine in a final volume of 1 ml OptiMEM. After 4 h, cells were allowed to recover over night by addition of DMEM containing 2x FCS and antibiotics). Medium was changed in the morning on day 2 and expanded in the afternoon for the experiment on day 3. For expression of recombinant proteins in knockdown cells (rescue experiments), siRNA transfection complexes were removed from the cells after 4 h on day 1 instead of leaving the transfection on overnight. Plasmids were then transfected on day 2 using JetPrime (Polyplus transfections) according to the manufacturer's instructions. Cells were subjected to the respective experiment on day 3.

### *2.4.5 Immunofluorescence*

For microscopy, coverslips were coated with matrigel (BD Biosciences) by incubating with ~50 µl matrigel per 18 mm coverslip for at least one hour at 37°C. Cells were seeded to matrigel-coated coverslips one day before immunostaining. Cells were immediately fixed with PFA fixing solution (400 µl for a 12-well) for 10 to 45 min at room temperature or with 100 % methanol (500 µl pre-cooled to -20°C) for 5 min at -20°C. Fixed cells were washed twice with PBS and were then blocked against unspecific antibody binding with 3.3 % goat serum and permeabilized using 0.1 % Triton X-100 for intracellular immunostainings by incubating 20 min at room temperature with goat serum dilution buffer (GSDB).

Primary antibodies were diluted in GSDB, centrifuged for 5 min at 13000 rpm and 35 µl were spotted onto parafilm in a humidity chamber. Coverslips were placed upside down on the spotted antibody solution and incubated for 1 h at room temperature or over night at 4°C. Coverslips were flipped back into the well-plate and washed 3 times for 5 min with IF wash buffer. Secondary goat α-mouse or α-rabbit antibodies coupled to Alexa 488, 568 or 647 were applied at a dilution of 1:200 as described above and incubated for 1 h at room temperature. Coverslips were washed 2 times for 5 min in IF wash buffer with detergent and 2 times without detergent. Coverslips were dipped into ddH2O to remove salt and mounted onto microscopy slides using 16 µl Immumount mounting solution (Thermo Electron) supplemented with 1 µg/ml DAPI.

### 2.4.6 EGF uptake

HeLa cells were seeded on MatriGel-coated glass coverslips and starved for 3 h in serum-free medium. Cells were stimulated for the indicated time points with serum-free medium containing AF647-EGF at 37°C and washed two times with PBS containing 2 mM $MgCl_2$ at room temperature. Upon fixation with 4 % PFA/ 4 % sucrose in PBS for 10 min, cells were analyzed by confocal microscopy.

### 2.4.7 Surface binding of EGF

HeLa cells were seeded on MatriGel-coated glass coverslips and starved for 3 h in serum-free medium. Cells were incubated with 500 ng/ml AF647-EGF for 30 min at 9°C, transferred to ice and washed two times with ice-cold PBS containing 2 mM $MgCl_2$. Upon fixation with pre-cooled 4 % PFA/ 4 % sucrose in PBS for 10 min at room temperature, cells were analyzed by immunofluorescence microscopy. For quantification of surface EGF-level, cells were analyzed by quantitative epifluorescence microscopy. A subtraction of the area of the DAPI-staining from the surface EGF signal was needed to decrease background fluorescence. Sum fluorescence intensity per cell was then calculated and normalized to the control condition. For co-localization studies with surface-bound EGF, cells were analyzed by confocal microscopy. The amount of the respective protein co-localizing with surface EGF was calculated with an intersection mask. Sum fluorescence intensity of this mask was normalized to total fluorescence intensity of EGF.

### 2.4.8 Fluorescence microscopy

Fluorescence microscopy is a technique that uses the phenomenon of fluorescence to specifically detect biomolecules in fixed or live cells. A fluorophore is excited with light of a specific wavelength and relaxes into the electronic ground state, emitting light of a defined, but longer wavelength. Generally, two different kinds of fluorophores are available: Fluorescent dyes coupled to antibodies that can be used to specifically label either endogenous or overexpressed proteins and genetically encoded fluorescent proteins that allow monitoring overexpressed proteins both in fixed and live cells. Depending on experimental requirements, different microscopic techniques were used.

Epifluorescence microscopy. For the quantitative analysis of fluorescence intensities on a per cell basis, e.g. for the analysis of ligand internalization experiments, epifluorescence widefield microscopy was used. Since no measures are taken to enhance

resolution in z, epifluorescence detection samples a large volume of the cell, thereby achieving a good excitation to emission ratio, and is hence ideally suited for the quantitative assessment of total labeling intensity. The epifluorescence setups used were from Zeiss [Zeiss Axiovert 200M with DG4 excitation unit and Coolsnap HQ2 EM-CCD camera (Roper Scientific) operated by Slidebook software (Intelligent Imaging)] or Nikon (Nikon Eclipse Ti, equipped with Andor sCMOS camera, Okolab incubator for live imaging and Nikon PerfectFocus autofocus system).

Spinning disc confocal microscopy. Experiments that required the resolution of subcellular structures were routinely analyzed by spinning disc confocal microscopy [Ultra View ERS Rapid Confocal Imager (Perkin Elmer) equipped with an EM-CCD-camera (Hamamatsu) and connected to a Zeiss Axiovert 200M microscope]. Confocal spinning-disc microscopy uses two rotating pinhole discs to acquire confocal images without point-by-point scanning of the specimen. This greatly reduces acquisition time and photobleaching of fluorophores. The microscope was operated with Volocity (Improvision, Perkin Elmer).

### *2.4.9 Image analysis and quantification*

Qualitative and quantitative image analysis were performed using Volocity software for spinning disc confocal images and ImageJ (Schneider et al. 2012) for epifluorescence microscopy data. Quantitative data were processed using Microsoft Excel and figures arranged using Adobe Illustrator.

## 2.5 Statistics

Statistics were done using the unpaired t-test for all quantified experiments except for the data shown in Fig. 3.2 D (EGFR-level after knockdown of SEPT9) and in Fig. 3.19 B,C (EGFR ubiquitylation after knockdown of SEPT9). Here, a one-sample t-test was used. All statistical calculations were done using the GraphPad QuickCalcs Web site:

http://www.graphpad.com/quickcalcs/ttest1/

http://www.graphpad.com/quickcalcs/oneSampleT1/

# 3 Results

## 3.1 SEPT9 controls EGFR degradation

The ability of cells to grow and divide is mainly controlled by the level of growth factor receptors like the EGF receptor present at the plasma membrane. These levels are tightly regulated by EGFR synthesis and by sorting of internalized receptor between degradative and recycling pathways. Given that septins play a role in membrane trafficking events (described in chapter 1.2.2; page 29) and that both SEPT9 and EGFR are often misregulated in breast cancer (described in chapter 1.4; page 34), we addressed the functional consequences of RNAi-mediated SEPT9 depletion on EGFR trafficking. Therefore, we generated antibodies against SEPT9 and obtained two different siRNAs targeting conserved stretches in the G-domain to silence all eight isoforms of SEPT9. HeLa cells were treated with these siRNAs for 48 h and analyzed by immunoblotting and indirect immunofluorescence microscopy using our home-brew antibody against SEPT9. All long isofoms were efficiently reduced (Fig. 3.1 A,B). Depletion of short isoforms could not be detected due to a lack of corresponding antibodies (epitopes are depicted in Fig. 1.10; page 31). Slight differences regarding cell morphology could be observed (Fig. 3.1 C). SiRNA #2 caused multinucleated cells and abnormally shaped nuclei, a cytokinetic defect already described (Estey et al. 2010). Furthermore, these cells lost their fibroblast-like morphology and formed more focal adhesions, as visualized by immunolocalization of the marker protein paxillin. In contrast, knockdown cells using siRNA #1 showed normal nuclei and a tendency to increased proliferation. We further analyzed the cellular localization of endogenous SEPT9 by confocal microscopy (Fig. 3.1 D,E). The localization is consistent with reports showing prominent fiber-like structures in the perinuclear area, thinner filaments in the cell periphery, and an additional pool at the cell cortex (panel D; Surka et al. 2002). As expected, SEPT9 also localized to the midbody during cytokinesis (panel E; Kechad et al. 2012).

### *3.1.1 Depletion of SEPT9 in fibroblasts decreases surface levels of EGFR*

We visualized surface EGFR by applying AlexaFluor (AF) 647-EGF to the living cells at low temperature to prohibit internalization. Cell culture media usually contain growth factors including EGFR ligands. Therefore, we serum-starved cells beforehand in order to maximize the available amount of receptors at the plasma membrane.

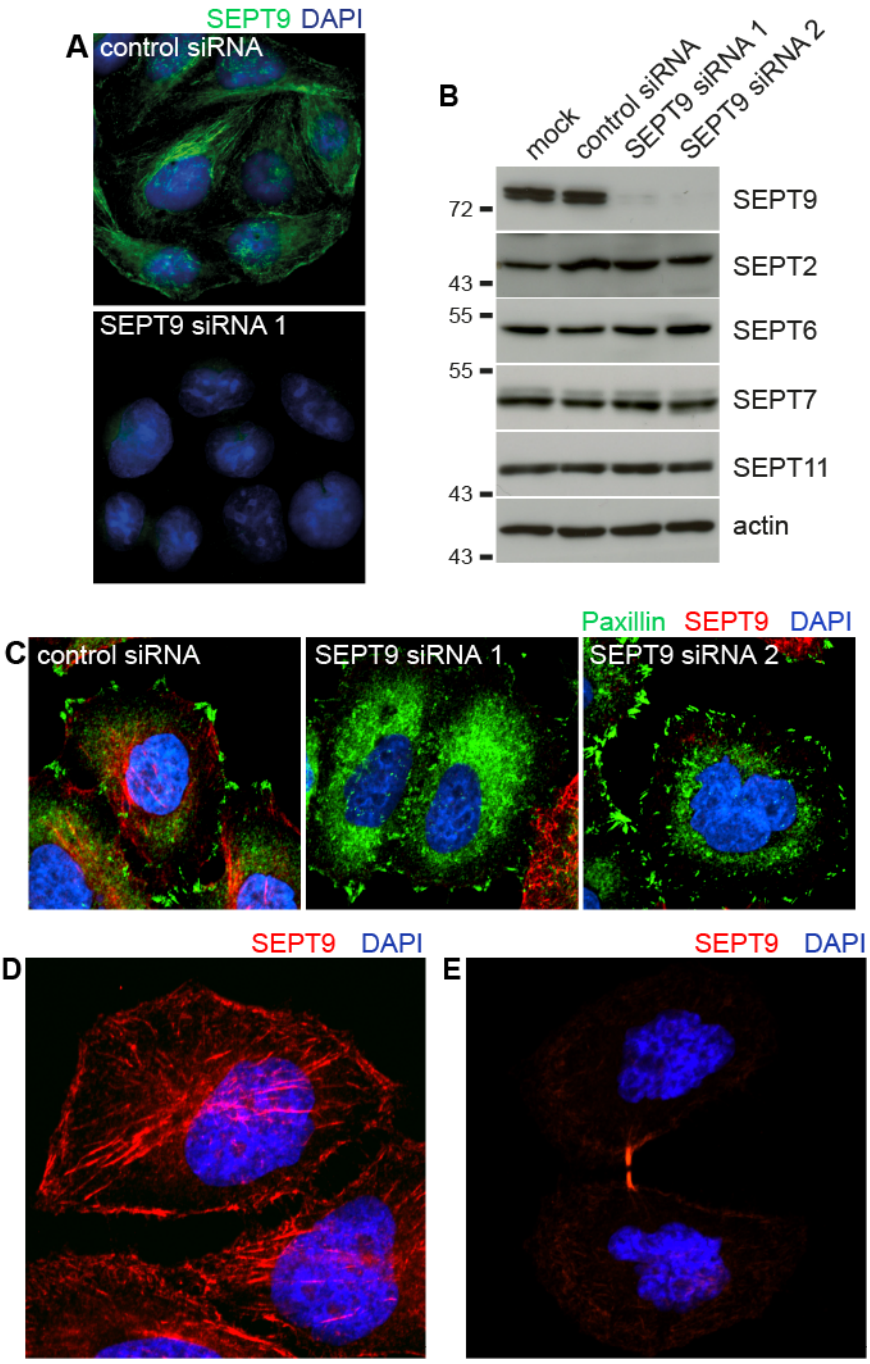


**Fig. 3.1: Verification of siRNAs and home-brew antibodies against SEPT9**

**(A)** HeLa cells were treated with control or SEPT9-specific siRNAs for 48 h. Upon fixation, cells were immunostained with home-brew antibodies against SEPT9 ('2320') and analyzed by epifluorescence microscopy. **(B)** SiRNA-treated HeLa cells were analyzed by immunoblotting using the indicated antibodies in order to confirm a reduction in protein level of SEPT9. **(C)** Cell morphology after knockdown of SEPT9. Confocal images of siRNA-treated HeLa cells immunostained with antibodies against SEPT9 ('2320', red) and the focal adhesion marker paxillin (green). **(D,E)** Cellular localization of endogenous SEPT9. Confocal images of HeLa cells immunostained with antibodies against SEPT9 ('2320') during interphase **(D)** or late telophase, where it localizes to the midbody **(E)**.

Cellular depletion of SEPT9 displayed a near 50% reduction in EGFR surface levels when compared to control cells (Fig. 3.2 B,C). Total receptor levels were slightly reduced as well (Fig. 3.2 D). We controlled the specificity of this phenotype by silencing a member of another septin group, SEPT7. This septin isoform displays the only member of its group and has unique functions in filament stability. It is postulated to form part of every heterooligomeric septin complex and cannot be substituted by other septins. SEPT7 knockdown cells, in contrast to SEPT9, displayed normal surface EGFR level. We further characterized the decrease in surface level by labeling surface EGFR without prior starvation using antibodies specific to the luminal domain. The reduced surface level caused by the loss of SEPT9 could also be observed in steady state (Fig. 3.2 E), indicating that the decrease is the result of a longterm-effect and not a consequence of the starvation. The amounts of other surface proteins, such as β1-integrin, remained unchanged.

### *3.1.2 SEPT9 regulates sorting of EGFR between lysosomal and recycling pathways*

As alterations in surface receptor level may be linked to a misregulation of endosomal sorting pathways, we investigated a potential defective trafficking in SEPT9-depleted cells. Activated EGFRs can be either recycled back to the plasma membrane or sorted for lysosomal degradation in a dose-dependant manner. Low EGF doses activate the recyling pathway, whereas increasing doses trigger degradation (Sigismund et al. 2005). We monitored EGFR degradation by stimulating cells with 500 ng/ml EGF in presence of cycloheximide in order to block new synthesis of EGFR. Loss of SEPT9 significantly accelerated receptor degradation, reflected by an about two-fold decrease in half-lives from 2 h to 1.1 h and 1.2 h, respectively (Fig. 3.3 A,B). Next, we performed pulse-chase experiments using radioactively labeled $^{125}$I-EGF, a powerful and sensitive tool enabling the user to monitor degradation and recycling simultaneously. Stimulation with 20 ng/ml EGF, where recycling is favoured over degradation under control conditions, followed by a 40 min chase resulted in nearly 30% of the total internalized EGF to be recycled to the plasma membrane and a smaller fraction to be degraded (Fig. 3.3 C; column 1,2). In absence of SEPT9, more receptors were sorted into the degradative pathway, and less recycling was measured. The relative amount of intact EGF remaining in the cell resembles the fraction of activated EGFR, which is still located along sorting routes (Fig. 3.3 C; column 3). Loss of SEPT9 did not alter this fraction, indicating that the kinetics of the

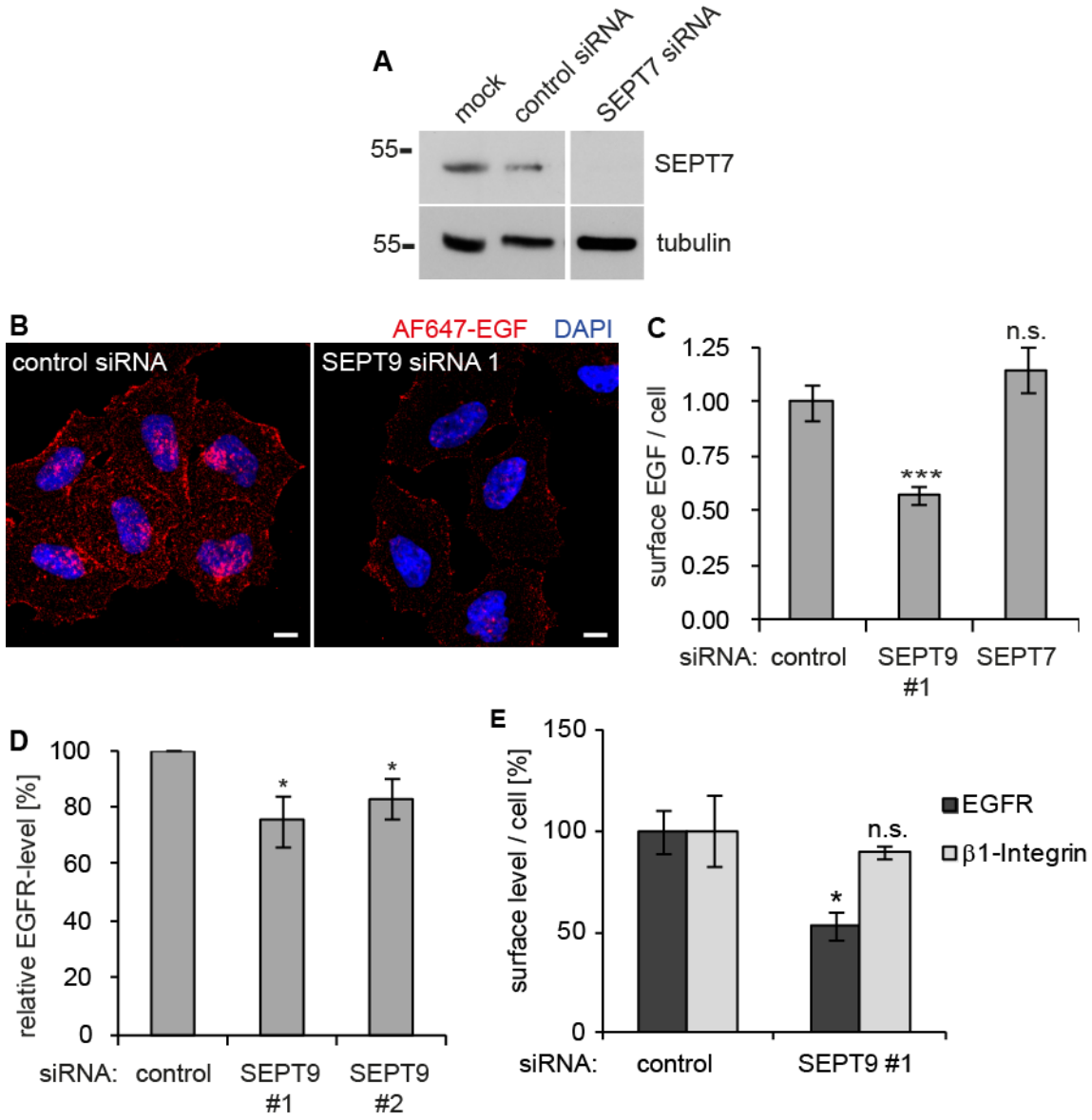


**Fig. 3.2: Depletion of SEPT9 decreases surface level of EGFR.**

HeLa cells were treated with control or septin-specific siRNA for 48 h. **(A)** Cells were lysed and analyzed by immunoblotting using specific antibodies against the indicated proteins. **(B, C)** Loss of SEPT9 decreases surface-associated EGF level. Cells were serum-starved for 3 h and AF647-EGF was bound to the cells surface at 9°C for 30 min. After fixation, cells were analyzed by quantitative epifluorescence microscopy. Representative images are shown in **(B)**. Scale bar: 10 µm. Surface-associated EGF per cell was calculated in **(C)** (n = 10). **(D)** Densitometric quantification of total EGFR level (n = 7). **(E)** SEPT9 depletion leads to a reduction of surface-associated EGFR. Cells were immunostained without prior starvation for cell surface β1-integrin or EGFR, respectively. Surface level per cell was quantified by epifluorescence microscopy (n=3). Results are shown as mean ± s.e.m. from n experiments; *P<0.05; **P<0.01; ***P<0.001; n.s., not significant.

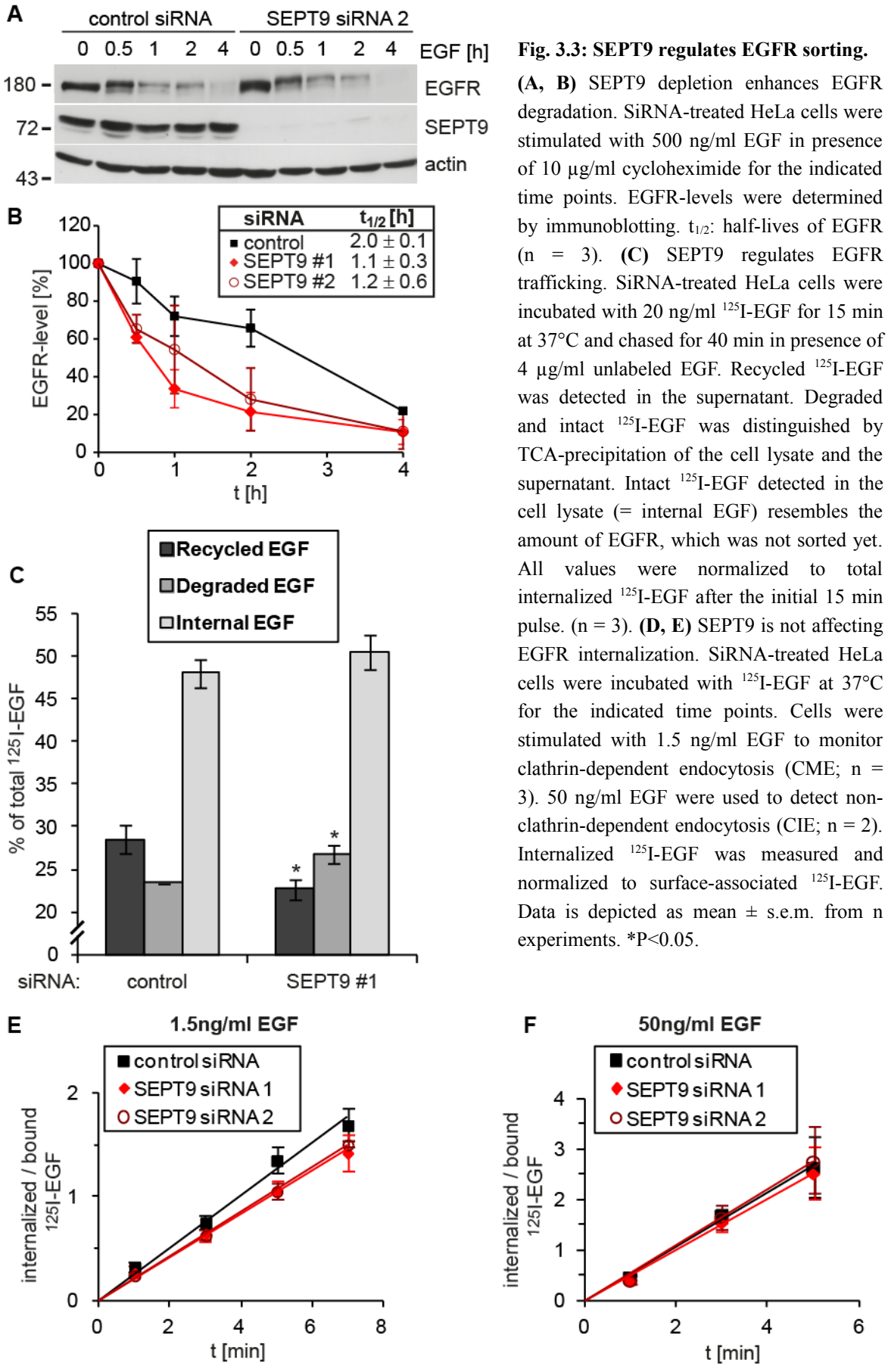


**Fig. 3.3: SEPT9 regulates EGFR sorting.**

**(A, B)** SEPT9 depletion enhances EGFR degradation. SiRNA-treated HeLa cells were stimulated with 500 ng/ml EGF in presence of 10 µg/ml cycloheximide for the indicated time points. EGFR-levels were determined by immunoblotting. $t_{1/2}$: half-lives of EGFR (n = 3). **(C)** SEPT9 regulates EGFR trafficking. SiRNA-treated HeLa cells were incubated with 20 ng/ml $^{125}$I-EGF for 15 min at 37°C and chased for 40 min in presence of 4 µg/ml unlabeled EGF. Recycled $^{125}$I-EGF was detected in the supernatant. Degraded and intact $^{125}$I-EGF was distinguished by TCA-precipitation of the cell lysate and the supernatant. Intact $^{125}$I-EGF detected in the cell lysate (= internal EGF) resembles the amount of EGFR, which was not sorted yet. All values were normalized to total internalized $^{125}$I-EGF after the initial 15 min pulse. (n = 3). **(D, E)** SEPT9 is not affecting EGFR internalization. SiRNA-treated HeLa cells were incubated with $^{125}$I-EGF at 37°C for the indicated time points. Cells were stimulated with 1.5 ng/ml EGF to monitor clathrin-dependent endocytosis (CME; n = 3). 50 ng/ml EGF were used to detect non-clathrin-dependent endocytosis (CIE; n = 2). Internalized $^{125}$I-EGF was measured and normalized to surface-associated $^{125}$I-EGF. Data is depicted as mean ± s.e.m. from n experiments. *P<0.05.

individual sorting pathways are not affected. Since enhanced endocytic uptake might also accelerate degradation, we monitored internalization rates using $^{125}$I-EGF. We stimulated cells with 1.5 ng/ml EGF for short periods and determined the ratio of internalized over surface-bound EGF, which provides a direct measure for the kinetics irrespective of impaired EGFR surface level. Depletion of SEPT9 showed no effect on clathrin-mediated internalization (Fig. 3.3 D), the dominant internalization pathway triggered at a low ligand concentration (Sigismund et al. 2008). Clathrin-independent pathways activated by stimulation with a higher EGF dose were also unaffected (Fig. 3.3 E). Taken together these results demonstrate that SEPT9 modulates sorting of EGFRs into the degradative pathway without affecting receptor internalization.

### *3.1.3 SEPT9 stabilizes heterooligomeric septin filaments*

Septin GTPases constitute a part of the cytoskeleton (Mostowy & Cossart 2012) and are known to associate with other cytoskeletal components such as actin or tubulin (Surka et al. 2002; Kechad et al. 2012). Since endosomal trafficking is highly dependent on transport along microtubules (Soldati & Schliwa 2006) and F-actin (Gasman et al. 2003), we aimed to exclude indirect effects that may arise from a potential disruption of cytoskeletal networks in SEPT9 depleted cells. Whereas the tubulin network looked unaltered, actin stress fibers were not as prominently stained as in control cells (Fig. 3.4 A,B). Endogenous SEPT2 localized to small fiber-like structures in the perinuclear area and in the periphery (Fig. 3.4 C). Additionally, a nuclear localization in a subpopulation of cells could be observed. Loss of SEPT9 caused SEPT2-fibers to disintegrate, supporting the role of SEPT9 as a regulator of SEPT2/6/7-complex assembly (M. S. Kim et al. 2011). Total levels of septin isoforms, which form part of SEPT9-containing complexes, were unaffected by SEPT9 depletion (Fig. 3.1 B). This indicates that SEPT9 is rather involved in septin localization, than in protein stability.

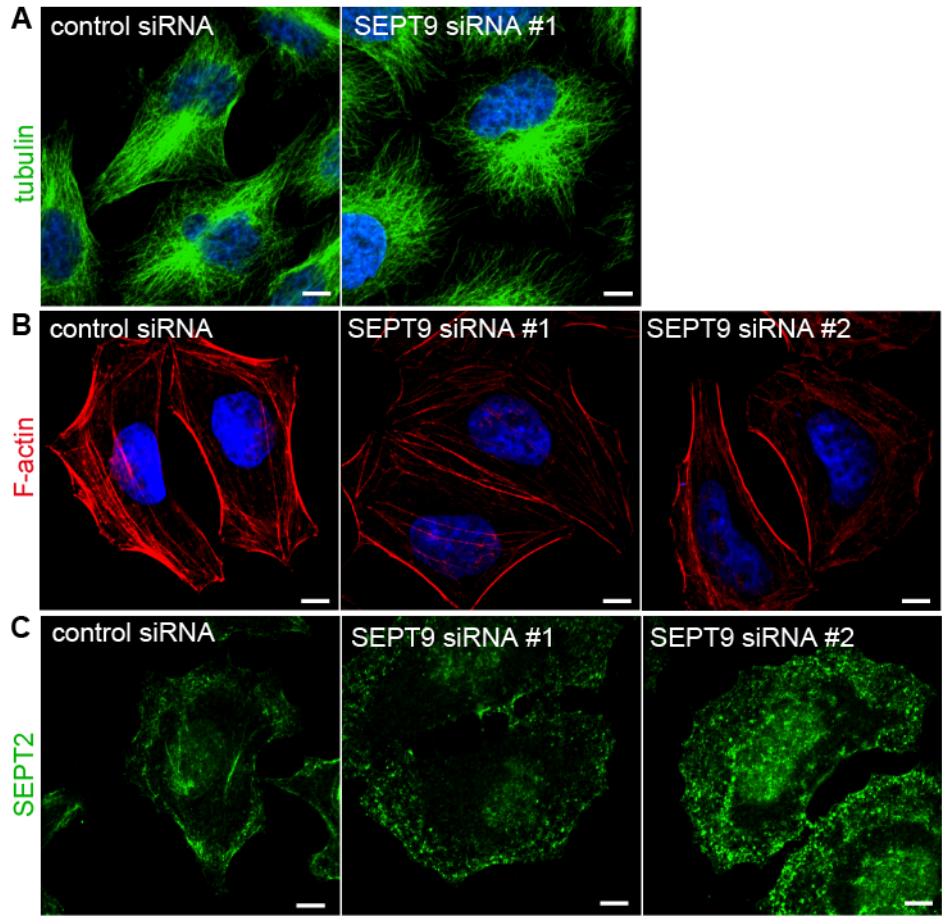


**Fig. 3.4: Cytoskeleton after knockdown of SEPT9**

Confocal images of siRNA-treated HeLa cells stained with phalloidin to visualize F-actin **(B)** and antibodies against tubulin **(A)** or SEPT2 **(C)**, respectively. Scale bar: 10 µm.

## 3.2 SEPT9 forms a complex with the adaptor protein CIN85

### *3.2.1 The N-terminus of SEPT9 is important for stabilizing EGFRs*

RNAi-mediated silencing of target proteins displays a powerful tool to study a given protein's functions, but a disadvantage of this technique is the possibility of unspecific 'off-target' effects (Birmingham et al. 2006). Therefore, knockdown/rescue experiments are substantial to control the observed phenotype for specificity. Expression of full-length SEPT9_v3, or of a truncation mutant comprising the G-domain alone (SEPT9ΔN) did not significantly alter the surface receptor level (Fig. 3.5 column 2,3). Treatment with SEPT9-specific siRNA caused, as already observed (Fig. 3.2 B,C), a decrease of surface-bound EGF to nearly 50% (column 4). Importantly, re-expression of full-length SEPT9_v3 caused surface EGFR levels to recover almost completely (column 5), whereas SEPT9ΔN, a

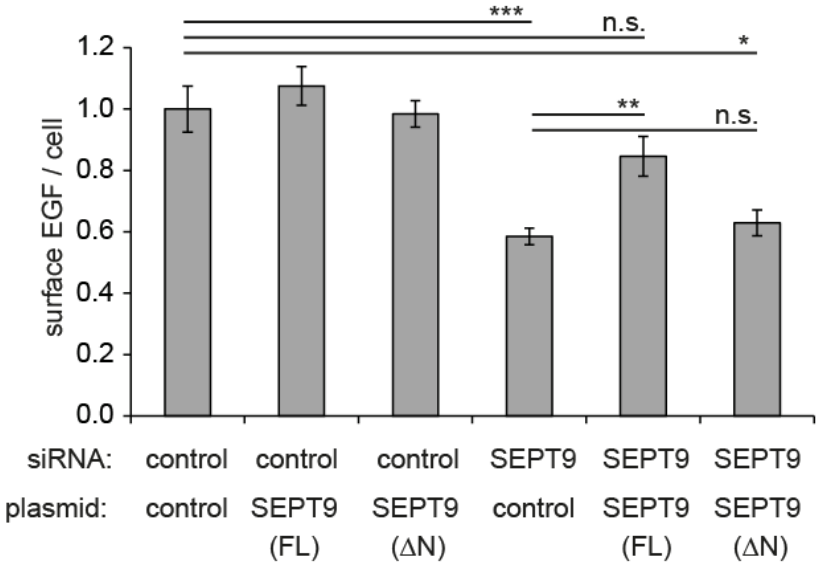


**Fig. 3.5: Knockdown/Rescue experiment for downregulation of EGFR surface level**

SiRNA-treated HeLa cells were retransfected after 24 h with full-length (FL) SEPT9_v3 or a HA-tagged ΔN-mutant, respectively. After additional 24 h, AF647-EGF was bound to the cells surface and surface-associated EGF per cell was calculated by quantitative epifluorescence microscopy. Please note, that surface EGF-level recover only upon reexpression of full-length SEPT9_v3. Data is depicted as mean ± s.e.m. from 8 experiments; *P<0.05; **P<0.01; ***P<0.001; n.s., not significant.

truncated mutant lacking the N-terminal domain, failed to achieve a similar effect (column 6). This finding indicates that the observed phenotypes are specific, and also suggests a critical role of the SEPT9 N-terminal domain, which provides a first insight into the molecular mechanisms underlying a possible role of SEPT9 in stabilizing EGFRs.

### *3.2.2 SEPT9 associates with all three SH3 domains of CIN85*

Closer inspection of the primary sequence of SEPT9 revealed the N-terminal domain to be enriched in proline residues. We therefore speculated that this region might link SEPT9 to SH3 domain-containing proteins and tested for binding of various endocytic adaptor proteins (Fig. 3.6 A). Based on our observation that SEPT9 depletion affects EGFR degradation, we included the adaptor CIN85. This protein regulates various steps of endosomal sorting of EGFRs including receptor downregulation (Dikic 2003). We also tested several regulators of clathrin-mediated endocytosis (McMahon & Boucrot 2011). Endophilin assists pit formation by membrane bending, but also displays one of several recruiting factors for dynamin. Transferrin receptor trafficking protein (TTP) is involved in the maturation of clathrin-coated pits and recruits cargo, such as transferrin receptor, to the

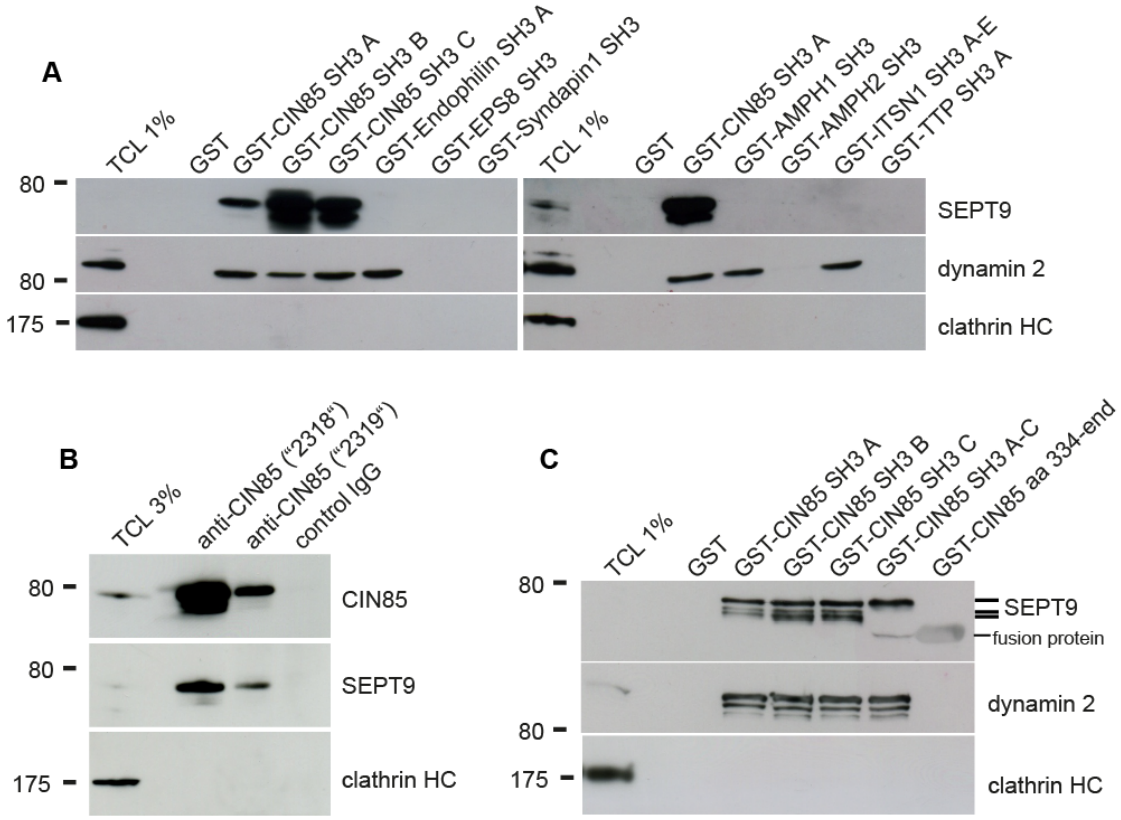


**Fig. 3.6: SEPT9 forms a complex with the adaptor protein CIN85**

**(A)** Affinity-purification of endogenous SEPT9 from HeLa cell extract using different SH3 domains as bait. Affinity-purified material was analyzed by immunoblotting using the indicated antibodies. AMPH: amphiphysin; ITSN: intersectin; TTP: transferrin receptor trafficking protein. **(B)** Two different CIN85-antibodies co-immunoprecipitate endogenous SEPT9 from A431 cell extracts. Precipitates were analyzed by immunoblotting with the indicated antibodies. **(C)** Affinity-purification of endogenous SEPT9 from HeLa cell extract using different truncations of CIN85 as bait.

forming pit. Amphiphysin acts as a linker protein between the clathrin coat and dynamin, whereas intersectin (ITSN) is needed for CCP formation. Given that septins are associated to cytoskeletal re-arrangements, we also inspected the adaptors EPS8 and syndapin 1, which connect clathrin-dependent and -independent endocytosis to actin remodelling events (Hansen et al. 2011; Cunningham et al. 2013). Only the three SH3-domains of CIN85 were able to retain SEPT9 from cell extracts on a glutathione-S-transferase (GST)-affinity matrix. In line with previous observations, also other binding partners like dynamin-2 were able to associate with CIN85 SH3 domains (Schroeder et al. 2010a). Based on this finding, we considered this adapter protein as a candidate factor linking SEPT9 to EGFR sorting.

The generation and affinity-purification of two different polyclonal antibodies, which detect a short stretch in the C-terminus of CIN85, enabled us to search for a native

complex in A431 cells. In comparison to other established cell lines, this cell type shows high expression levels of both, CIN85 and SEPT9 (data not shown), as well as a high copy number of EGFR. We detected a significant fraction of endogenous SEPT9 to co-immunoprecipitate with native CIN85 (Fig. 3.6 B). Further characterization using various GST-coupled truncations of CIN85 revealed that the SH3 domains were sufficient to mediate binding to SEPT9 from cell extracts (Fig. 3.6 C). A deletion variant of CIN85 lacking the SH3-domains (CIN85 aa334-end) was unable to interact with SEPT9.

### *3.2.3 CIN85 binds to a PR-rich motif located in the N-terminus of SEPT9*

*In silico* analysis of the primary sequence of SEPT9 predicted three atypical proline-arginine (PR) motifs located in its N-terminus, which would fit the consensus sequence PxxxPR known to mediate interactions with CIN85-SH3s (Fig. 3.7 A) (Kowanetz et al. 2003). The PR motif located at PR129/130 is highly conserved between species (Fig. 3.7 B).

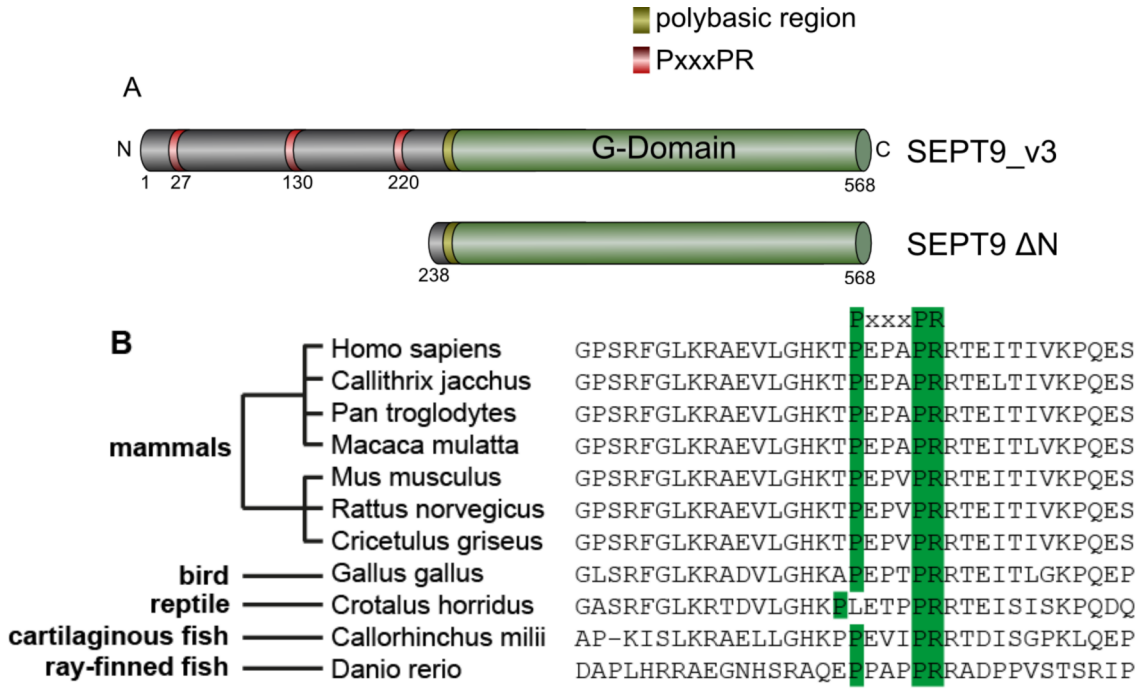


**Fig. 3.7: *In silico* analysis of the N-terminal region of SEPT9**

**(A)** Domain structure of SEPT9_v3 (full length) and a N-terminally truncated mutant. Putative CIN85 binding motifs (PxxxPR) are indicated in red. **(B)** SEPT9 sequences from different species were aligned using TCOFFEE to show conservation of the PxxxPR binding motif located at PR129/130. The class of the respective species is indicated on the left side. The green boxes indicate the position of the PxxxPR motif.

To elucidate whether this particular motif is implicated in binding of SEPT9 to CIN85, we performed biochemical mapping experiments using different truncations or point mutations of PxxxPR to PxxxAA in order to inactivate the putative binding sites. The SEPT9 N-terminal domain (GST-SEPT9_v3 aa1-220) was sufficient to promote the interaction with CIN85 (Fig. 3.8 A), whereas the isolated G-domain (GST-SEPT9 ΔN) was unable to associate with CIN85. Mutational inactivation of the proline-rich motif located at PR129/30 abolished CIN85 binding to SEPT9_v3. No such effect could be observed when the remaining two PR-motifs were mutated. To exclude that complex formation is mediated by a third binding partner, we probed the GST-baits used above with purified SH3-domains of CIN85 ($His_6$-CIN85 SH3 A-C). A similar binding pattern could be observed, although inactivation of the PR129/30-motif did not abolish binding completely (Fig. 3.8 B). This result indicates that binding of CIN85 to SEPT9 is direct, but that additional, yet unidentified determinants might contribute to the interaction.

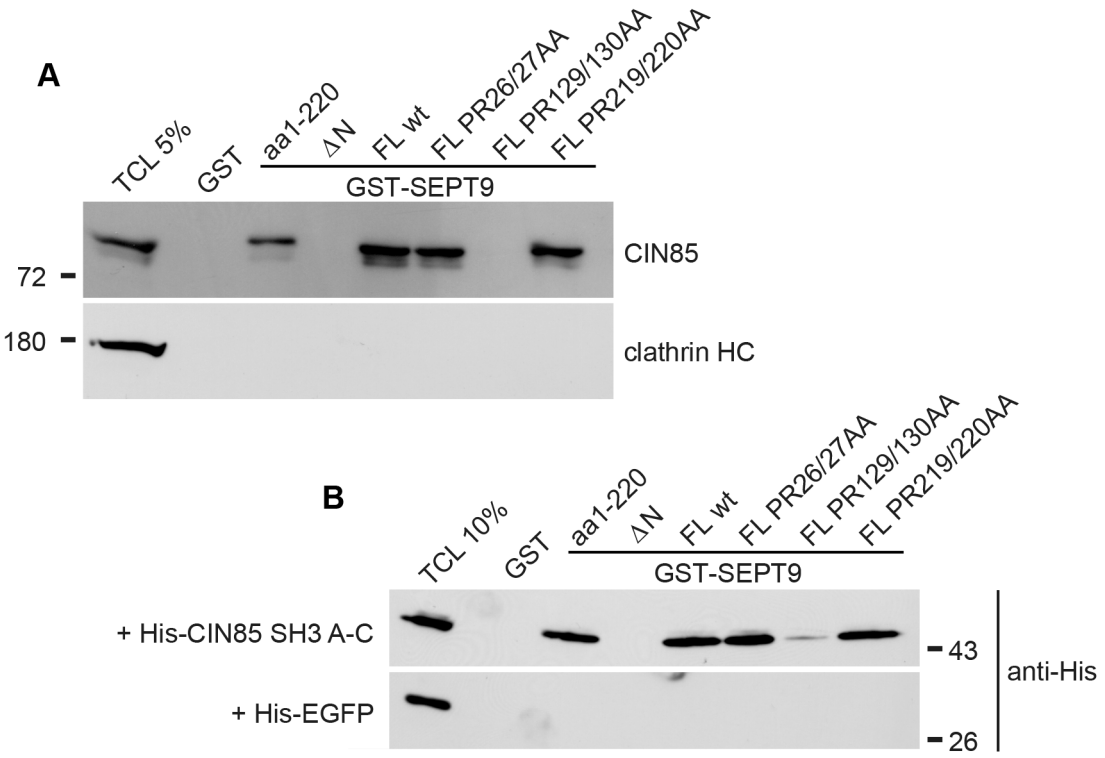


**Fig. 3.8: CIN85 binds to a PR-enriched motif in the N-terminus of SEPT9_v3**

**(A,B)** Affinity-purification using wild-type (wt), truncated or mutated versions of GST-fused SEPT9_v3 as baits. Affinity-purified material was analyzed by immunoblotting using the indicated antibodies. **(A)** CIN85 was affinity-purified from HeLa cell extracts. **(B)** GST-SEPT9_v3 versions were incubated with purified $His_6$-CIN85 SH3 A-C. Bound SH3 domains were detected by immunoblotting using a $His_6$-tag specific antibody. His-EGFP was used as a control. TCL: total cell lysate; wt: wild-type; FL: full-length; HC: heavy chain.

We expanded our studies to other septin isoforms and focused on SEPT9-containing septin filaments such as the SEPT2/6/7/9 complex (M. S. Kim et al. 2011). Indeed, SEPT2 and SEPT6 were co-purified on GST-fused CIN85 SH3 A-C (Fig. 3.9). But this association required the presence of SEPT9, validating that CIN85 binds directly to SEPT9 only.

Collectively, our results demonstrate that an atypical PR motif links SEPT9 to all three SH3 domains of CIN85, which provides a potential functional link of SEPT9 to endolysosomal sorting of EGFR. Furthermore, our data suggest that this interaction serves to recruit SEPT9-containing complexes, rather than SEPT9 monomers to activated receptors.

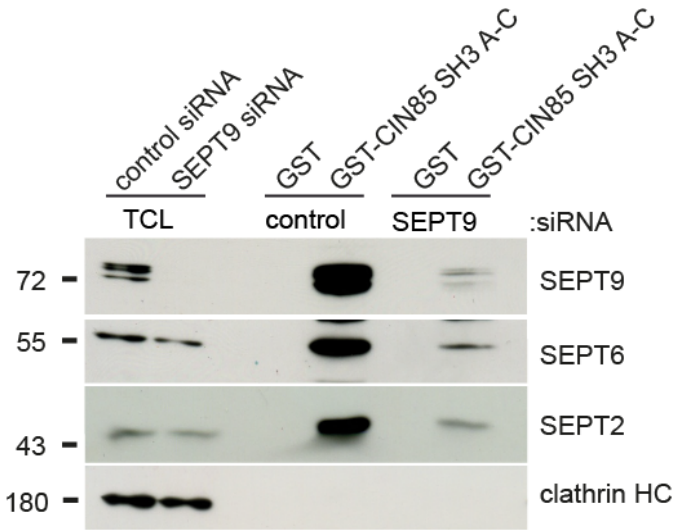


**Fig. 3.9: CIN85 associates with septin complexes by binding to SEPT9**

GST-fused CIN85 SH3 A-C was used to affinity-purify septin isoforms from HeLa cells treated with either control siRNA or SEPT9-specific siRNA #1. TCL: total cell lysate.

## 3.3 CIN85 recruits SEPT9 to activated EGFR at the cell surface

### *3.3.1 SEPT9-containing complexes are recruited to activated EGFR at the plasma membrane*

Next, we investigated the subcellular localization of the SEPT9/CIN85 complex. Therefore, we obtained siRNAs and antibodies against CIN85 and confirmed their specificity (Fig. 3.10 A,B). Treatment of Hela cells with CIN85-specific siRNA caused a significant reduction of the immunostaining. Also total level of CIN85 were reduced without affecting total levels of SEPT9. We further analyzed the subcellular distribution under steady-state conditions using confocal microscopy (Fig. 3.10 C). Endogenous CIN85 localized to some extent to endosomal-like structures, but the main pool showed a cytoplasmic distribution. A subset of cells showed an additional pool located at the cell cortex.

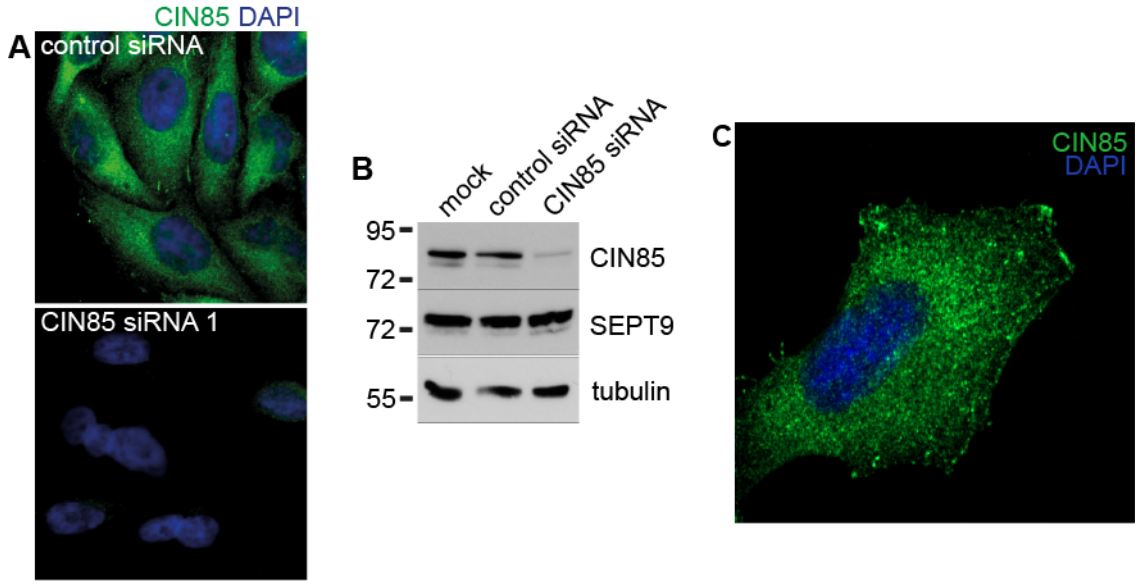


**Fig. 3.10: Verification of siRNA and home-brew antibodies against CIN85.**

**(A)** SiRNA-treated HeLa cells were immunostained with home-brew antibodies against CIN85 '6665' and analyzed by epifluorescence microscopy. **(B)** HeLa cells were analyzed by immunoblotting using the indicated antibodies in order to confirm a reduction of total levels of CIN85 upon siRNA-treatment. **(C)** HeLa cells were immunostained with antibodies against CIN85 '6665' and analyzed by confocal microscopy.

We probed for a potential colocalization first by overexpression of mRFP-tagged CIN85, which induced the formation of enlarged, aberrant endosomes, as already described (Zhang et al. 2009). These structures accumulated late endosomal markers, such as

LAMP1, and were clearly distinct from early, EEA1-containing endosomes (Fig. 3.11). A direct comparison to the neighbouring non-expressing cells illustrates that CIN85 overexpression caused SEPT9 filaments to disintegrate by translocating the endogenous protein onto CIN85-positive organelles.

However, longer expression times caused mRFP-CIN85 to aggregate into enlarged MVB-like structures, limiting the use of this tool. Therefore, we monitored the localization of endogenous CIN85 and SEPT9 upon stimulation with EGF. CIN85, in complex with the E3 ligase Cbl, associates with activated EGFRs at the plasma membrane and remains associated during internalization and endolysosomal sorting (Dikic 2003; Haglund et al. 2005). We probed cells with EGF at low temperature in order to prohibit internalization.

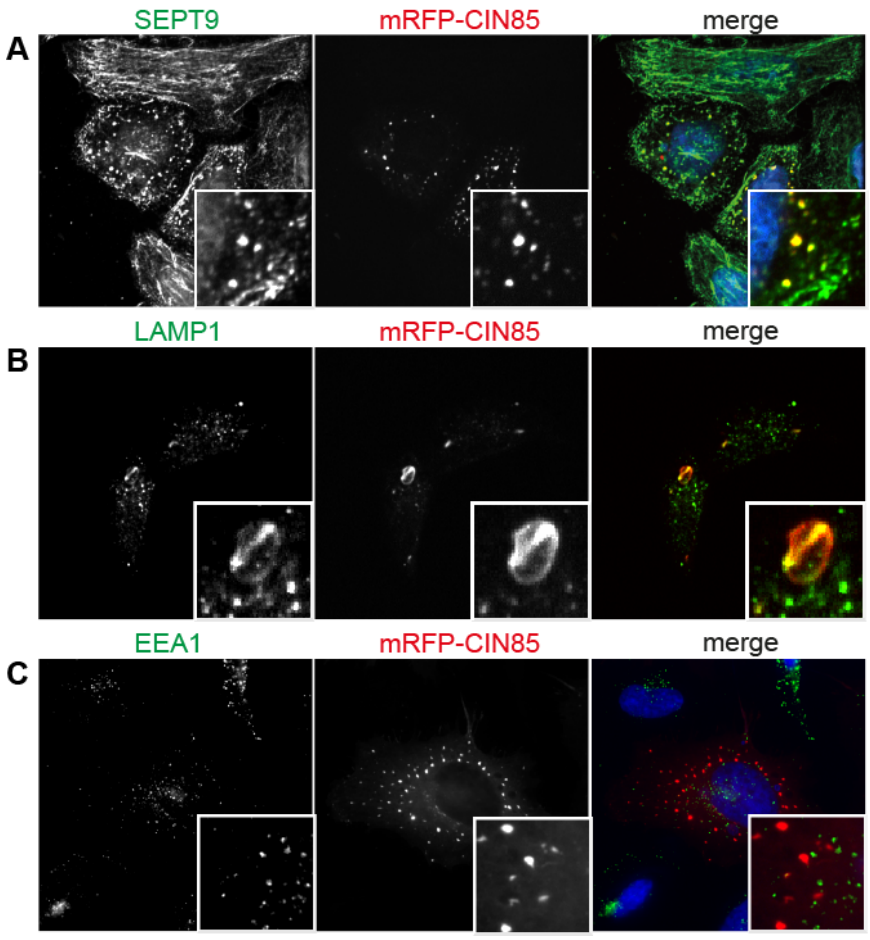


**Fig. 3.11: Overexpression of mRFP-CIN85 recruits endogenous SEPT9**

HeLa cells were transiently transfected with mRFP-CIN85, fixed after 24 h and stained with specific antibodies against SEPT9 **(A)**, the late endosomal marker LAMP1 **(B)** and the early endosomal marker EEA1 **(C)**. Cells were analyzed by epifluorescence microscopy.

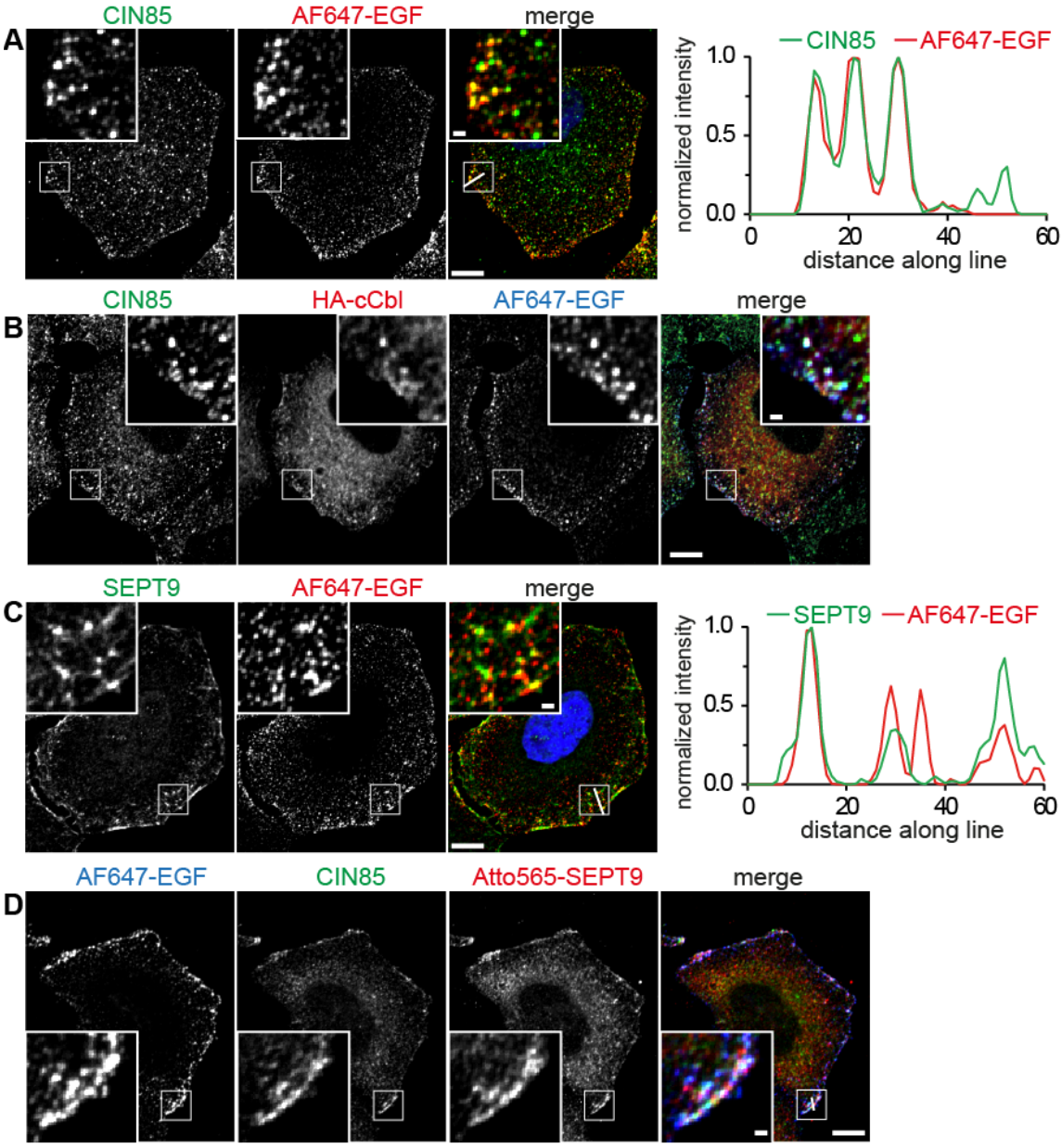


**Fig. 3.12: SEPT9 and CIN85 colocalize at the plasma membrane with activated EGFR**

**(A-D)** Confocal images of HeLa cells treated with 500 ng/ml AF647–EGF at 9°C and stained for CIN85 or SEPT9, respectively. Note that SEPT9 filaments are disrupted upon treatment at low temperatures. Right panels: fluorescence intensity profiles along lines depicted in the merged images. Boxed areas are shown at higher magnification in the insets. **(B)** Cells were transiently transfected with HA-cCbl. **(D)** Cells were immunostained with CIN85 and a SEPT9-antibody, which was directly couled to Atto-565.

We chose this experimental setup to monitor the recruitment of adaptor proteins to endocytic sites at the plasma membrane. As expected, stimulation with EGF induced the recruitment of CIN85 to activated EGFRs at the surface of cells, as monitored by its colocalization with AF647-labelled EGF (Fig. 3.12 A). At these sites CIN85 also colocalized with haemagglutinin epitope (HA)-tagged c-Cbl (Fig. 3.12 B). Importantly, also endogenous SEPT9 colocalized with similar structures (Fig. 3.12 C). The line profile illustrates that only a subfraction of cortical SEPT9 colocalized with activated receptor. Please note that septin filaments get partially disrupted at low temperatures. To answer the question, whether both proteins localize to the same pool of activated EGFR, we aimed to localize SEPT9 and CIN85 simultaneously. Since both antibodies were produced in rabbits, we coupled SEPT9-antibodies directly to a fluorescent dye and found both proteins to be colocalized on the same EGF-positive structures (Fig. 3.12 D).

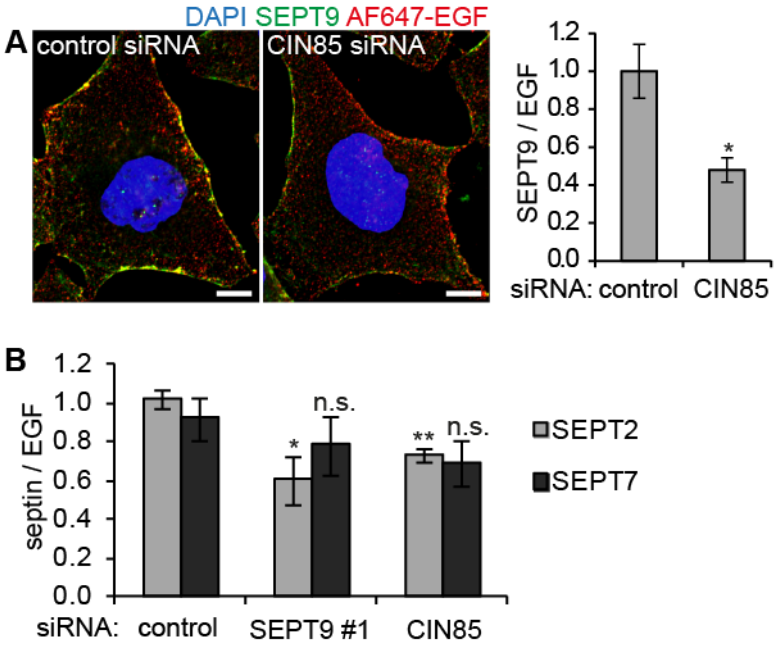


**Fig. 3.13: CIN85 recruits septin oligomers to the plasma membrane**

**(A)** Loss of CIN85 decreases colocalization of SEPT9 with surface-associated EGF. *Left panel:* Confocal images of siRNA-treated cells, which were stimulated with 500 ng/ml AF647-EGF at 9°C and stained for SEPT9. Scale bar: 10 µm. *Right panel:* Colocalization of surface-bound AF647-EGF with SEPT9 was quantified by calculating the amount of SEPT9 found in EGF-positive structures (data were corrected for total EGF bound to the cell surface) (n = 3). **(B)** Loss of CIN85, as well as SEPT9, decreases colocalization of SEPT2 and surface-bound EGF. SiRNA-treated cells were treated and quantified as in (A), but stained for SEPT2 or SEPT7, respectively (n = 3 for SEPT2; n = 2 for SEPT7). All data are depicted as mean ± s.e.m. from n experiments; *P<0.05; **P<0.01; n.s., not significant.

We hypothesized that the recruitment of SEPT9/CIN85 complex to the plasma membrane is mediated by CIN85 and analyzed SEPT9 colocalization with surface-associated EGF in HeLa cells depleted of CIN85. Treatment of cells with CIN85-specific siRNAs efficiently decreased total levels of CIN85 without affecting SEPT9 levels (Fig. 3.13 A). Loss of CIN85 significantly reduced the degree of colocalization between SEPT9 and EGF-positive structures (Fig. 3.13 B). A similar effect could be observed for other septin isoforms co-assembling with SEPT9 such as SEPT2 (Fig. 3.13 C; light gray). Also SEPT7 showed a tendency to less colocalization, but failed to reach statistical significance (dark grey). Depletion of SEPT9 caused a similar effect on SEPT2 and SEPT7. These results indicate that septin complexes are recruited to the plasma membrane in a CIN85/SEPT9-dependent manner, rather than SEPT9 mono- or multimers.

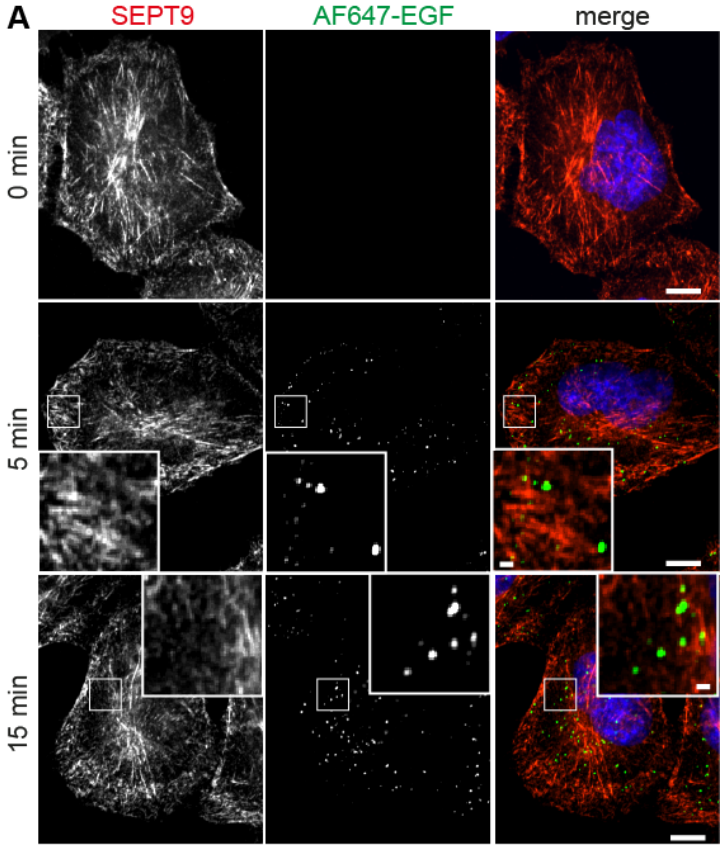


**Fig. 3.14: SEPT9 does not localize to internalized EGF**

HeLa cells were starved and stimulated with 100 ng/ml AF647-EGF at 37°C for the indicated time points. Fixed cells were stained for SEPT9 and analyzed by confocal microscopy. Please note, that cells were treated at 37°C, which leaves SEPT9 filaments unaffected. Scale bar: 10 µm; insets: 1 µm.

### 3.3.2 SEPT9 localizes to activated EGFR exclusively at the plasma membrane

The degradative sorting of EGFRs is initiated at the plasma membrane and persists during intracellular trafficking. CIN85 has been previously suggested to play a role during several steps of endosomal sorting (Dikic 2003; Schroeder et al. 2012). Therefore, we considered a native complex of SEPT9 and CIN85 on endosomes.

To test this hypothesis, we monitored the localization of endogenous SEPT9 during transport of AF647-EGF to early (5 min) and late (15 min) endosomes. SEPT9 remained associated with filaments in the cell periphery during the starvation (0 min) and the EGF stimulation, and displayed no colocalization with internalized EGFRs (Fig. 3.14).

We further validated this negative finding by overexpressing key regulators of endosomal sorting at various stages (Fig. 3.15). First, we stalled endosomal sorting at the level of early endosomes by overexpression of GTP-locked (Q79L) EGFP-Rab5, which induced the formation of giant endosomes (Wegner et al. 2010). These enlarged structures did not accumulate endogenous CIN85 or SEPT9, respectively (panel A/B), but, as expected, the early endosomal marker EEA1 (panel C). Since we detected less recycling in absence of SEPT9 (Fig. 3.3 C), we considered a native SEPT9/CIN85-complex on recycling endosomes. However, neither SEPT9 (Fig. 3.15 panel D) nor CIN85 (panel E) translocated to the recycling compartment, as visualized by overexpressed wild-type EGFP-Rab11.

Given that CIN85 still associates with the EGF receptor at the level of multivesicular bodies (MVBs) and that septins are implicated in ESCRT assembly during mitosis at the site of abscission (Renshaw et al. 2014), we also considered a potential function of the SEPT9/CIN85 complex during the formation of MVBs. We overexpressed a dominant negative version of the ATPase Vps4A (E228Q), which fails to mediate dissociation of the ESCRT-III complex (Baumgärtel et al. 2011). This triggers the accumulation of enlarged, degradative endosomes. As expected, these structures accumulated endogenous CIN85 (Fig. 3.15, panel G), but failed to recruit SEPT9 (panel F). Collectively, these data largely exclude the possibility that a native complex of SEPT9 and CIN85 is assembled on endosomes.

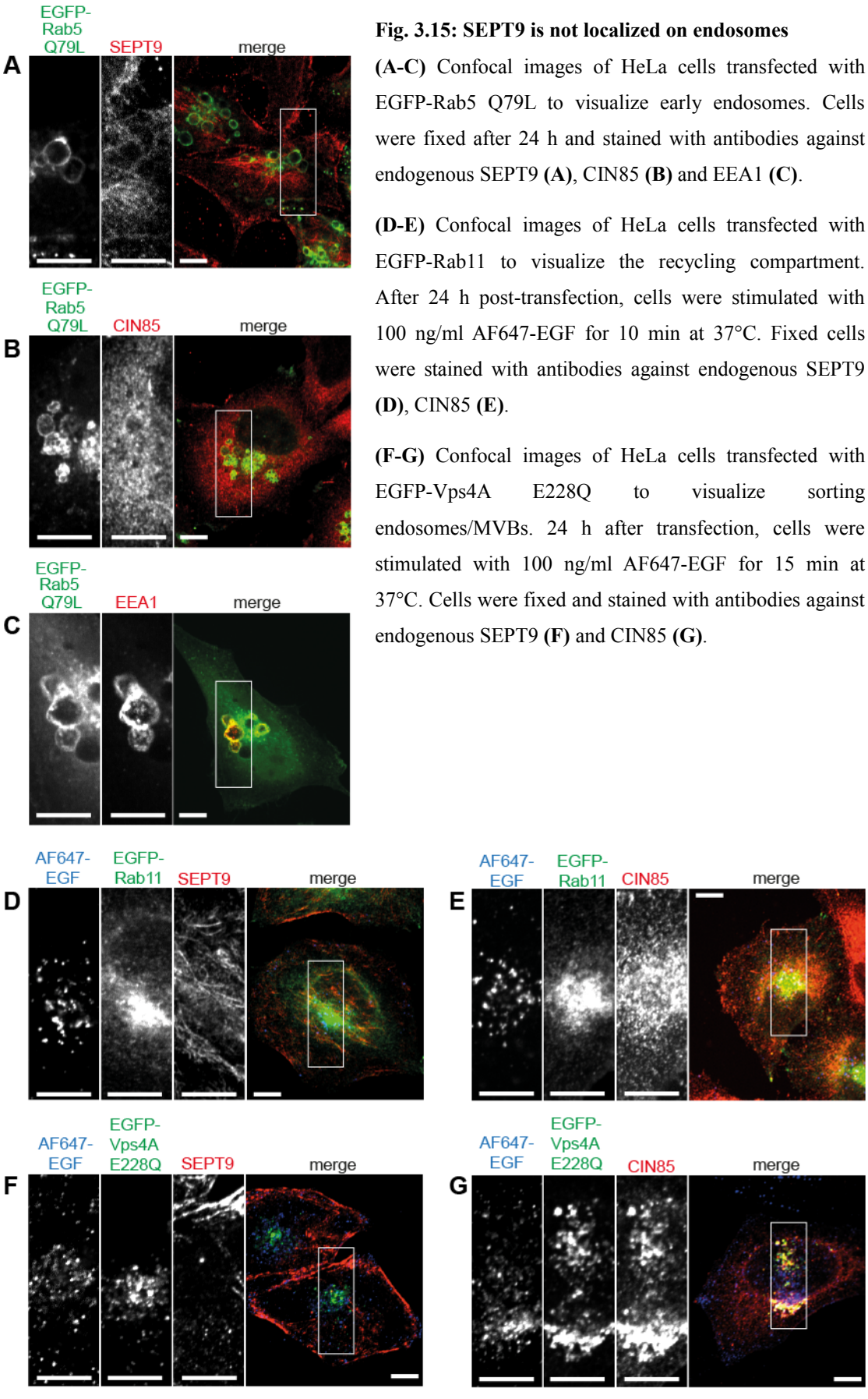


**Fig. 3.15: SEPT9 is not localized on endosomes**

**(A-C)** Confocal images of HeLa cells transfected with EGFP-Rab5 Q79L to visualize early endosomes. Cells were fixed after 24 h and stained with antibodies against endogenous SEPT9 **(A)**, CIN85 **(B)** and EEA1 **(C)**.

**(D-E)** Confocal images of HeLa cells transfected with EGFP-Rab11 to visualize the recycling compartment. After 24 h post-transfection, cells were stimulated with 100 ng/ml AF647-EGF for 10 min at 37°C. Fixed cells were stained with antibodies against endogenous SEPT9 **(D)**, CIN85 **(E)**.

**(F-G)** Confocal images of HeLa cells transfected with EGFP-Vps4A E228Q to visualize sorting endosomes/MVBs. 24 h after transfection, cells were stimulated with 100 ng/ml AF647-EGF for 15 min at 37°C. Cells were fixed and stained with antibodies against endogenous SEPT9 **(F)** and CIN85 **(G)**.

### 3.3.3 EGF stimulation induces SEPT9 association with membranes

Given that septins show the ability to bind to membrane surfaces enriched in phosphoinositides (Zhang et al. 1999; Tanaka-Takiguchi et al. 2009; Bertin et al. 2010), we followed the idea that SEPT9, probably incorporated into a SEPT2/6/7-complex, might associate directly with the plasma membrane. We stimulated cells with increasing doses of EGF at 13°C, where internalisation is prohibited, but adaptor proteins are still recruited to the cell surface. Biochemical cytosol/membrane fractionation of these cells gained insight into the subcellular distribution of SEPT9. As expected, the EGF receptor was detected exclusively in the membrane fraction and EGF stimulation induced the recruitment of the signaling adaptor Grb2 from the cytosol to the membrane (Fig. 3.16 A). Only a small pool of SEPT9 associated with membranes in starved cells. Ligand stimulation induced the recruitment of several septin isoforms (SEPT9, SEPT2, SEPT7) from the cytosol to membranes in a dose-dependent manner. The turnover of SEPT9 from cytosolic to membrane-associated was quantified in (Fig. 3.16 B). These results further validate that a SEPT9-containing complex associates with the plasma membrane upon receptor activation. In conclusion, these results demonstrate that SEPT9 is transiently recruited to ligand-activated EGFRs at the plasma membrane in a CIN85-dependent manner, but is excluded from this complex during, or soon after internalization.

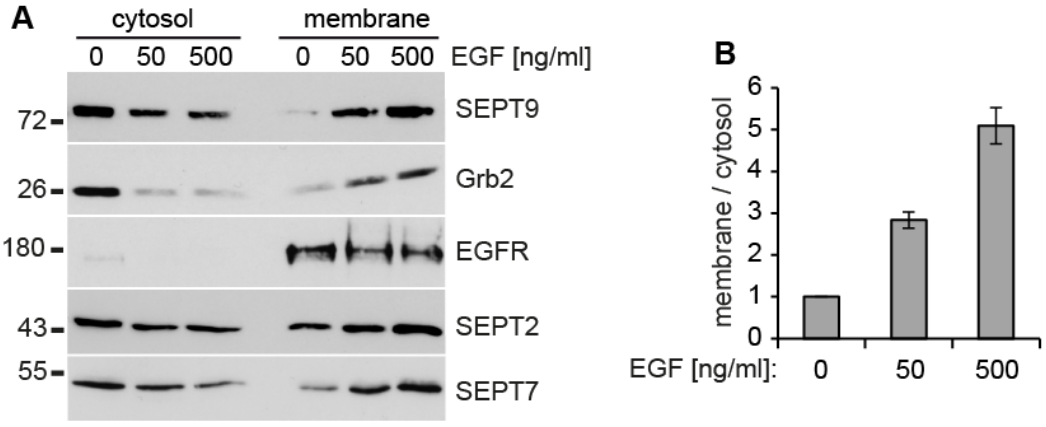


**Fig. 3.16: EGF stimulation induces translocation of septins to membrane**

**(A,B)** Membrane/cytosol fractionation of HeLa cells stimulated with the indicated EGF concentrations for 60 min at 14°C. Equal amounts of both fractions were analyzed by immunoblotting. The ratio of membrane-associated to cytosolic SEPT9 was quantified in **(B)** and is shown as mean ± s.e.m. from 3 experiments.

### 3.3.4 SEPT9 impairs ERK signaling

Given that signaling adaptors, in particular Grb-2, can influence ubiquitin-mediated downregulation of the EGFR (Schmidt & Dikic 2005), we looked at downstream signaling of AKT and MAPK upon loss of SEPT9. As expected, EGF stimulation significantly increased the levels of phosphorylated AKT (P-AKT) (Fig. 3.17 A,B), as monitored by an ELISA-based detection of P-AKT at Ser473. This residue is targeted by PDK2, also known as mTORC2. In line with the decreased receptor surface level, depletion of SEPT9 reduced the level of P-AKT (Ser473) irrespective of the applied EGF dose. This reduction was not caused by altered levels of total AKT (Fig. 3.17 B).

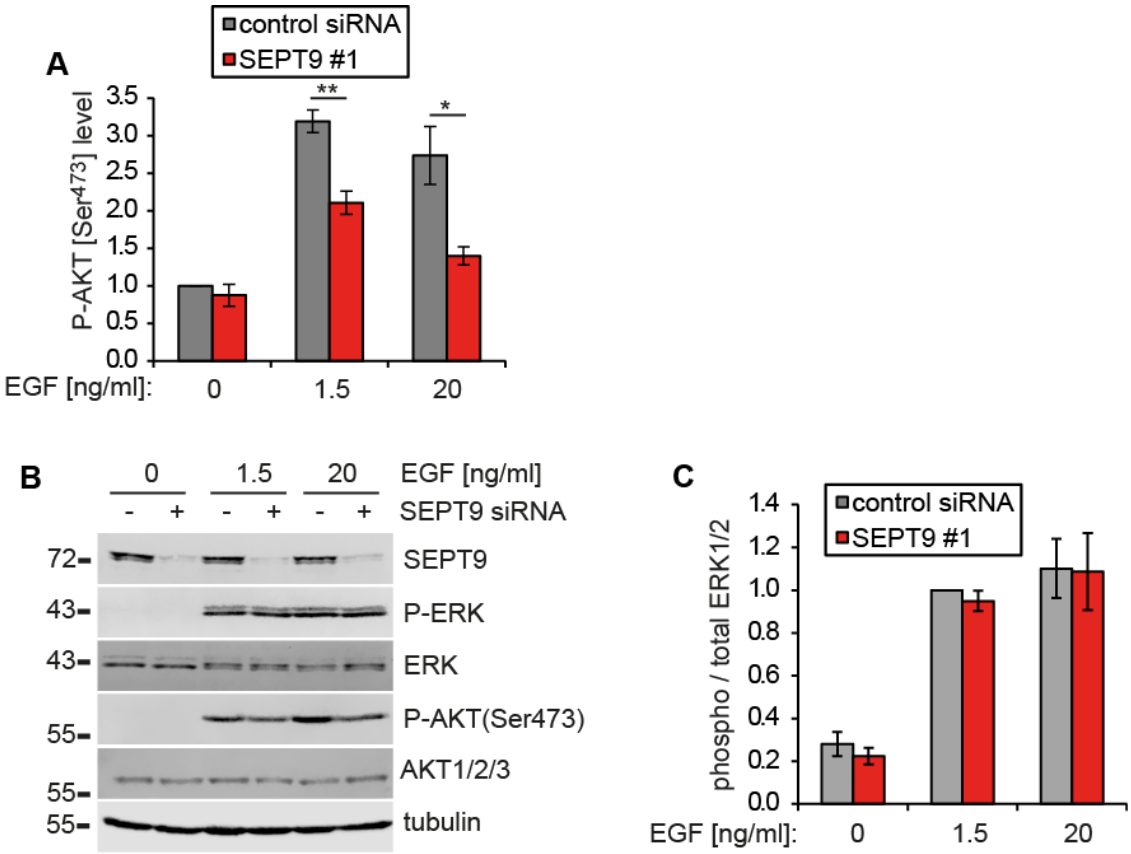


**Fig. 3.17: Effect of SEPT9 depletion on downstream EGFR signaling**

SiRNA-treated HeLa cells were stimulated with the indicated concentrations of EGF for 5 min at 37°C. **(A)** Cell lysates were subjected to ELISA for measuring phospho-AKT [Ser$^{473}$] levels. All values were normalized to the starved control knockdown cells (0 ng/ml EGF). **(B,C)** Cell lysates were analyzed by immunoblotting using the indicated antibodies. Phospho-ERK1/2-levels were quantified in **(C)** and corrected for total ERK1/2-level. Values were normalized to control knockdown cells stimulated with 1.5 ng/ml EGF, since P-ERK1/2 was barely detectable in unstimulated cells. Results are shown as mean ± s.e.m. from n = 3 experiments. Please note, that these values were <u>not</u> corrected for the decreased EGFR surface level in SEPT9 knockdown cells.

Next, we monitored MAPK signaling by immunoblotting using an antibody specific for the active diphosphorylated form of the MAP kinase ERK. Two isoforms are expressed in HeLa cells, which are phosphorylated at T202;Y204 (ERK1) and T185;Y187 (ERK2), respectively. In contrast to AKT, phospho-ERK1/2-level were unaffected and did not correlate with the decreased EGFR surface level (Fig. 3.17 B,C). Together, these findings indicate that SEPT9 knockdown cells can compensate the partial loss of surface receptors with regard to ERK signaling but not to AKT signaling.

## 3.4 SEPT9 regulates Cbl-dependent ubiquitylation of EGF receptors

### *3.4.1 SEPT9 and the E3 ligase Cbl occupy the same binding site on CIN85*

Our findings strongly support a model, by which SEPT9 modulates degradative sorting by associating with EGFR signaling complexes exclusively at the plasma membrane but not on endosomes. The major signal, which determines sorting of EGFR to either recycling or degradation, is its ubiquitylation. A key player responsible for this modification is the E3 ligase Cbl, which is recruited already at the plasma membrane and, as already described above, interacts with CIN85 SH3 domains (Schmidt & Dikic 2005). We thus hypothesized that SEPT9, which we had found to associate with all three SH3 domains of CIN85 (see Fig. 3.6 A,C) competes with Cbl for binding to CIN85. To test this hypothesis we followed a structural approach, in analogy to a recent study, where binding of a Cbl-b-derived peptide to the SH3 A domain of CIN85 was analyzed (Ceregido et al. 2013). We designed a SEPT9-derived peptide containing the PR129/130-signature motif and applied NMR spectroscopy to gain insights into the molecular mechanisms underlying the association of SEPT9 with CIN85 (performed in cooperation with Peter Schmieder). Incubation of the $^{15}$N-labelled SH3 A domain of CIN85 with the SEPT9-derived peptide further confirmed a direct association (Fig. 3.18 A). Moreover, titration of the peptide induced changes in chemical shifts of amino acids clustering in two patches at the C-terminus of the SH3 domain. In addition, a few single residues located in the N-terminal part contributed to ligand binding (Fig. 3.18 B,C). A comparison to Cbl-b-binding (Ceregido et al. 2013) illustrates that both ligands occupied the same binding surface on SH3 A domain of CIN85 (Fig. 3.18 B). This finding led us to the assumption that SEPT9 and Cbl might compete for the same binding sites in CIN85 SH3 domains.

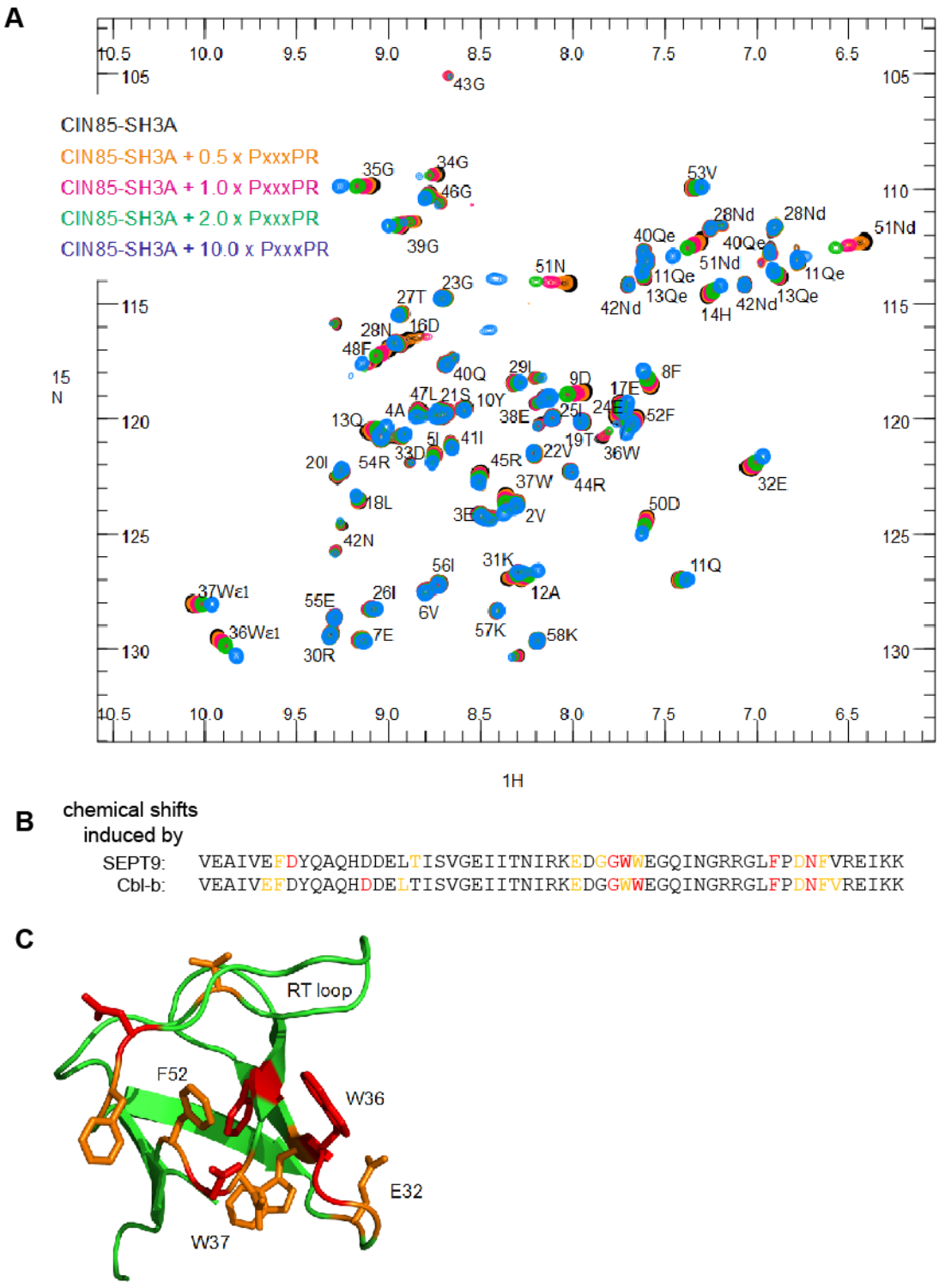


**Fig. 3.18: SEPT9 and Cbl-b share the same binding pocket on CIN85**

**(A)** Overlay of the $^{1}H$, $^{15}N$ HSQC spectra of $^{15}N$-labeled CIN85 SH3 A alone with spectra from samples containing increasing amounts of the SEPT9-derived peptide PxxxPR (no peptide, 0.5x, 1x, 2x, 10x molar equivalents). The resonance assignment is shown next to the peaks. **(B,C)** Sequence and ribbon model of CIN85 SH3 A based on the X-ray structure B2Z8. Residues for which peptide-induced chemical shift changes were observed are highlighted in red and orange. For comparison, Cbl-b-induced chemical shift perturbations in (B) were taken from (Ceregido et al. 2013). These measurements were perfomed by Dr. Peter Schmieder; Leibniz Institute for Molecular Pharmacology, Berlin.

### 3.4.2 SEPT9 competes with Cbl for binding to CIN85

To further follow the idea of SEPT9 competing with Cbl for binding to CIN85, we performed affinity chromatography experiments using GST-tagged CIN85 SH3 A and the SEPT9-derived peptide. As expected, CIN85 SH3 A was able to retain SEPT9 and c-Cbl from cell extracts (Fig. 3.19 A). Titration with the SEPT9-derived peptide occupied binding surfaces of the SH3 domain, thereby decreasing binding of full-length SEPT9. Importantly, also c-Cbl binding was lost from the SH3 domain in a dose-dependent manner. A control peptide, where the conserved PR residues of the binding motif were mutated to alanines, failed to compete with binding of full-length SEPT9 and c-Cbl.

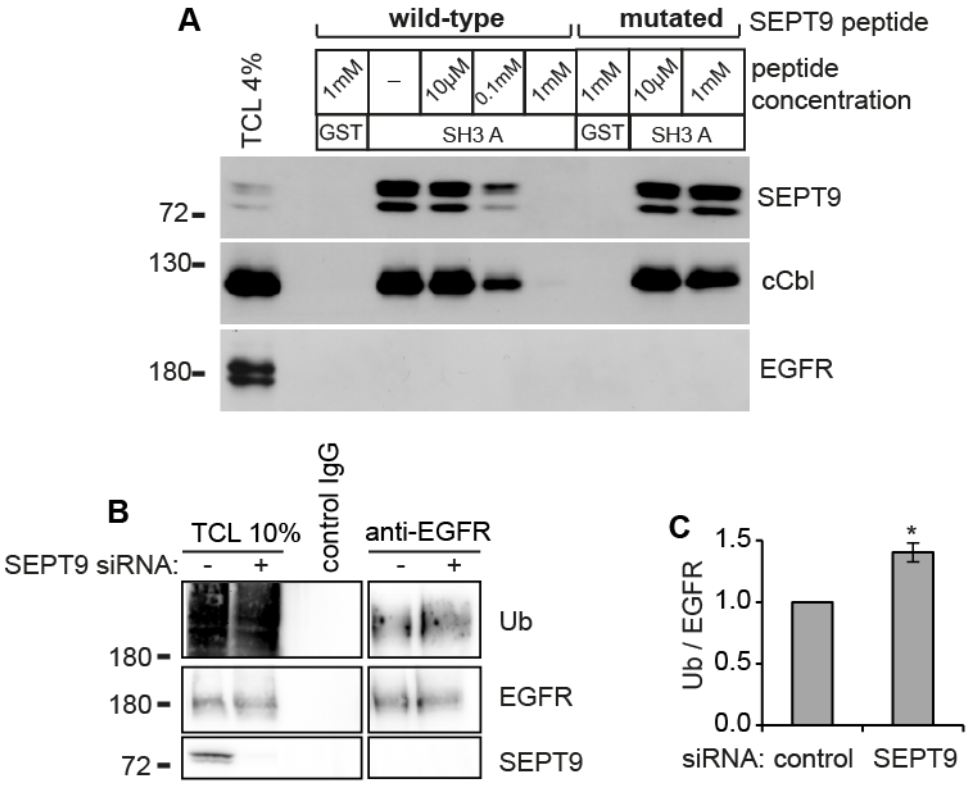


**Fig. 3.19: SEPT9 regulates EGFR ubiquitylation.**

**(A)** SEPT9 and c-Cbl compete for the same binding surface in CIN85. HeLa cells were stimulated with 500 ng/ml EGF at 9°C and subjected to affinity purification using the SH3 A domain of CIN85 as bait. Extracts had been supplemented with increasing concentrations of a SEPT9-derived or a control peptide. **(B,C)** SEPT9 inhibits EGFR ubiquitylation in HeLa cells. SiRNA-treated HeLa cells were stimulated with 100 ng/ml EGF for 30 min at 13°C. Cell extracts were subjected to immunoprecipitation using an EGFR-specific antibody and analyzed by immunoblotting using an ubiquitin-specific antibody. **(C)** The amounts of ubiquitin were quantified by densitometry and normalized to the amount of affinity-purified EGFR. The result is shown as mean ± s.e.m from n = 4 experiments. TCL, total cell lysate; *P<0.05.

The second isoform, Cbl-b, could not be addressed in this experiment due to a lack of corresponding antibodies. This result further confirmed that binding of SEPT9 and Cbl to a single CIN85-SH3 domain is mutually exclusive. In addition, these findings support a model, by which SEPT9 competes with both isoforms, c-Cbl, as well as Cbl-b, for binding to CIN85.

These structural and biochemical data suggest a molecular mechanism by which SEPT9 inhibits EGFR degradation by regulating Cbl-mediated ubiquitylation. To test this hypothesis, we directly assessed EGFR ubiquitylation by affinity-purification of endogenous EGFR from SEPT9 knockdown cells, which were stimulated with EGF at 13°C to inhibit receptor internalization and degradation. Quantitative immunoblotting using an antibody specific for poly- and mono-ubiquitin revealed significantly more ubiquitylated receptor in absence of SEPT9 (Fig. 3.19 B,C). Together, these results provide a molecular explanation for the accelerated degradation observed in SEPT9-depleted cells.

### *3.4.3 SEPT9 regulates Cbl-b-mediated downregulation of EGFR*

In order to further dissect mechanistic details of SEPT9 function, we made use of a proteomic approach based on SILAC (stable isotope labeling with amino acids in cell culture). We cultured cells in presence of amino acids containing heavy or light isotopes, respectively. The cells were surface-stimulated at low temperatures to restrict the analysis to interactors assembled at the level of the plasma membrane and affinity-purified endogenous EGFR from control or SEPT9 knockdown cells. Equal amounts of EGFR from control cells containing heavy isotopes and from SEPT9 knockdown cells containing light isotopes were mixed and analyzed by LC-MS/MS (performed in cooperation with Dr. Eberhard Krause; Leibniz Institute for Molecular Pharmacology, Berlin). The ratio of heavy to light isotopes provides information on changes in the interactome of the receptor. The proteomic analysis identified multiple proteins associated with EGFR under control conditions, which can be roughly divided into adaptors controlling EGFR degradation, signaling or internalization (Fig. 3.20). A full and detailed list of all interactors is provided in appendix 1. In absence of SEPT9, we found three adaptor proteins to be slightly enriched at activated receptors. It should be noted that these hits showed only modest effects and should be interpreted with care.

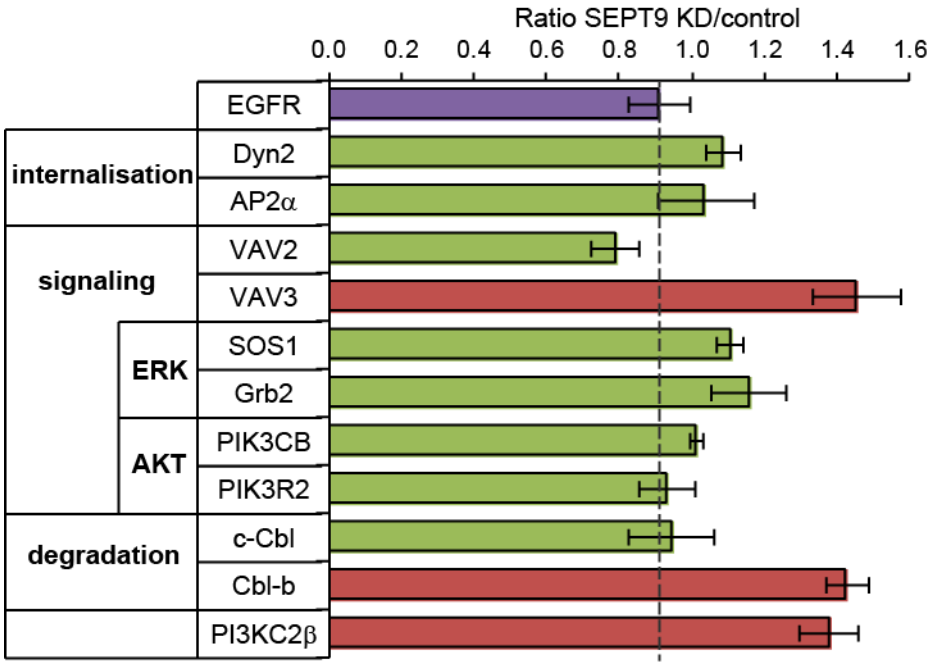


**Fig. 3.20: Proteomic analysis of the EGFR-Interactome after loss of SEPT9**

HeLa cells were kept in medium containing either heavy isotopes of arginine and lysine or light isotopes, respectively, for 8 days in total. Upon siRNA-treatment cells were surface-stimulated with 500 ng/ml EGF and subjected to affinity-purification of EGFR using specific antibodies. Eluates with equal amounts of EGFR from control cells containing heavy isotopes (H) and from SEPT9 knockdown cells containing light isotopes (L) were mixed and analyzed by MS/MS (performed in cooperation with Dr. Eberhard Krause; Leibniz Institute for Molecular Pharmacology, Berlin). The reverse experiment with SEPT9 knockdown cells being labeled was performed in parallel. The ratio L/H (or H/L for the reverse experiment) is shown as mean ± s.e.m from n = 2 experiments for a selected set of proteins. Purple: reference protein; green: unaffected proteins; red: affected proteins. For full list and details see also appendix 1.

As expected, AP-2 and dynamin 2 (Dyn2), both mediators of internalization, were found unaffected by the loss of SEPT9, consistent with unaltered internalization rates in SEPT9 knockdown cells (Fig. 3.3 E,F).

Among the signaling-related proteins, two members of the Vav family were detected, VAV2 and VAV3. The third member of this family, VAV1, is specifically expressed in the hematopoietic system and should not be expressed in HeLa cells (Hornstein et al. 2004). EGF stimulation induces tyrosine-phosphorylation of all three isoforms. They encode a *dbl* homology (DH) region, which exhibits Rho GEF activity; a PI-interacting PH domain; one SH2-domain; two SH3-domains; a proline-rich motif for binding to other SH3-domains; an acidic-rich region and a calponin-homology (CH) region, which binds to actin. These Rho GEFs associate with several signaling adaptors (Zeng et al. 2000; Duan et al. 2011). Whether they also bind directly to EGFR through their SH2-domain was not characterized

yet. VAV proteins are suggested to couple downstream signaling to local Rho activation, thereby regulating EGF-induced cell migration (Fernández-Espartero et al. 2013). Depletion of SEPT9 caused a slightly higher abundance of VAV3, but not VAV2, indicating that SEPT9 might affect Rho-mediated actin remodeling events.

Grb-2 and SOS1 are key activators of MAPK signaling and were unaffected by the absence of SEPT9. Therefore, it can be concluded that the increased phospho-ERK levels observed in SEPT9 knockdown cells (see Fig. 3.17 B,C) are not a consequence of a different abundance of these adaptor proteins. The AKT signaling cascade is initiated mainly by PI3K, which consist of a catalytical (PIK3CB) and a regulatory (PIK3R2) subunit (Engelman et al. 2006). Both of them associated with EGFR in a SEPT9-independent manner. This finding confirms that the reduction of phospho-AKT in absence of SEPT9 (see Fig. 3.17 A,B) is most likely a consequence of the decreased surface receptor level. In addition to this heterodimeric (class I) PI3K, a member of the monomeric class II PI3K, PI3KC2β, was detected. This kinase was slightly enriched at activated receptors in SEPT9 knockdown cells. In contrast to the class I and III PI3K, the functional implication and the lipid specificity of the class II PI3K in EGFR endocytosis is only poorly characterized. It may contribute to the generation of 3' phosphoinositides, in particular PI(3)P and PI(3,4)P2, during internalization (described in chapter 11; page 12).

As expected, two isoforms of Cbl, Cbl-b and c-Cbl, were highly abundant. Importantly, only Cbl-b showed a slightly increased binding in absence of SEPT9, whereas c-Cbl was not affected. Both isoforms share redundant functions in the downregulation of RTKs (Levkowitz et al. 1999), but seem to be recruited in a slightly different temporal manner (Pennock & Wang 2008). In addition, several isoform-specific functions are described in T-cells. For instance, only Cbl-b controls Vav-dependent cytoskeletal remodelling (Schmidt & Dikic 2005). Assuming that this function of Cbl-b is transferrable to EGFR downregulation, the specific enrichment of this isoform would provide an explanation for the simultaneous enrichment of a VAV member. Together, these findings indicate that SEPT9 regulates Cbl-b-mediated downregulation of EGF receptors, which might be connected to VAV3-dependent actin remodelling events.

## 3.5 Identification of novel SEPT9 interaction partners

### *3.5.1 Proteomic analysis of the SEPT9_v3 interactome*

Our finding that the mechanisms underlying SEPT9 function are based on the modulation of specific isoforms supports the idea that SEPT9 associates with several other components of the endocytic network. Additionally, loss of CIN85 decreased recruitment of SEPT9 to activated receptors to 50%, indicating that additional factors are needed for translocation of SEPT9 to the plasma membrane. We aimed to identify these yet unknown factors using a proteomic approach. We affinity-purified overexpressed SEPT9_v3-myc$_6$ from HEK cells and analyzed the eluates by LC-MS/MS (performed by Claudia Gras, in cooperation with Dr. Eberhard Krause; Leibniz Institute for Molecular Pharmacology, Berlin). A full and detailed list of all hits is provided in appendix 2. As expected, CIN85, as well as several septin isoforms, were identified as interactors of SEPT9_v3 (Fig. 3.21). Also other endocytic adaptors, such as AP-2, dynamin 2 and endophilin B, were co-purified, which might be associated indirectly with SEPT9_v3 through binding to CIN85. Among the adaptor proteins, which we assumed to bind in a CIN85-independent manner, we detected a member of sorting nexins, SNX9. All SNX proteins are characterized by a lipid-binding PX domain and most of them are implicated in the endocytic sorting routes (Cullen & Korswagen 2011). SNX9, however, regulates CME at the plasma membrane and might contribute to the recruitment of SEPT9 to the forming pit upon stimulation. Cytoskeleton-associated protein 4 (CKAP4) is an epithelial cell surface receptor for antiproliferative factor (APF) and is suggested to be able to heterodimerize with EGFR (Conrads et al. 2006; Li et al. 2014). This receptor was also identified in the EGFR-interactome at the plasma membrane (see appendix 1) and therefore displays another candidate factor for SEPT9-recruitment. Furthermore, we detected the HECT-type E3 ligase Itch, as well as the deubiquitylating enzyme USP9X, which form part of an EGF-induced negative feedback-loop that downregulates endocytic adaptors: Soon after EGF receptor activation, Cbl and endophilin become targets of Itch ligase activity, thereby marking them for proteasomal degradation (Azakir & Angers 2009). USP9X protects Itch by inhibiting its own EGF-induced autoubiquitylation. Further studies are needed to elucidate, whether SEPT9 participates in degradation not only of EGFR, but also of endocytic adaptors, such as Cbl, by recruiting Itch and/or USP9X to activated receptors.

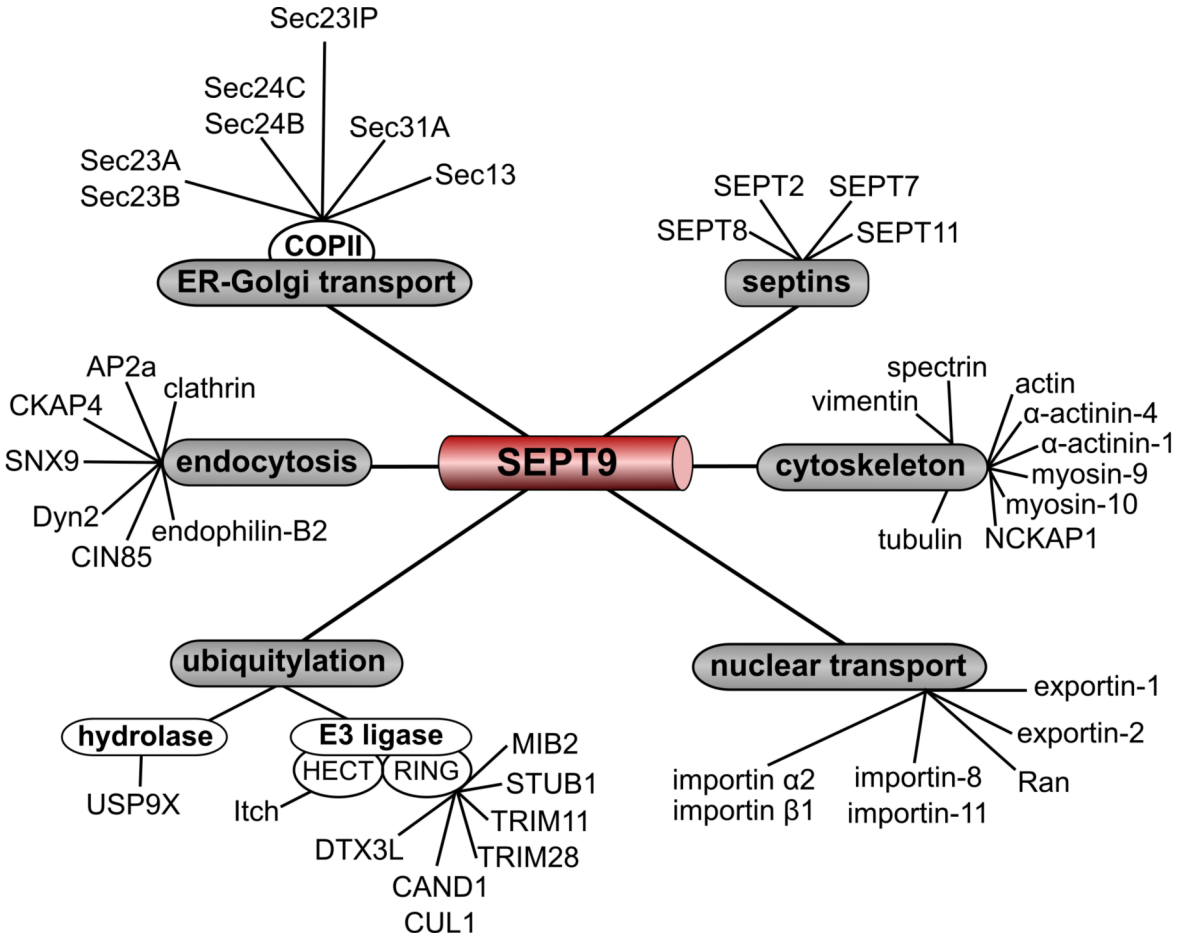


**Fig. 3.21: Proteomic analysis of the SEPT9 interactome**

SEPT9_v3-myc$_6$ was stably expressed in HEK cells and affinity-purified using specific myc-antibodies. Eluates were analyzed by LC-MS/MS (performed by Claudia Gras, in cooperation with Eberhard Krause). A selection of hits was grouped according to cellular processes or components. A full and detailed list is provided in appendix 2.

Along with Itch and USP9X, several other E3 ligases, mainly RING-type ligases, associated with SEPT9_v3. Also cullin 1 (CUL1), a subunit of the multimeric RING-type ligases, and CAND1, a regulator of ligase assembly, were co-purified with SEPT9_v3. These putative interactors further support the hypothesis that SEPT9 is involved in protein stability also of other ubiquitylated targets than the EGF receptor. Accordingly, SEPT9 was shown to be able to regulate the stability of the MAP kinase JNK (Gonzalez et al. 2009).

Furthermore, several components of the COPII-coat were highly enriched. Also Sec23IP, which defines sites for COPII vesicle budding (ER exit sites; ERES) was detected, indicating that SEPT9 is implicated in ER-golgi trafficking by regulating the biogenesis of COPII-vesicles.

In addition, multiple importins and exportins were identified as potential SEPT9

interactors. This is consistent with an implication of SEPT9 in nuclear transport of hypoxia-inducible factor 1α (HIF1α) by interacting with importin-α (Golan & Mabjeesh 2013; Amir et al. 2009).

### *3.5.2 Implications of SEPT9 in membrane trafficking – preliminary data*

Our proteomic analysis provides evidence, that SEPT9 associates with multiple regulators of ubiquitin-dependent protein stability including cullin-containing E3 ligases. We further investigated whether this function can be transferred to other cellular processes, which involve membrane trafficking events. Given that SEPT9, together with F-actin and other septin isoforms, contributes to anti-bacterial autophagy (Mostowy & Cossart 2011b), and that cullin ligases were recently implicated in autophagy (McEwan & Dikic 2014), we considered a potential implication of SEPT9 in autophagy. Immunolocalization of the autophagy marker p62 revealed an upregulation of p62 upon loss of SEPT9 in HeLa cells (Fig. 3.22), indicating that SEPT9 depletion impairs the selective degradation of ubiquitylated cargo by the autophagic machinery. Future studies will need to address the molecular mechanisms underlying underlying SEPT9 functions in autophagy.

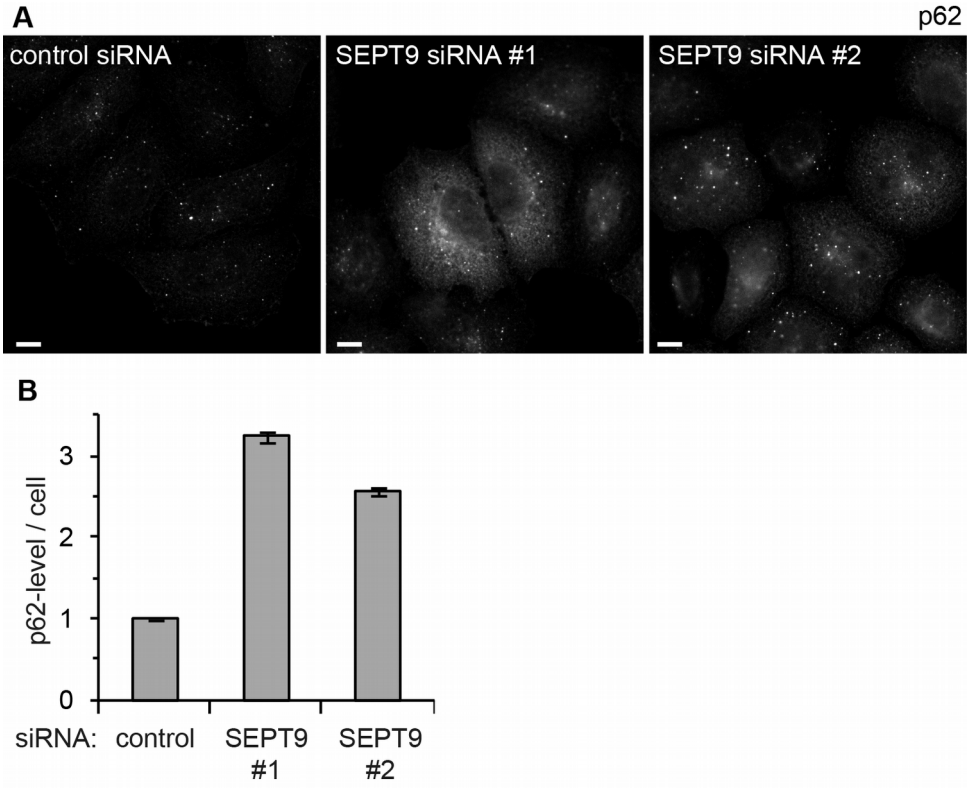


**Fig. 3.22: Loss of SEPT9 causes increased p62-level.**

**(A,B)** SiRNA-treated Hela cells were immunostained with p62-specific antibodies and analyzed using epifluorescence microscopy. Scale bar: 10 µm. Sum intensity / cell was quantified in **(B)** from n = 2 experiments and is shown as mean ± s.e.m.

# 4 Discussion

## 4.1 CIN85 recruits SEPT9-containing complexes to sites of activated EGFR at the plasma membrane

In this study, we implicated the GTPase SEPT9 in Cbl-b-mediated downregulation of the EGF receptor. Our biochemical data (Fig. 3.9; page 79 and Fig. 3.16; page 87) in combination with our colocalisation studies (Fig. 3.13; page 83) support the hypothesis that a SEPT2/6/7/9 oligomeric complex is recruited to sites of EGFR activation at the plasma membrane. Further, we provide evidence that the adaptor protein CIN85 mediates the recruitment of septin complexes to the plasma membrane by interacting with SEPT9, thereby connecting SEPT9 to the EGFR signalosome. We show that CIN85 binds to a proline-rich motif located at aa 125-130 in the N-terminus of SEPT9 (_v3). Our *in vitro* binding studies indicate that this interaction is direct and specific for SEPT9 (Fig. 3.8 B; page 78). However, mutational inactivation of the binding motif in SEPT9 failed to abolish binding completely. Although the inactivation of the two remaining putative binding motifs did not affect the association with CIN85, these motifs might still participate in binding. Loss of CIN85 reduced SEPT9 recruitment to EGFR to ~50% (Fig. 3.13 A; page 83), indicating that also other, unidentified factors contribute to septin localisation at the plasma membrane. A potential factor might be the direct association of septin isoforms to membrane components like PIPs. Studies using recombinant yeast septin complexes revealed a short basic stretch in the N-terminal region of septins that mediates binding to PIPs (Tanaka-Takiguchi et al. 2009). A corresponding stretch is also present in human SEPT9 located at amino acids 271-276 (SEPT9_v3). In combination with our fractionation assay (Fig. 3.16; page 87) we hypothesize that PI(4,5)P2 and PI(3,4,5)P3 accumulating in vicinity of stimulated EGFRs might aid the initial recruitment of SEPT9-containing filaments to the plasma membrane and support their retention at the cell surface. Mutational inactivation of this binding motif in SEPT9 would help to illuminate if membrane association indeed contributes to the recruitment of SEPT9 to activated EGFR. However, whether a septin oligomer or rather a filamentous structure inhibits receptor downregulation, remains an open question. Also, whether oligomers are recruited or formed new in proximity to the receptor, could not be shown here. The simultaneous monitoring of different septin isoforms upon stimulation would allow conclusions about the potential *de novo* formation of septin complexes at the plasma membrane. The use of

TIRF microscopy would be a benefit here, as this technique restricts the detection to events occurring at the plasma membrane. Co-expression of fluorophore-tagged SEPT7 and SEPT9 would further allow the analysis of living cells, assuming that the ligand-induced recruitment to the plasma membrane can also be observed for overexpressed, tagged septin isoforms.

## 4.2 SEPT9 regulates Cbl-b-dependent ubiquitylation of EGF receptors

Our structural (Fig. 3.18; page 90), biochemical (Fig. 3.19; page 91) and proteomic (Fig. 3.20; page 93) data provide evidence that SEPT9 attenuates receptor ubiquitylation by competing with Cbl for binding to CIN85. Thereby, SEPT9 indirectly controls receptor sorting by priming them for ESCRT-dependent sorting into multivesicular bodies. Of note, SEPT9 and Cbl can bind to all three SH3 domains of CIN85 (Kowanetz et al. 2003), potentially allowing the existence of a tripartite CIN85/SEPT9/Cbl complex. How are simultaneous or competing interactions on the three SH3 domains regulated? In a conceivable model the competition of SEPT9 and Cbl is regulated by local concentrations and different affinities for the three SH3 domains of CIN85. An alternative idea is based on a hypothetical model of CIN85 activation: Under unstimulated conditions CIN85 is found in a closed conformation, where SH3 A and B fold back on the Pro-rich-domain (Fig. 4.1; Havrylov et al. 2010). Here, several binding sites, maybe including the SEPT9/Cbl binding site(s), are blocked. Upon EGF stimulation, secondary modifications, such as phosphorylation or ubiquitylation, cause a switch to an open conformation, in which all binding sites for interactors are fully exposed. Assuming that SEPT9 binding to one available SH3 domain stabilizes the closed conformation before stimulation, binding of further Cbl molecules could be prevented upon activation. The assisting role of CIN85 on Cbl activity would be lost, although Cbl and CIN85 are present at the same activated receptor. As a consequence Cbl-mediated ubiquitylation would be inhibited.

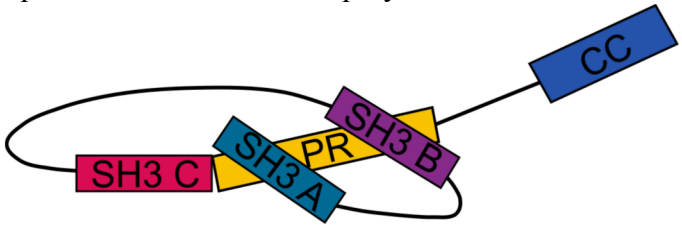


**Fig. 4.1: Hypothetical model for inactive CIN85 conformation**

The SH3 A and B domain of CIN85 fold back on the proline-rich region (PR), thereby blocking binding sites. *CC*: coiled coil. Modified from Havrylov et al. 2010.

Interestingly, our proteomic analysis of the EGFR interactome restricted the competing effect to one specific isoform, Cbl-b. The second isoform, c-Cbl, was also recruited to activated receptor, but in a SEPT9-independent manner. Here, c-Cbl was more abundant than Cbl-b, quantified by the number of peptides identified for the respective isoform (appendix 1). In conclusion, the isoform-specific effect is unlikely to be caused by different local concentrations. Furthermore, this effect is presumably not caused by different affinities of c-Cbl and Cbl-b for CIN85, since ITC measurements showed similar binding affinities to the SH3 domains of CIN85 (Kowanetz et al. 2003). Our biochemical and structural data indicate that the potential to compete with CIN85 is present *in vitro* for both isoforms (Fig. 3.18, Fig. 3.19A; page 91). However, in the cell type used in this study the presence of SEPT9 affected exclusively Cbl-b, indicating that complex formation is regulated by additional, yet unidentified factors.

Our proteomic analysis of the SEPT9 interactome identified CIN85, as expected, but also other endocytic adaptors as potential interaction partners (Fig. 3.21; page 96; appendix 2). Several of these are involved in CME (endophilin-B2, clathrin, SNX9, AP2a, Dyn2), but presumably not affected by SEPT9, since endocytosis is unchanged upon loss of SEPT9 (Fig. 3.3E,F; page 72). Nonetheless, they might support the recruitment of SEPT9 to the plasma membrane. Of note, an interaction between CIN85 and Dyn2 on MVBs has recently been implicated in recycling of EGFRs (Schroeder et al. 2010b). However, a direct role of SEPT9 in this process is unlikely, since we found no evidence for the localization of SEPT9 on recycling endosomes (Fig. 3.15 D; page 86).

Besides Cbl-b numerous other factors have been found to associate with the SH3 domains of CIN85 (Borthwick et al. 2004; Gout et al. 2000; Haglund et al. 2005; Kowanetz et al. 2004; Nikolaienko et al. 2009; Schmidt et al. 2004; Büchse et al. 2011), including proteins involved in EGFR signaling and subcellular trafficking. It is not unlikely that SEPT9 also regulates the formation of those complexes, at least as far as they are assembled at the plasma membrane, and thereby serves to coordinate their activities in time and space. For instance, Sprouty 2 can sequester Cbl away from activated receptor presumably by a mechanism akin to SEPT9 (Haglund et al. 2005). Whether SEPT9 modulates the function of, or acts in concert with Sprouty2, remains to be determined.

Whereas both Cbl isoforms are assumed to have redundant roles in EGFR ubiquitylation, a possible explanation for the isoform-specific effects we observed could be deduced from Cbl function in B and T cells. In this system, both isoforms are expressed

and well characterized in their respective functions. Cbl is recruited into T-cell receptor (TCR) and B-cell receptor (BCR) complexes and fulfils similar functions during receptor downregulation as described above for EGFR (reviewed in Schmidt & Dikic 2005; Lutz-Nicoladoni et al. 2015). However, additional roles were associated to Cbl-b. In T-cells, Cbl-b negatively controls signaling to a Wiskott-Aldrich syndrome protein (WASP)-dependent pathway through ubiquitylation of VAV proteins, thereby inhibiting actin remodelling (Bachmaier et al. 2000; Chiang et al. 2000; Miura-Shimura et al. 2003). We found both, VAV2 and VAV3, to be associated with EGFR in our proteomic approach (Fig. 3.20; page 93). VAV proteins are Rho GEFs that are phosphorylated on tyrosine residues upon EGF stimulation and associate with several signaling adaptors of AKT-, ERK- and PLCγ-dependent signaling pathways (Zeng et al. 2000; Duan et al. 2011). We found only VAV3 to be recruited to EGFR in a SEPT9-sensitive manner. Assuming that the VAV-dependent pathway is also relevant during EGFR signaling, SEPT9 could inhibit VAV3 recruitment to the plasma membrane, thereby regulating the interaction between Cbl-b and its substrate VAV3. In conclusion, SEPT9 might inhibit Cbl-b mediated ubiquitylation of VAV3, thereby activating VAV3-dependent Rho signaling.

An interesting question addresses the biological outcome targeted by this pathway. One of the major downstream targets of Rho GTPases are modulators of actin polymerization (Schmitz et al. 2000). Actin filaments have been suggested to support endocytosis (Boulant et al. 2011; Ferguson et al. 2009; Merrifield et al. 2002; Boucrot et al. 2014), but also endosomal transport (Gasman et al. 2003) and sorting (Puthenveedu et al. 2010; Derivery et al. 2009; Ohashi et al. 2011). Our data largely exclude a role of SEPT9 during endocytosis (Fig. 3.3 C; page 72). However, VAV proteins have been suggested to modulate EGFR sorting towards degradation at the level of endosomes (Thalappilly et al. 2010).

Actin remodeling not only modulates intracellular membrane traffic, but also underlies cell migration, which in turn can be induced by EGF stimulation (Mariotti et al. 2001; Sparatore et al. 2005; Hu et al. 2011; Kawahara et al. 2002). This is presumably mediated by heterodimerization and crosstalk of signaling pathways between EGFR and integrins (Ware et al. 1998). SEPT9-containing complexes might modulate EGF induced migration by assisting Rho-dependent cytoskeletal re-arrangements. In this scenario increased VAV-induced actin remodelling in absence of SEPT9 would activate migratory events. Accordingly, cultured embryonic fibroblasts derived from conditional SEPT9

knock-out mice have been shown to migrate slower than wild-type cells (Füchtbauer et al. 2011). However, if the SEPT9-sensitive recruitment of VAV3 to EGFR at the plasma membrane contributes to actin-dependent sorting of EGFR on endosomes, remains to be determined. SEPT9 might also recruit a different Rho-GEF to EGFR, such as SA-RhoGEF (Nagata & Inagaki 2005), and modulate this factor upon EGF stimulation.

Another hypothesis for a migratory implication describes that SEPT9 might affect the heterodimerization of EGFR with integrins upon EGF stimulation, maybe through the formation of a diffusion barrier. SEPT9 presumably does not affect the stability or subcellular localization of integrins, since surface levels of β1-integrin are unaffected by loss of SEPT9 (Fig. 3.2; page 71). Apparently, further investigations are needed here, since crosstalk from β1-integrin to EGFR is unidirectional (Moro et al. 2002). Thus, SEPT9 might rather affect different integrin isoforms, like i.e. α6β4-integrin, which are regulated upon EGF binding (Braun et al. 1994; Mariotti et al. 2001; Rabinovitz et al. 2004; Rabinovitz et al. 1999).

Given that SEPT9 stabilizes focal adhesions (Dolat et al. 2014) and that CIN85 interacts with the focal adhesion kinases FAK and Pyk2 (Schmidt et al. 2003), it is possible that a CIN85/SEPT9 complex additionally assembles at focal adhesions upon EGF stimulation to modulate cellular adhesion. Cbl regulates cellular attachment by associating with Pyk2 at focal adhesions (Sanjay et al. 2001). SEPT9 might use a similar mechanism here to sequester Pyk2 away from CIN85, thereby potentially modulating cellular adhesion.

Our proteomic analysis revealed a mild increase in PI3KC2β abundance at EGFR (Fig. 3.20; page 93; appendix 1). This class II PI3K presumably produces PI(3)P and/or PI(3,4)P2 upon EGF stimulation (described in chapter 1.1.1; page 12). Theoretically, more PI(3)P on early endosomes in absence of SEPT9 would affect sorting kinetics and early trafficking pathways would be faster. An increased production of PI(3,4)P2 would promote the recruitment of AKT, resulting in enhanced AKT signaling. However, none of these phenotypes can be observed in SEPT9 depleted cells (Fig. 3.3C; page 72 and Fig. 3.17A; page 88). Further studies first have to confirm the increased abundance of PI3KC2β and – more importantly – discover the precise role of this PIP kinase isoform in EGFR associated pathways.

## 4.3 Septin complexes form diffusion barriers

Mammalian septins can form diffusion barriers to restrict diffusion of proteins within cellular membranes (described in chapter 1.2.2; page 27). SEPT9, in complex with other isoforms, might initiate the formation of a diffusion barrier in close proximity of active EGFRs, thereby rigidifying the plasma membrane. Assuming that this barrier is inhibiting the recruitment of CIN85, it could sequester a pool of CIN85 at the plasma membrane, which is no longer available to regulate EGFR ubiquitylation. In absence of SEPT9, this pool may be activated and assist EGFR ubiquitylation, leading to more degradation and – after several cycles of endocytosis – decrease surface receptor level. Moreover, these filaments might serve as scaffolds that recruit further binding partners of the SEPT9 N-terminal domain, or of other septin isoforms co-assembled in the same complex (Hall & Russell 2012).

This study focuses on the best-described SEPT2/6/7/9-complex. However, SEPT9 also forms part of other septin complexes, which are only poorly characterized (Nagata et al. 2004). These isoforms were not experimentally addressed here but could also play so far undiscovered roles. Several aspects indicate a specialized, regulatory role of SEPT9, thereby rendering it a unique member of the family. First, SEPT9 can bind to SEPT2/6/7 complexes in a non-stoichiometric manner, whereby long isoforms of SEPT9 stabilize the formation of higher order oligomers (M. S. Kim et al. 2011). Second, it is assumed that some septin isoforms share redundant functions, potentially allowing the replacement of one missing isoform in a septin oligomer. However, SEPT9 encodes a quite unique and relatively long N-terminal domain, that displays no homology to other septin isoforms. A hypothetical tertiary structure with the bulky N-terminus folding back on the G-domain might allow for an intramolecular regulation of GTPase activity. In this respect, SEPT9 shows the fastest hydrolysis rate of GTP of all septins tested so far (Zent & Wittinghofer 2014). As filament formation and stability depend on the nucleotide binding state of individual septin monomers, it is possible that interactions with the N-terminal region could affect the GTPase activity of SEPT9 in filaments. These changes could induce a remodeling of local septin structures. Other septin isoforms presumably lack the ability to take over these functions. Analysis of the GTP hydrolysis rate of SEPT9 with or without CIN85 would give further insight into this hypothesis. However, these experiments are obstructed by difficulties of the purification of recombinant SEPT9. An optimization of the purification protocol would be needed before being able to address this question.

## 4.4 Putative isoform-specific effects of SEPT9

Studying SEPT9 function is impeded by the fact that the SEPT9 mRNA undergoes extensive splicing and thereby gives rise to eight isoforms that differ in their N-terminal domains (compare Fig. 1.10; page 31). Upon overexpression, these isoforms localize to different cellular compartments, indicating that they exhibit specific functions (Connolly et al. 2011). It is therefore possible that distinct isoforms localize at different stages during EGFR trafficking. The antibody produced for these studies detects only the long isoforms, all of which harbour the atypical proline-rich motif implicated in CIN85 binding. Our data using this antibody demonstrate a colocalization with EGFR exclusively at the plasma membrane, since we were unable to detect SEPT9 on endosomes (Fig. 3.12; page 82). We did not exclude the presence of short isoforms on endosomes. In any case these would have to be recruited by factors other than CIN85, since they lack the necessary motif in the N-terminal domains. We also excluded additional binding of CIN85 to the G-Domain of SEPT9 (Fig. 3.8; page 78), which is preserved in all isoforms. Our knockdown/rescue experiments indicate that SEPT9_v3 is recruited to the plasma membrane and regulates EGFR stability (Fig. 3.5; page 75). Whether also other long isoforms participate or share redundant roles, has not been investigated here.

SEPT9_v1 has been reported to be able to stabilize JNK, a MAP kinase isoform activated upon EGF stimulation (Gonzalez et al. 2009). This function is mediated by the isoform-specific 27 amino acid-long stretch at the N-terminus. Of note, we found a potential function of SEPT9 in modulating ERK signaling, since phospho-ERK level in SEPT9 knockdown cells do not correlate with the decrease of receptor surface level (Fig. 3.17; page 88). This compensation could be explained by the enrichment of Cbl-b at the receptor, which has been suggested to stabilize Grb-2 at EGFR (Huang & Sorkin 2005). However, our proteomic analysis of the EGFR interactome largely excluded changes in the direct association of signaling adaptors to the receptor (Fig. 3.20; page 93). How can ERK-signaling then be upregulated, if it is not modulated at the early initiation phase at the plasma membrane? SEPT9-containing complexes might build a diffusion barrier for the membrane-associated Ras, thereby hindering access to its GEF, SOS. Such an effect would not necessarily be detectable in the EGFR interactome as Ras associates only indirectly with the receptor's cytoplasmic tail (described in chapter 1.1.1; page 11). SEPT9 might also influence downstream events of MAPK signaling, which were not further addressed in this study. We largely excluded an endosomal localization of SEPT9,

but active MAP kinase gets uncoupled from the endosomal sorting pathway and translocates to the cytoplasm. Here, SEPT9_v1 might associate with active JNK, and possibly also with active ERK, and mediate the degradation of these MAP kinases. The existence of a cytoplasmic pool of SEPT9 is verified by our immunostainings and cytosol/membrane fractionation experiments. However, a detailed analysis is needed to clarify if this function is also present for ERK, since unchanged total ERK level (Fig. 3.17 B; page 88) rather indicate that SEPT9 does not regulate ERK stability.

The putative association of SEPT9 to MAPK signaling is supported by our proteomic data that identified the E3 ligase Itch and its corresponding ubiquitin-hydrolase USP9X as potential SEPT9 interactors (Fig. 3.21; page 96; appendix 2). These proteins were associated to a negative-feedback loop on Cbl activity through JNK signaling (Azakir & Angers 2009). In resting cells, Itch activity is inhibited by auto-ubiquitylation. EGF stimulation leads to JNK-dependent phosphorylation of Itch, thereby facilitating an interaction between Itch and USP9X. This enzyme deubiquitylates – and activates – Itch. Itch then targets Cbl for proteasomal degradation by ubiquitylation. In this pathway, SEPT9 might assist Cbl downregulation by promoting USP9X/Itch complex formation. Modulation of this negative feedback loop could provide an additional mechanism for SEPT9 in stabilizing EGFR.

Whether the interaction with CIN85 participates in the modulation of ERK signaling was not addressed here. In head and neck squamous cell carcinomas, CIN85 was shown to be able to modulate EGFR-mediated ERK signaling (Wakasaki et al. 2010). A potential role of SEPT9/CIN85 in MAPK signaling needs to be analyzed in more detail in future studies.

Taken altogether, the following model for SEPT9 function at activated EGFR can be inferred from the data obtained in this study:

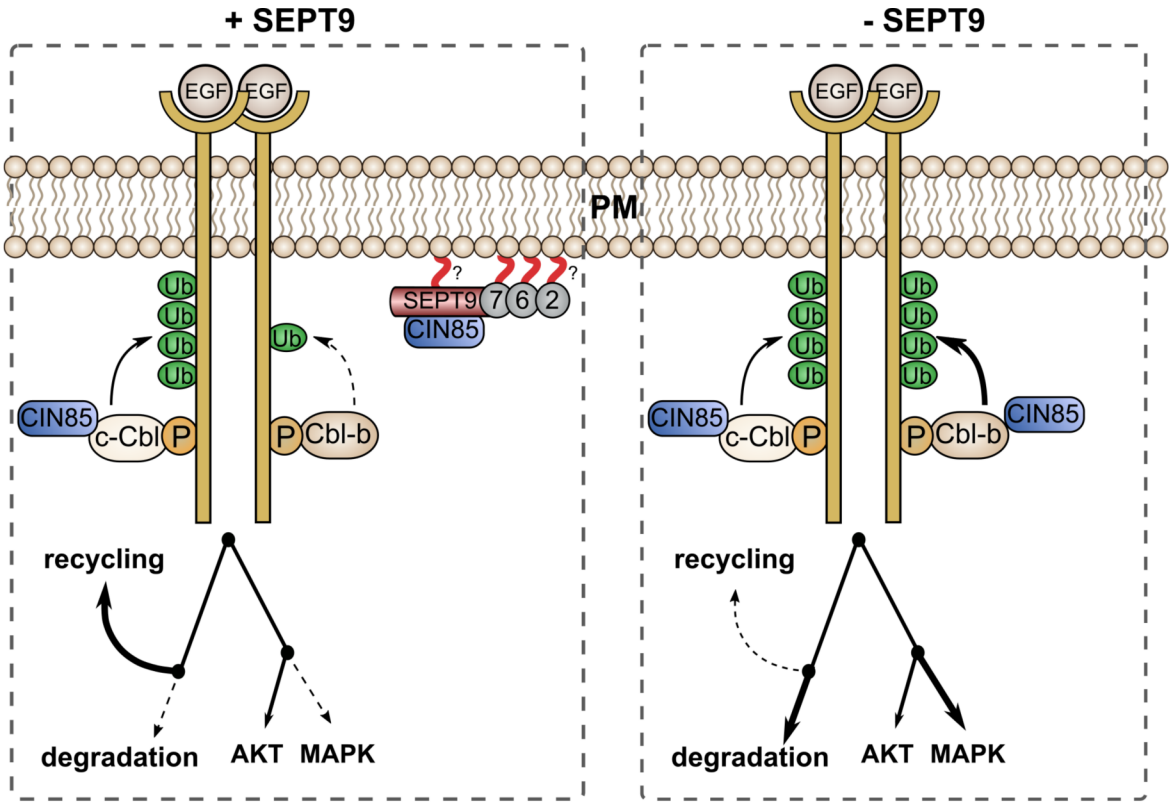


**Fig. 4.2: Hypothetical model of SEPT9 function in stabilizing EGFR at the plasma membrane.**

Upon EGF stimulation, two isoforms of the E3 ligase Cbl, in complex with CIN85, associate with a phosphotyrosine-residue of the activated EGFR at the plasma membrane (PM). Cbl targets EGFR for degradation by ubiquitylation. CIN85 recruits a SEPT9-based complex to sites of activated EGFR at the PM. This localization might be further stabilized by binding of septin subunits to PI(4,5)P2 or PI(3,4,5,)P3 in the PM. By associating with CIN85, SEPT9 competes with the E3 ligase Cbl-b for binding (right receptor side). As a consequence, the assisting role of CIN85 on ligase activity is lost, leading to less ubiquitylation. The isoform c-Cbl (left receptor side) is not affected by SEPT9. Active EGFRs transduce the signal by activating AKT and MAPK signaling pathways. Only MAPK signaling, in particular ERK, is inhibited by SEPT9 presumably by regulating ERK stability. Upon internalisation, the receptor is either recycled back to the plasma membrane or degraded in the lysosome. The SEPT9-induced reduction of EGFR ubiquitylation causes less degradation and enhances the recycling pathway.

## 4.5 A putative role of septin complexes in EGFR trafficking

We provide evidence for the recruitment of a SEPT2/6/7/9-complex to the plasma membrane and showed that SEPT9 is not internalized. We dissected a detailed mechanism for SEPT9 function, but did not explore the relevance of other septin isoforms in detail. Interestingly, three studies indicate a possible function of other septin isoforms in RTK trafficking at later stages of endocytosis. First, a proteomic analysis of endosomal compartments identified phosphorylated SEPT2 cosedimented with early endosomes and SEPT11 with late endosomes (Stasyk et al. 2007). A second large-scale RNAi-based screen identified potential implications of several septin isoforms in endocytosis of different ligands (Liberali et al. 2014). Additionally, a recent study implicates SEPT6 and SEPT7 in AP-3 and ESCRT-dependent biogenesis of MVBs (Traikov et al. 2014). AP-3 facilitates an ubiquitin-independent sorting route to lysosomes through an Alix-dependent pathway (Faúndez et al. 1998; Le Borgne et al. 1998; Poirier et al. 2002; Reusch et al. 2002; Peden et al. 2004; Kent et al. 2012; Dores et al. 2012). SEPT6 and SEPT7 interact with AP-3 on early endosomes and influence the association of ESCRT-components. Interestingly, this process involves the E3 ligase TAL, which ubiquitylates TSG101.

In combination with these studies our data indicate that distinct septin complexes assemble at different levels of endosomal sorting. A SEPT2/6/7/9-complex assembles at the plasma membrane and inhibits receptor ubiquitylation. Upon or during internalization SEPT9 is released, but SEPT2/6/7 may remain associated with active EGFR on AP-3 positive endosomes and regulate ubiquitin-independent lysosomal degradation of EGFR. However, the ubiquitin-independent pathway is only poorly understood and further studies are needed to illuminate the complex role of septin isoforms in EGFR trafficking. In particular the question at which stage SEPT6 and SEPT7 are recruited to activated EGFR remains an open question. Of note, our data indicate that SEPT7 is recruited to activated EGFR at the plasma membrane (Fig. 3.16; page 87), but is dispensable for the regulation of EGFR stability (Fig. 3.2 C; page 71). SEPT9 colocalizes with EGFR exclusively at the plasma membrane (Fig. 3.13A; page 83 and Fig. 3.14; page 84), however, the SEPT2/6/7 complex might be internalized with activated EGFR. Given that SEPT9 shows the unique ability to regulate septin filament assembly (M. S. Kim et al. 2011), SEPT9 might have downstream effects on SEPT6/7 assembly on early endosomes. Colocalisation studies of these septins with an early endosomal marker, such as EEA1, after loss of SEPT9 could

illuminate such an effect. How could such an effect be mediated? As already discussed, SEPT9 might affect Cbl-b/VAV-mediated Rho signaling. Growing evidence supports the hypothesis that Rho signaling can disrupt SEPT9-containing filament assembly (Ito et al. 2005; Nagata & Inagaki 2005). This effect was shown to be mediated by an interaction between SEPT9 and Rhotekin, a regulator of Rho activity. Assuming that Rhotekin, or another septin-binding Rho effector, accumulates at the plasma membrane upon EGF stimulation, ligand-induced Rho signaling might disrupt septin filaments in proximity to activated receptor. A putative involvement of Rho signaling could be experimentally addressed by monitoring the behaviour of septin isoforms upon stimulation with EGF in presence of a Rho inhibitor, such as the exoenzyme C3 (Rubin et al. 1988; Tan et al. 2007). If filaments get disrupted by Rho signaling, altered colocalisation of SEPT6 or SEPT7 should be observed on early endosomes upon inhibitor treatment.

## 4.6 Conclusions and Outlook

### *4.6.1 Trafficking of other RTKs*

This study focuses on trafficking of EGFR as a model system for RTKs. To which degree are these findings transferable to other RTKs, or even to other classes of receptors? The closest relatives of EGFR, HER2-4, act as coreceptors for EGFR (described in chapter 1.1; page 9) and might therefore be directly affected by SEPT9. Cbl also binds and ubiquitylates HER-2 and HER-4, but not HER-3 (Lenferink et al. 1998; Klapper et al. 2000; Meijer et al. 2013; Cao et al. 2007). CIN85, like its paralog CD2AP, is recruited to HER-2, but might also affect HER-4 (Minegishi et al. 2013). In conclusion, it is likely that SEPT9 also affects ubiquitylation of at least HER-2.

Cbl also ubiquitylates other receptor tyrosine kinases, such as FGFR, PDGFR, VEGFR, CSF-1R, HGFR (also known as c-Met), macrophage stimulating protein receptor (Ron), c-Kit and ephrin (EphR) receptors (Miyake et al. 1999; Wilhelmsen et al. 2002; Szymkiewicz et al. 2002; Duval et al. 2003; Penengo et al. 2003; Fasen et al. 2008). Interestingly, CIN85/CD2AP have been shown to contribute to the downregulation of c-Met, PDGFR, c-Kit, VEGFR (Petrelli et al. 2002; Kobayashi et al. 2004). Moreover, several septins including SEPT9 are recruited to stimulated c-Met during invasion of the pathogens *Listeria* and *Shigella* into HeLa cells (Mostowy et al. 2009). The subsequent entry of bacteria appears to depend on CIN85, as well as Cbl-mediated ubiquitylation of

c-Met (Veiga & Cossart 2005). In conclusion, CIN85 might here also act as the major component of the endocytic network, which recruits SEPT9 to the invading pathogen. However, in contrast to EGFR, SEPT9 would not disassociate during internalization, but form intracellular cage-like structures to entrap the pathogen. Further experiments are needed to clarify, whether this intracellular localisation of SEPT9 is specific for an anti-bacterial defense mechanism or also occurs for internalisation of c-Met upon ligand-activation. Binding of the pathogen to c-Met is supposed to mimick ligand binding and causes phosphorylation of multiple intracellular target genes. Interestingly, SEPT9 is phosphorylated at Ser30 upon *Shigella* infection (Schmutz et al. 2013). Whether this modification also occurs upon activation with HGF, or can even be observed upon EGFR activation, would be an interesting question.

Another interesting aspect in this pathway is the role of SEPT9 in targeting the pathogen for autophagy. We showed in this study, that knockdown of SEPT9 leads to an upregulation of p62, an autophagy receptor that promotes degradation of ubiquitylated targets (Fig. 3.22; Komatsu et al. 2007; Pankiv et al. 2007). p62 interacts with both, ubiquitin-conjugated cargo and LC3 on the forming autophagosome. Increased p62 levels negatively correlate with autophagy, indicating an inactivation of autophagy-mediated degradation in SEPT9-depleted cells. SEPT9 might target not only pathogens, but also other cellular proteins, for degradation through autophagy.

In addition, a comprehensive view of the SEPT9 interactome revealed a multitude of E3 ubiquitin ligases (Fig. 3.21; page 96; appendix 2). These potential binding partners included CUL1, a subunit of E3 (SCF) ligases, and CAND1, a key inhibitor of SCF assembly and stability (Zheng et al. 2002; Liu et al. 2002). SEPT9 might regulate the stability of these E3 ligases themselves, but also of their ubiquitylation targets. The potential mechanism for this role might be adapted from our findings. In this study we discovered that SEPT9 can inhibit Cbl activity by competing with an activator of ligase activity, CIN85. Cbl belongs to the monomeric RING-type E3 ligases and is regulated by phosphorylation and/or interaction partners. In comparison, ligase activity of the multimeric RING-type ligases, like the SCF complexes, can be controlled by the assembly of the subunits. CAND1 binds to unneddylated CUL1 and suppresses SCF complex formation (Goldenberg et al. 2004). Neddylation of CUL1 by NEDD8 causes dissociation of CAND1, thereby allowing for complex formation and subsequent activation of the E3 ligase. SEPT9 might bind to the inactive CUL1/CAND1-complex and further stabilize this

interaction by preventing recruitment of NEDD8.

Both results support a role of SEPT9 in the ubiquitylation-network of the cell and is in line with the main finding of this study. Of note, p62 plays diverse roles in the cell, meaning that p62 aggregation is not necessarily connected to autophagy. For instance, Cullin ligases, which might be associated with SEPT9, in combination with p62 aggregation were shown to promote apoptosis (Jin et al. 2009). Further studies would have to focus on autophagy in order to connect the p62 accumulation to an autophagy-related defect. Established markers of autophagy include LC3 conversion and phosphorylation of S6-kinase, a target of mTORC (Nojima et al. 2003; Kim et al. 2002).

In line with the possibility, that SEPT9 is associated to ubiquitylation, an assessment of the ubiquitin-modified proteome revealed that SEPT9 itself presumably gets ubiquitylated at a single lysin residue (W. Kim et al. 2011). SEPT9-ubiquitylation by Cbl is rather unlikely, since we did not detect any indications of a Cbl/SEPT9-complex. The ubiquitin-associated enzymes, which we identified here as potential SEPT9 interactors, might be responsible for dynamically modulating the degree of SEPT9-ubiquitylation. Given that SEPT7 gets ubiquitylated in mammalian cells (Chahwan et al. 2013), SEPT9 might recruit these E3 ligases to septin complexes, thereby mediating ubiquitylation also of other septin isoforms.

### *4.6.2 Biological role of SEPT9 in cancer*

Our biochemical fractionation data revealed a significat recruitment of septins to sites of active receptor only by applying comparably high doses of EGF. This could be due to the fact that only a small pool of receptors is activated at low ligand doses. In this case, the amount of SEPT9 recruited to the membrane could be too small to be detected by immunoblotting. Another possibility is that septin recruitment correlates with the contribution of CIE, which only occurs at high EGF doses. This link would be unidirectional, since SEPT9 is not affecting internalisation (Fig. 3.3 E,F; page 72). This is in line with the observation that several mechanisms act in a cooperative manner during EGFR endocytosis (Goh et al. 2010). In the human body, the exposure of cells to increasing doses of growth factors displays a risk factor, since downstream signaling regulates proliferation and apoptosis rates. Cells might have evolved different ways of internalization in order to prevent a 'hyperstimulation' that would enhance proliferation and simultanously inhibit apoptosis - a hallmark of cancer cells. An interesting question is

where this response is needed on a systemic level. In HeLa cells a concentration of more than ~ 20 ng/ml EGF is needed to monitor degradation with sensitive techniques like radioactively labeled EGF. In this study, we also used concentrations of up to 500 ng/ml EGF. In the human body, the EGF concentration highly depends on the body fluid. Rather low EGF concentrations of 1 – 5 ng/ml are found in plasma and saliva. However, also high ligand doses ranging from 50 – 500 ng/ml are present in bile, urine, milk and prostate fluid (Richards et al. 1983; Grau et al. 1994; Dvorak et al. 2003). It should be noted, that the concentrations used here to stimulate HeLa cells might not be directly transferable to non-cancer epithelial cells, since cancer cells often display increased EGFR or HER2 level (Abramson et al. 2014). Additionally, body fluids confront cells with a multitude of external stimuli. Stimulation of EGFR with different ligands and extensive crosstalk of downstream signaling creates a complex regulation of the biological outcome, which is hard to mimick in cell culture experiments.

In cells exposed to increasing doses of EGF, the switch to CIE would be needed to couple stronger receptor activation to enhanced degradation in order to inhibit proliferation. In this context, the recruitment of septins would act antagonistic to this downregulation, since SEPT9 stabilizes activated receptors.

Long SEPT9 isoforms have been shown upregulated in various tumors, in particular breast cancer (described in chapter 1.4; page 34). Here, SEPT9 upregulation can be found in HER2-positive carcinomas and basal-like carcinomas, which show a strong correlation with EGFR misregulation (Abramson et al. 2014). As already discussed in chapter 4.6.1 (page 108), SEPT9 most likely not only affects EGFR, but also HER-2 ubiquitylation. In conclusion, SEPT9 overexpression in breast cancer cells correlates with misfunctions in HER signaling.

SEPT9, along with other septin isoforms, plays an important role during cytokinesis. However, a misregulation of the cell cycle in cancer cells due to altered SEPT9 levels is rather unlikely, since no significant correlation between SEPT9 levels and proliferation rates could be observed (Scott et al. 2005). Based on our findings, SEPT9 might exhibit a high oncogenic potential in promoting breast tumorigenesis by regulating EGFR stability. This is supported by our rescue experiments, which show that CIN85-associated septin filaments need to contain long isoforms of SEPT9 to protect EGFRs from degradation (Fig. 3.5; page 75).

However, further studies are needed to clarify the mechanism(s) SEPT9 might use to promote tumorigenesis. It also remains to be determined if and to which extent the interaction with CIN85 at activated EGFR may contribute to cancer progression. This process is mainly driven by increasing the migratory potential of cancer cells, which promotes cancer cell invasion. In cultured cells, EGF is known to enhance invasiveness of many breast cancer cells (Wells et al. 2002; Aaronson 1991; Price et al. 1999). As already discussed above, SEPT9 might modulate EGF-induced migration by activating Rho-dependent actin remodelling (page 101). An attractive idea is that this link provides a mechanism for how SEPT9 overexpression – or a misregulation of the ratio of specific isoforms – could enhance cell motility. In line with this hypothesis, Rho signaling was shown to mediate cancer cell invasion (Sahai & Marshall 2003). Several studies also indicate that crosstalk between EGFR/integrin signaling pathways, in particular MAPK signaling, contributes to EGF-induced migration (Wang et al. 1998; Moro et al. 2002; Kawahara et al. 2002). As SEPT9 might modulate ERK and JNK signaling (discussed in chapter 4.4; page 104), it is possible that the CIN85/SEPT9 complex promotes migratory events by mediating crosstalk through MAPK signaling. A potential connection between SEPT9 and growth factor-induced breast cancer cell invasiveness could be experimentally addressed by RNAi-mediated knockdown of SEPT9 in MDA-MB231 cells. This breast cancer cell line migrates upon EGF stimulation and, more importantly, displays an overexpression of long SEPT9 isoforms (Connolly et al. 2011; Price et al. 1999).

In conclusion, SEPT9 could be targeted in future studies as a candidate for a novel biomarker in order to improve the characterization of EGFR-positive breast carcinomas. These carcinomas are sorted into the subgroup triple-negative breast cancer (TNBC), which still lacks reliable biomarkers due to its heterogenity. TNBC-patients are faced with poor prognosis, since targeted therapies, such as the EGFR kinase inhibitor gefitinib, result in only low response rates (Minckwitz et al. 2005). The efficiency of this treatment might increase if combined for instance with the administration of a cell penetrating, SEPT9-derived peptide, which hinders binding of SEPT9 to CIN85.

### 4.6.3 Putative complex formation of CIN85/CD2AP with other septin isoforms

The presence of an endogenous SEPT9/CIN85 complex raises the question whether CIN85 might participate in the potential funtions of other septin isoforms. *In silico* analysis of the aminoacid sequence revealed the presence of putative CIN85-binding motifs also in SEPT1, SEPT4 and SEPT7. Biological functions of SEPT1 are poorly characterized and this isoform was neglected in this study due to a lack of specific antibodies.

SEPT4 is highly expressed in heart, adrenal gland and adult brain (Paavola et al. 1999; Zieger et al. 2000; Larisch et al. 2000). In neurons, SEPT4 might take over the role of SEPT9 and might form a complex with CIN85. CIN85 regulates endocytosis of the dopamin receptor, a G-protein coupled receptor (GPCR) (Shimokawa et al. 2010). A SEPT4/CIN85 complex might regulate the stability also of this receptor, as it is also regulated by mono-ubiquitylation (Kim 2008). This is supported by several studies, which show that SEPT4 might be implicated in different neuropathies (Ihara et al. 2003; Ihara et al. 2007).

SEPT7 could be considered as a potential interactor for CIN85 in epithelial cells. However, loss of CIN85 did not significantly alter colocalisation of cortical SEPT7 with activated EGFR (Fig. 3.13; page 83), indicating that the interaction of CIN85 with septin complexes occurs exclusively through SEPT9, at least at the plasma membrane. In podocytes, SEPT7 was found associated with CD2-associated protein (CD2AP), a homolog of CIN85 (Wasik et al. 2012). CD2AP and CIN85 share the same domain structure and mostly redundant roles. The main difference are a few specific functions described for CD2AP, which are attributed to the presence of four actin-binding motifs in the C-terminal region of CD2AP (Dikic 2002). Both proteins are widely expressed, but only CIN85 shows a high expression in neurons. The experimental differentiation between direct binding to CD2AP or CIN85 is impeded by heterodimerization of these two proteins through their coiled-coil-domain. Of note, the SEPT7/CD2AP interaction was not proved to be direct and could also be mediated by SEPT9.

SEPT9 might potentially be able to bind to both, CIN85 and CD2AP. A complex with CD2AP could be formed at sites, where intense actin remodelling is needed. For example, CD2AP, similar to SEPT9, localizes to the midbody, where the formation of an actomyosin ring is needed to constrict the plasma membrane (Monzo et al. 2005). In dividing cells, SEPT4 also localizes to the midbody in a SEPT9-independent manner (Füchtbauer et al. 2011), indicating that CD2AP might associate with a SEPT9/4-containing heterooligomer,

which mediates abscission. In this case, CD2AP would represent a linker between septin and actin filaments. Of note, also the ESCRT machinery and endosomal trafficking promote the constriction and cleavage of the membrane during cytokinesis (Morita et al. 2007; Gould & Lippincott-schwartz 2009). Therefore, the connection between SEPT9 and the machineries mediating endosomal membrane trafficking could also be implicated in the cytokinetic function of SEPT9. Accordingly, the Rab GTPase Rab35, which is implicated in endosomal recycling processes, was shown to regulate septin localisation at the midbody (Kouranti et al. 2006).

Furthermore, CD2AP plays a role at the immunological synapse (Dustin et al. 1998). This synapse describes the interface between a lymphocyte, like a T cell, and an antigen-presenting cell. Recognition of the antigen is mediated by an oligomeric T-cell receptor complex (TCR). A CD2AP/Cbl complex assembles at the TCR (Chiang et al. 2000; Kirsch et al. 2001). Three findings support a putative physiological importance of SEPT9 in this cell type: (i) SEPT9 shows the highest expression levels in lymphoid cells (Scott et al. 2005). (ii) A T-cell specific SEPT9 knock-out mouse is characterized by a defective T-cell differentiation, in particular a misregulated homeostasis of CD8-positive T-cells (Lassen et al. 2013). (iii) SEPT9 was identified as a candidate tumour suppressor of a subtype of lymphoid cancer (Giefing et al. 2008). In conclusion, a SEPT9/CD2AP complex might also regulate the stability of TCR-components. According to our findings, especially the Cbl-b/VAV pathway might be affected in T-cells by SEPT9.

A detailed analysis of SEPT9 function in the lymphoid system could additionally provide helpful data to illuminate the poorly characterized pathogenesis of HNA (described in chapter 1.3.2; page 33). This neuropathy was associated to point mutations in SEPT9 and is characterized by episodic pain attacks and amyotrophy mainly in one shoulder. Common triggers of attacks are events that strain the immune system, such as immunization, infection, surgery or stress (Laccone et al. 2008). Malfunctions of the immune response, maybe caused by mutated SEPT9 at the immunological synapse of CD8-positive T cells, might explain these episodic attacks.

# 5 Bibliography

Aaronson, S. a., 1991. Growth Factors and Stringent Regulation of Mitogenic Responsiveness to Growth Factors. *Science*, 254(5035), pp.1146–1153.

Abramson, V.G. et al., 2014. Subtyping of triple-negative breast cancer: Implications for therapy. *Cancer*.

Adhikari, A. & Chen, Z.J., 2009. Diversity of Polyubiquitin Chains. *Developmental Cell*, 16(4), pp.485–486.

Ahmad, G. et al., 2014. Cbl-family ubiquitin ligases and their recruitment of CIN85 are largely dispensable for epidermal growth factor receptor endocytosis. *The International Journal of Biochemistry & Cell Biology*, 57, pp.123–134.

Alessi, D.R. et al., 1997. Characterization of a 3-phosphoinositide-dependent protein kinase which phosphorylates and activates protein kinase Balpha. *Current biology : CB*, 7(4), pp.261–269.

Alwan, H. a J., Van Zoelen, E.J.J. & Van Leeuwen, J.E.M., 2003. Ligand-induced lysosomal epidermal growth factor receptor (EGFR) degradation is preceded by proteasome-dependent EGFR de-ubiquitination. *Journal of Biological Chemistry*, 278(37), pp.35781–35790.

Amir, S. et al., 2006. MSF-A interacts with hypoxia-lnducible factor-1a and augments hypoxia-inducible factor transcriptional activation to affect tumorigenicity and angiogenesis. *Cancer Research*, 66(2), pp.856–866.

Amir, S. et al., 2009. SEPT9_v1 up-regulates hypoxia-inducible factor 1 by preventing its RACK1-mediated degradation. *Journal of Biological Chemistry*, 284(17), pp.11142–11151.

Ashizawa, A. et al., 2012. The ubiquitin system and Kaposi's sarcoma-associated herpesvirus. *Frontiers in Microbiology*, 3(FEB), pp.1–10.

Azakir, B. a. & Angers, A., 2009. Reciprocal regulation of the ubiquitin ligase Itch and the epidermal growth factor receptor signaling. *Cellular Signalling*, 21(8), pp.1326–1336.

Babst, M., 2011. MVB vesicle formation: ESCRT-dependent, ESCRT-independent and everything in between. *Current opinion in cell biology*, 23(4), pp.452–7.

Bachmaier, K. et al., 2000. Negative regulation of lymphocyte activation and autoimmunity by the molecular adaptor Cbl-b. *Nature*, 403(6766), pp.211–216.

Bai, X. et al., 2013. Novel septin 9 repeat motifs altered in neuralgic amyotrophy bind and bundle microtubules. *The Journal of cell biology*, 203(6), pp.895–905.

Banfic, H. et al., 2009. Epidermal growth factor stimulates translocation of the class II phosphoinositide 3-kinase PI3K-C2beta to the nucleus. *The Biochemical journal*, 422(1), pp.53–60.

Barbieri, M.A. et al., 2000. Epidermal Growth Factor and Membrane Trafficking. *The Journal of cell biology*, 151(3), pp.539–550.

Baumgärtel, V. et al., 2011. Live-cell visualization of dynamics of HIV budding site interactions with an ESCRT component. *Nature cell biology*, 13(4), pp.469–474.

Beites, C.L., Campbell, K. a & Trimble, W.S., 2005. The septin Sept5/CDCrel-1 competes with alpha-SNAP for binding to the SNARE complex. *The Biochemical journal*, 385(Pt 2), pp.347–353.

Bertin, A. et al., 2010. Phosphatidylinositol-4,5-bisphosphate promotes budding yeast septin filament assembly and organization. *Journal of molecular biology*, 404(4), pp.711–31.

Birmingham, A. et al., 2006. 3' UTR seed matches, but not overall identity, are associated with RNAi off-targets. *Nature methods*, 3(3), pp.199–204.

Le Borgne, R. et al., 1998. The mammalian AP-3 adaptor-like complex mediates the intracellular transport of lysosomal membrane glycoproteins. *Journal of Biological Chemistry*, 273(45), pp.29451–29461.

Borinstein, S.C. et al., 2000. SETA is a multifunctional adapter protein with three SH3 domains that binds Grb2, Cbl, and the novel SB1 proteins. *Cellular Signalling*, 12(11-12), pp.769–779.

Borthwick, E.B. et al., 2004. Multiple domains of Ruk/CIN85/SETA/CD2BP3 are involved in interaction with p85alpha regulatory subunit of PI 3-kinase. *Journal of molecular biology*, 343(4), pp.1135–46.

Boucrot, E. et al., 2014. Endophilin marks and controls a clathrin-independent endocytic pathway . *Nature*, 517(7535), pp.460–465.

Boulant, S. et al., 2011. Actin dynamics counteract membrane tension during clathrin-mediated endocytosis. *Nature cell biology*, 13(9), pp.1124–1131.

Braun, T. et al., 1994. MyoD expression marks the onset of skeletal myogenesis in Myf-5 mutant mice. *Development (Cambridge, England)*, 120(11), pp.3083–3092.

Breitschopf, K. et al., 1998. A novel site for ubiquitination: The N-terminal residue, and not internal lysines of MyoD, is essential for conjugation and degradation of the protein. *EMBO Journal*, 17(20), pp.5964–5973.

Bright, N. a et al., 1997. Dense core lysosomes can fuse with late endosomes and are re-formed from the resultant hybrid organelles. *Journal of cell science*, 110 ( Pt 1, pp.2027–2040.

Bright, N.A., Gratian, M.J. & Luzio, J.P., 2005. Endocytic delivery to lysosomes mediated by concurrent fusion and kissing events in living cells. *Current Biology*, 15(4), pp.360–365.

Buccione, R., Orth, J.D. & McNiven, M. a, 2004. Foot and mouth: podosomes, invadopodia and circular dorsal ruffles. *Nature reviews. Molecular cell biology*, 5(8), pp.647–657.

Büchse, T. et al., 2011. CIN85 interacting proteins in B cells-specific role for SHIP-1. *Molecular & cellular proteomics : MCP*, 10(10), p.M110.006239.

Buck, E. et al., 2006. Inactivation of Akt by the epidermal growth factor receptor inhibitor erlotinib is mediated by HER-3 in pancreatic and colorectal tumor cell lines and contributes to erlotinib sensitivity. *Molecular cancer therapeutics*, 5(8), pp.2051–2059.

Cai, B. et al., 2013. Differential roles of C-terminal eps15 homology domain proteins as vesiculators and tubulators of recycling endosomes. *Journal of Biological Chemistry*, 288(42), pp.30172–30180.

Cao, Z. et al., 2007. Neuregulin-induced ErbB3 downregulation is mediated by a protein stability cascade involving the E3 ubiquitin ligase Nrdp1. *Molecular and cellular biology*, 27(6), pp.2180–2188.

Caudron, F. & Barral, Y., 2009. Septins and the Lateral Compartmentalization of Eukaryotic Membranes. *Developmental Cell*, 16(4), pp.493–506.

Ceregido, M.A. et al., 2013. Multimeric and differential binding of CIN85/CD2AP with two atypical proline-rich sequences from CD2 and Cbl-b*. *The FEBS journal*, 280(14), pp.3399–415.

Cerveira, N., Bizarro, S. & Teixeira, M.R., 2011. MLL-SEPTIN gene fusions in hematological malignancies. *Biological chemistry*, 392(8-9), pp.713–24.

Chahwan, R. et al., 2013. Dma/RNF8 proteins are evolutionarily conserved E3 ubiquitin ligases that target septins. *Cell cycle (Georgetown, Tex.)*, 12(6), pp.1000–8.

Chardin, P. et al., 1993. Human Sos1: a guanine nucleotide exchange factor for Ras that binds to GRB2. *Science (New York, N.Y.)*, 260(5112), pp.1338–1343.

Chiang, Y.J. et al., 2000. Cbl-b regulates the CD28 dependence of T-cell activation. *Nature*, 403(6766), pp.216–220.

Chih, B. et al., 2012. A ciliopathy complex at the transition zone protects the cilia as a privileged membrane domain. *Nature cell biology*, 14(1), pp.61–72.

Clayton, A.H. a et al., 2005. Ligand-induced dimer-tetramer transition during the activation of the cell surface epidermal growth factor receptor-A multidimensional microscopy analysis. *Journal of Biological Chemistry*, 280(34), pp.30392–30399.

Conner, S.D. & Schmid, S.L., 2003. Regulated portals of entry into the cell. *Nature*, 422(6927), pp.37–44.

Connolly, D. et al., 2014. Septin 9 amplification and isoform-specific expression in peritumoral and tumor breast tissue. *Biological chemistry*, 395(2), pp.157–67.

Connolly, D. et al., 2011. Septin 9 isoform expression, localization and epigenetic changes during human and mouse breast cancer progression. *Breast cancer research : BCR*, 13(4), p.R76.

Conrads, T.P. et al., 2006. CKAP4/p63 is a receptor for the frizzled-8 protein-related antiproliferative factor from interstitial cystitis patients. *Journal of Biological Chemistry*, 281(49), pp.37836–37843.

Couet, J., Sargiacomo, M. & Lisanti, M.P., 1997. Interaction of a Receptor Tyrosine Kinase , EGF-R , with Caveolins. *The Journal of biological chemistry*, 272(48), pp.30429–30438.

Crljen, V., Volinia, S. & Banfic, H., 2002. Hepatocyte growth factor activates phosphoinositide 3-kinase C2 beta in renal brush-border plasma membranes. *The Biochemical journal*, 365(Pt 3), pp.791–799.

Cullen, P.J. & Korswagen, H.C., 2011. Sorting nexins provide diversity for retromer-dependent trafficking events. *Nature Cell Biology*, 14(1), pp.29–37.

Cunningham, D.L. et al., 2013. Novel Binding Partners and Differentially Regulated Phosphorylation Sites Clarify Eps8 as a Multi-Functional Adaptor. *PLoS ONE*, 8(4).

Dannhauser, P.N. & Ungewickell, E.J., 2012. Reconstitution of clathrin-coated bud and vesicle formation with minimal components. *Nature Cell Biology*, 14(6), pp.634–639.

Dawson, J.P., Bu, Z. & Lemmon, M. a., 2007. Ligand-Induced Structural Transitions in ErbB Receptor Extracellular Domains. *Structure*, 15(8), pp.942–954.

Derivery, E. et al., 2009. The Arp2/3 Activator WASH Controls the Fission of Endosomes through a Large Multiprotein Complex. *Developmental Cell*, 17(5), pp.712–723.

Dikic, I., 2002. CIN85/CMS family of adaptor molecules. *FEBS letters*, 529(1), pp.110–5.

Dikic, I., 2003. Mechanisms controlling EGF receptor endocytosis and degradation. *Biochemical Society transactions*, 31(Pt 6), pp.1178–81.

Doherty, G.J. & McMahon, H.T., 2009. Mechanisms of endocytosis. *Annual review of biochemistry*, 78, pp.857–902.

Dolat, L. et al., 2014. Septins promote stress fiber–mediated maturation of focal adhesions and renal epithelial motility. *Journal of Cell Biology*, 207(2), pp.225–235.

Domin, J. et al., 1997. Cloning of a human phosphoinositide 3-kinase with a C2 domain that displays reduced sensitivity to the inhibitor wortmannin. *The Biochemical journal*, 326 ( Pt 1, pp.139–147.

Dores, M.R. et al., 2012. AP-3 regulates PAR1 ubiquitin-independent MVB/lysosomal sorting via an ALIX-mediated pathway. *Molecular Biology of the Cell*, 23(18), pp.3612–3623.

Dou, H. et al., 2012. Structural basis for autoinhibition and phosphorylation-dependent activation of c-Cbl. *Nature structural & molecular biology*, 19(2), pp.184–192.

Duan, L. et al., 2011. Negative regulation of EGFR-Vav2 signaling axis by Cbl ubiquitin ligase controls EGF receptor-mediated epithelial cell adherens junction dynamics and cell migration. *Journal of Biological Chemistry*, 286, pp.620–633.

Dustin, M.L. et al., 1998. A novel adaptor protein orchestrates receptor patterning and cytoskeletal polarity in T-cell contacts. *Cell*, 94, pp.667–677.

Duval, M. et al., 2003. Vascular endothelial growth factor-dependent down-regulation of Flk-1/KDR involves Cbl-mediated ubiquitination. Consequences on nitric oxide production from endothelial cells. *Journal of Biological Chemistry*, 278(22), pp.20091–20097.

Dvorak, B. et al., 2003. Increased epidermal growth factor levels in human milk of mothers with extremely premature infants. *Pediatric Research*, 54(1), pp.15–19.

Eden, E.R. et al., 2012. The Role of EGF Receptor Ubiquitination in Regulating Its Intracellular Traffic. *Traffic*, 13(2), pp.329–337.

Engelman, J. a, Luo, J. & Cantley, L.C., 2006. The evolution of phosphatidylinositol 3-kinases as regulators of growth and metabolism. *Nature reviews. Genetics*, 7(August), pp.606–619.

Estey, M.P. et al., 2010. Distinct roles of septins in cytokinesis: SEPT9 mediates midbody abscission. *The Journal of cell biology*, 191(4), pp.741–9.

Estey, M.P., Kim, M.S. & Trimble, W.S., 2011. Septins. *Current biology : CB*, 21(10), pp.R384–7.

Ettenberg, S. a et al., 1999. Cbl-B Inhibits Epidermal Growth Factor Receptor Signaling. *Oncogene*, 18(10), pp.1855–1866.

Fasen, K., Cerretti, D.P. & Huynh-Do, U., 2008. Ligand binding induces Cbl-dependent EphB1 receptor degradation through the lysosomal pathway. *Traffic*, 9(2), pp.251–266.

Faúndez, V., Horng, J.T. & Kelly, R.B., 1998. A function for the AP3 coat complex in synaptic vesicle formation from endosomes. *Cell*, 93(3), pp.423–432.

Ferguson, K.M. et al., 2003. EGF activates its receptor by removing interactions that autoinhibit ectodomain dimerization. *Molecular Cell*, 11(2), pp.507–517.

Ferguson, S.M. et al., 2009. Coordinated actions of actin and BAR proteins upstream of dynamin at endocytic clathrin-coated pits. *Developmental cell*, 17(6), pp.811–822.

Fernández-Espartero, C.H. et al., 2013. GTP exchange factor Vav regulates guided cell migration by coupling guidance receptor signalling to local Rac activation. *Journal of cell science*, 126, pp.2285–93.

Franke, T.F. et al., 1997. Direct regulation of the Akt proto-oncogene product by phosphatidylinositol-3,4-bisphosphate. *Science (New York, N.Y.)*, 275(5300), pp.665–668.

Frech, M. et al., 1997. High affinity binding of inositol phosphates and phosphoinositides to the Pleckstrin homology domain of RAC protein kinase B and their influence on kinase activity. *Journal Of Biological Chemistry*, 272(13), pp.8474–8481.

Füchtbauer, A. et al., 2011. Septin9 is involved in septin filament formation and cellular stability. *Biological chemistry*, 392(8-9), pp.769–77.

Fujishima, K. et al., 2007. Targeted disruption of Sept3, a heteromeric assembly partner of Sept5 and Sept7 in axons, has no effect on developing CNS neurons. *Journal of Neurochemistry*, 102(1), pp.77–92.

Fukazawa, T. et al., 1996. Tyrosine phosphorylation of Cbl upon epidermal growth factor (EGF) stimulation and its association with EGF receptor and downstream signaling proteins. *Journal of Biological Chemistry*, 271(24), pp.14554–14559.

Futter, C.E. et al., 1996. Multivesicular endosomes containing internalized EGF-EGF receptor complexes mature and then fuse directly with lysosomes. *Journal of Cell Biology*, 132(6), pp.1011–1023.

Gadella, T.W. & Jovin, T.M., 1995. Oligomerization of epidermal growth factor receptors on A431 cells studied by time-resolved fluorescence imaging microscopy. A stereochemical model for tyrosine kinase receptor activation. *The Journal of cell biology*, 129(6), pp.1543–1558.

Galperin, E. et al., 2002. EHD3: a protein that resides in recycling tubular and vesicular membrane structures and interacts with EHD1. *Traffic (Copenhagen, Denmark)*, 3(8), pp.575–589.

Gardner, L.B. & Corn, P.G., 2008. Hypoxic regulation of mRNA expression. *Cell Cycle*, 7(13), pp.1916–1924.

Garrett, T.P.J. et al., 2003. The crystal structure of a truncated ErbB2 ectodomain reveals an active conformation, poised to interact with other ErbB receptors. *Molecular Cell*, 11(2), pp.495–505.

Gasman, S., Kalaidzidis, Y. & Zerial, M., 2003. RhoD regulates endosome dynamics through Diaphanous-related Formin and Src tyrosine kinase. *Nature cell biology*, 5(3), pp.195–204.

Ghazi-Tabatabai, S. et al., 2008. Structure and Disassembly of Filaments Formed by the ESCRT-III Subunit Vps24. *Structure*, 16(9), pp.1345–1356.

Giefing, M. et al., 2008. Identification of candidate tumour suppressor gene loci for Hodgkin and Reed-Sternberg cells by characterisation of homozygous deletions in classical Hodgkin lymphoma cell lines. *British Journal of Haematology*, 142(6), pp.916–924.

Gillooly, D.J. et al., 2000. Localization of phosphatidylinositol 3-phosphate in yeast and mammalian cells. *The EMBO journal*, 19(17), pp.4577–4588.

Gladfelter, A.S., 2010. Guides to the final frontier of the cytoskeleton : septins in filamentous fungi. *Current Opinion in Microbiology*.

Goh, L.K. et al., 2010. Multiple mechanisms collectively regulate clathrin-mediated endocytosis of the epidermal growth factor receptor. *The Journal of cell biology*, 189(5), pp.871–83.

Goh, L.K. & Sorkin, A., 2013. Endocytosis of Receptor Tyrosine Kinases. *Cold Spring Harb Perspect Biol*, (5), p.a017459.

Golan, M. & Mabjeesh, N.J., 2013. SEPT9-i1 is required for the association between HIF-1a and importin-a to promote efficient nuclear translocation. *Cell Cycle*, 12(14), pp.2297–2308.

Goldenberg, S.J. et al., 2004. Structure of the Cand1-Cul1-Roc1 complex reveals regulatory mechanisms for the assembly of the multisubunit cullin-dependent ubiquitin ligases. *Cell*, 119(4), pp.517–528.

Gonzalez, M.E. et al., 2007. High SEPT9_v1 expression in human breast cancer cells is associated with oncogenic phenotypes. *Cancer research*, 67(18), pp.8554–64.

Gonzalez, M.E. et al., 2009. Up-regulation of SEPT9_v1 stabilizes c-Jun-N-Terminal Kinase and contributes to its pro-proliferative activity in mammary epithelial cells. *Cell signal*, 21(4), pp.477–487.

Gould, G.W. & Lippincott-schwartz, J., 2009. New roles for endosomes: from vesicular carriers to multi-purpose platforms. , 10(April), pp.287–292.

Gout, I. et al., 2000. Negative regulation of PI 3-kinase by Ruk, a novel adaptor protein. *The EMBO journal*, 19(15), pp.4015–25.

Grau, M. et al., 1994. Relationship between Epidermal Growth Factor in Glands , Plasma , and Bile: Effects of Catecholamines and Fasting. *Endocrinology*, 135(5), pp.1854–1862.

Graus-Porta, D. et al., 1997. ErbB-2, the preferred heterodimerization partner of all ErbB receptors, is a mediator of lateral signaling. *EMBO Journal*, 16(7), pp.1647–1655.

Griffiths, E.K. et al., 2003. Cbl-3-deficient mice exhibit normal epithelial development. *Molecular and cellular biology*, 23(21), pp.7708–7718.

Grøvdal, L.M. et al., 2004. Direct interaction of Cbl with pTyr 1045 of the EGF receptor (EGFR) is required to sort the EGFR to lysosomes for degradation. *Experimental Cell Research*, 300, pp.388–395.

Haglund, K. et al., 2002. Cbl-directed monoubiquitination of CIN85 is involved in regulation of ligand-induced degradation of EGF receptors. *Proceedings of the National Academy of Sciences of the United States of America*, 99(19), pp.12191–12196.

Haglund, K. et al., 2005. Sprouty2 acts at the Cbl/CIN85 interface to inhibit epidermal growth factor receptor downregulation. *EMBO reports*, 6(7), pp.635–41.

Haigler, H., McKanna, J. & Cohen, S., 1979. Rapid induction of morphological changes in human carcinoma cells A-431 by epidermal growth factors. *The Journal of cell biology*, 83(October), pp.260–265.

Hall, P. a & Russell, S.E.H., 2012. Mammalian septins: dynamic heteromers with roles in cellular morphogenesis and compartmentalization. *The Journal of pathology*, 226(2), pp.287–99.

Hallberg, B., Rayter, S.I. & Downward, J., 1994. Interaction of Ras and Raf in intact mammalian cells upon extracellular stimulation. *Journal of Biological Chemistry*, 269(6), pp.3913–3916.

Hansen, C.G., Howard, G. & Nichols, B.J., 2011. Pacsin 2 is recruited to caveolae and functions in caveolar biogenesis. *Journal of cell science*, 124(Pt 16), pp.2777–2785.

Havrylov, S., Redowicz, M.J. & Buchman, V.L., 2010. Emerging roles of Ruk / CIN85 in vesicle-mediated transport , adhesion , migration and malignancy. *Traffic*, 11(6), pp.721–31.

Heuser, J. & Steer, C.J., 1989. Trimeric binding of the 70-kD uncoating ATPase to the vertices of clathrin triskelia: A candidate intermediate in the vesicle uncoating reaction. *Journal of Cell Biology*, 109(4 I), pp.1457–1466.

Hill, E. et al., 2001. The role of dynamin and its binding partners in coated pit invagination and scission. *Journal of Cell Biology*, 152(2), pp.309–323.

Ho, C.-W., Chen, H.-T. & Hwang, J., 2011. UBC9 autosumoylation negatively regulates sumoylation of septins in Saccharomyces cerevisiae. *The Journal of biological chemistry*, 286(24), pp.21826–34.

Hommelgaard, A.M. et al., 2005. Caveolae: Stable membrane domains with a potential for internalization. *Traffic*, 6(3), pp.720–724.

Honegger, a M. et al., 1989. Evidence that autophosphorylation of solubilized receptors for epidermal growth factor is mediated by intermolecular cross-phosphorylation. *Proceedings of the National Academy of Sciences of the United States of America*, 86(3), pp.925–929.

Hornstein, I., Alcover, A. & Katzav, S., 2004. Vav proteins, masters of the world of cytoskeleton organization. *Cellular Signalling*, 16(1), pp.1–11.

Hu, J., Mukhopadhyay, A. & Craig, A.W.B., 2011. Transducer of Cdc42-dependent actin assembly promotes epidermal growth factor-induced cell motility and invasiveness. *Journal of Biological Chemistry*, 286(3), pp.2261–2272.

Hu, Q. et al., 2010. A septin diffusion barrier at the base of the primary cilium maintains ciliary membrane protein distribution. *Science (New York, N.Y.)*, 329(July), pp.436–439.

Hu, Q., Nelson, W.J. & Spiliotis, E.T., 2008. Forchlorfenuron alters mammalian septin assembly, organization, and dynamics. *The Journal of biological chemistry*, 283(43), pp.29563–71.

Huang, F. et al., 2006. Differential regulation of EGF receptor internalization and degradation by multiubiquitination within the kinase domain. *Molecular Cell*, 21, pp.737–748.

Huang, F. & Sorkin, A., 2005. Growth Factor Receptor Binding Protein 2-mediated Recruitment of the RING Domain of Cbl to the Epidermal Support Receptor Endocytosis. *Molecular biology of the cell*, 16(March), pp.1268–1281.

Hynes, N.E. & MacDonald, G., 2009. ErbB receptors and signaling pathways in cancer. *Current Opinion in Cell Biology*, 21(2), pp.177–184.

Ihara, M. et al., 2003. Association of the cytoskeletal GTP-binding protein Sept4/H5 with cytoplasmic inclusions found in Parkinson's disease and other synucleinopathies. *The Journal of biological chemistry*, 278(26), pp.24095–102.

Ihara, M. et al., 2007. Sept4, a component of presynaptic scaffold and Lewy bodies, is required for the suppression of alpha-synuclein neurotoxicity. *Neuron*, 53(4), pp.519–33.

Ito, H. et al., 2005. Possible role of Rho/Rhotekin signaling in mammalian septin organization. *Oncogene*, 24(47), pp.7064–72.

Jiang, X. et al., 2003. Grb2 Regulates Internalization of EGF Receptors through Clathrin-coated Pits. *Molecular biology of the cell*, 14(March), pp.858–870.

Jin, Z. et al., 2009. Cullin3-Based Polyubiquitination and p62-Dependent Aggregation of Caspase-8 Mediate Extrinsic Apoptosis Signaling. *Cell*, 137(4), pp.721–735.

Joberty, G. et al., 2001. Borg proteins control septin organization and are negatively regulated by Cdc42. *Nature cell biology*, 3(10), pp.861–6.

Juvvadi, P.R. et al., 2013. Filamentous fungal-specific septin AspE is phosphorylated in vivo and interacts with actin, tubulin and other septins in the human pathogen Aspergillus fumigatus. *Biochemical and Biophysical Research Communications*, 431(3), pp.547–553.

Kawahara, E. et al., 2002. EGF and beta1 integrin convergently regulate migration of A431 carcinoma cell through MAP kinase activation. *Experimental cell research*, 272(1), pp.84–91.

Kechad, A. et al., 2012. Anillin acts as a bifunctional linker coordinating midbody ring biogenesis during cytokinesis. *Current biology : CB*, 22(3), pp.197–203.

Kent, H.M. et al., 2012. Structural Basis of the Intracellular Sorting of the SNARE VAMP7 by the AP3 Adaptor Complex. *Developmental Cell*, 22(5), pp.979–988.

Kim, D.H. et al., 2002. mTOR interacts with raptor to form a nutrient-sensitive complex that signals to the cell growth machinery. *Cell*, 110(2), pp.163–175.

Kim, D.-S. et al., 2004. Analysis of Mammalian Septin Expression in Human Malignant Brain Tumors. *Neoplasia*, 6(2), pp.168–178.

Kim, M.S. et al., 2011. SEPT9 occupies the terminal positions in septin octamers and mediates polymerization-dependent functions in abscission. *The Journal of cell biology*, 195(5), pp.815–26.

Kim, O.-J., 2008. A single mutation at lysine 241 alters expression and trafficking of the D2 dopamine receptor. *Journal of receptor and signal transduction research*, 28(5), pp.453–464.

Kim, W. et al., 2011. Systematic and quantitative assessment of the ubiquitin-modified proteome. *Molecular Cell*, 44(2), pp.325–340.

Kinoshita, M., 2003. Assembly of Mammalian Septins. *Journal of Biochemistry*, 134(4), pp.491–496.

Kinoshita, M. et al., 1997. Nedd5, a mammalian septin, is a novel cytoskeletal component interacting with actin-based structures. *Genes and Development*, 11, pp.1535–1547.

Kinoshita, M. et al., 2002. Self- and actin-templated assembly of Mammalian septins. *Developmental cell*, 3(6), pp.791–802.

Kirkham, M. & Parton, R.G., 2005. Clathrin-independent endocytosis: New insights into caveolae and non-caveolar lipid raft carriers. *Biochimica et Biophysica Acta - Molecular Cell Research*, 1745, pp.273–286.

Kirsch, K.H. et al., 2001. The Adapter Type Protein CMS/CD2AP Binds to the Proto-oncogenic Protein c-Cbl through a Tyrosine Phosphorylation-regulated Src Homology 3 Domain Interaction. *Journal of Biological Chemistry*, 276(7), pp.4957–4963.

Klapper, L.N. et al., 2000. Tumor-inhibitory antibodies to HER-2/ErbB-2 may act by recruiting c-Cbl and enhancing ubiquitination of HER-2. *Cancer Research*, 60(13), pp.3384–3388.

Klippel, a et al., 1997. A specific product of phosphatidylinositol 3-kinase directly activates the protein kinase Akt through its pleckstrin homology domain. *Molecular and cellular biology*, 17(1), pp.338–344.

Kobayashi, S. et al., 2004. The c-Cbl/CD2AP complex regulates VEGF-induced endocytosis and degradation of Flt-1 (VEGFR-1). *The FASEB journal : official publication of the Federation of American Societies for Experimental Biology*, 18(7), pp.929–931.

Koide, H. et al., 1993. GTP-dependent association of Raf-1 with Ha-Ras: identification of Raf as a target downstream of Ras in mammalian cells. *Proceedings of the National Academy of Sciences of the United States of America*, 90(18), pp.8683–8686.

Komada, M., 2008. Controlling receptor downregulation by ubiquitination and deubiquitination. *Current drug discovery technologies*, 5(1), pp.78–84.

Komatsu, M. et al., 2007. Homeostatic Levels of p62 Control Cytoplasmic Inclusion Body Formation in Autophagy-Deficient Mice. *Cell*, 131(6), pp.1149–1163.

Kornilova, E. et al., 1996. Lysosomal targeting of epidermal growth factor receptors via a kinase- dependent pathway is mediated by the receptor carboxyl-terminal residues 1022-1123. *Journal of Biological Chemistry*, 271(48), pp.30340–30346.

Kouranti, I. et al., 2006. Rab35 Regulates an Endocytic Recycling Pathway Essential for the Terminal Steps of Cytokinesis. *Current Biology*, 16, pp.1719–1725.

Kowanetz, K. et al., 2004. CIN85 Associates with Multiple Effectors Controlling Intracellular Trafficking of Epidermal Growth Factor Receptors. *Molecular biology of the cell*, 15(July), pp.1895–1903.

Kowanetz, K. et al., 2003. Identification of a novel proline-arginine motif involved in CIN85-dependent clustering of Cbl and down-regulation of epidermal growth factor receptors. *The Journal of biological chemistry*, 278(41), pp.39735–46.

Kremer, B.E., Adang, L. a & Macara, I.G., 2007. Septins regulate actin organization and cell-cycle arrest through nuclear accumulation of NCK mediated by SOCS7. *Cell*, 130(5), pp.837–50.

Kremer, B.E., Haystead, T. & Macara, I.G., 2005. Mammalian Septins Regulate Microtubule Stability through Interaction with the Microtubule-binding Protein. *Molecular biology of the cell*, 16(October), pp.4648–4659.

Kuhlenbäumer, G. et al., 2005. Mutations in SEPT9 cause hereditary neuralgic amyotrophy. *Nature genetics*, 37(10), pp.1044–6.

Kuo, Y.-C. et al., 2015. SEPT12 orchestrates the formation of mammalian sperm annulus by organizing core octameric complexes with other SEPT proteins. *Journal of Cell Science*, 128, pp.923–934.

Kurakin, A. V, Wu, S. & Bredesen, D.E., 2003. Atypical recognition consensus of CIN85/SETA/Ruk SH3 domains revealed by target-assisted iterative screening. *The Journal of biological chemistry*, 278(36), pp.34102–9.

Laccone, F. et al., 2008. Dysmorphic syndrome of hereditary neuralgic amyotrophy associated with a SEPT9 gene mutation--a family study. *Clinical genetics*, 74(3), pp.279–83.

Laemmli, U.K., 1970. Cleavage of structural proteins during the assembly of the head of bacteriophage T4. *Nature*, 227(5259), pp.680–685.

Landsverk, M.L. et al., 2009. Duplication within the SEPT9 gene associated with a founder effect in North American families with hereditary neuralgic amyotrophy. *Human Molecular Genetics*, 18(7), pp.1200–1208.

Larisch, S. et al., 2000. A novel mitochondrial septin-like protein, ARTS, mediates apoptosis dependent on its P-loop motif. *Nature cell biology*, 2(12), pp.915–921.

Lassen, L.B. et al., 2013. Septin9 is involved in T-cell development and CD8+ T-cell homeostasis. *Cell and Tissue Research*, 352(3), pp.695–705.

Leipe, D.D. et al., 2002. Classification and evolution of P-loop GTPases and related ATPases. *Journal of molecular biology*, 317(1), pp.41–72.

Lemmon, M. a & Schlessinger, J., 2010. Cell signaling by receptor tyrosine kinases. *Cell*, 141(7), pp.1117–34.

Lemmon, M.A., Schlessinger, J. & Ferguson, K.M., 2014. The EGFR Family : Not So Prototypical Receptor Tyrosine Kinases. *Cold Spring Harb Perspect Biol*, (6), p.a020768.

Lenferink, A.E.G. et al., 1998. Differential endocytic routing of homo- and hetero-dimeric ErbB tyrosine kinases confers signaling superiority to receptor heterodimers. *EMBO Journal*, 17(12), pp.3385–3397.

Lenormand, P. et al., 1993. Growth factors induce nuclear translocation of MAP kinases (p42mapk and p44mapk) but not of their activator MAP kinase kinase (p45mapkk) in fibroblasts. *Journal of Cell Biology*, 122(5), pp.1079–1088.

Leung, S.M. et al., 1998. SNAP-23 requirement for transferrin recycling in Streptolysin-O-permeabilized Madin-Darby canine kidney cells. *The Journal of biological chemistry*, 273(28), pp.17732–17741.

Levkowitz, G. et al., 1999. Ubiquitin ligase activity and tyrosine phosphorylation underlie suppression of growth factor signaling by c-Cbl/Sli-1. *Molecular cell*, 4, pp.1029–1040.

Li, L. et al., 2011. Proteins linked to extinction in contextual fear conditioning in the C57BL/6J mouse. *Proteomics*, 11(18), pp.3706–3724.

Li, S. et al., 2014. CKAP4 inhibited growth and metastasis of hepatocellular carcinoma through regulating EGFR signaling. *Tumor Biology*, 35(8), pp.7999–8005.

Liberali, P., Snijder, B. & Pelkmans, L., 2014. A Hierarchical Map of Regulatory Genetic Interactions in Membrane Trafficking. *Cell*, 157(6), pp.1473–1487.

Lidke, D.S. et al., 2010. ERK nuclear translocation is dimerization-independent but controlled by the rate of phosphorylation. *Journal of Biological Chemistry*, 285(5), pp.3092–3102.

Liu, J. et al., 2002. NEDD8 modification of CUL1 dissociates p120CAND1, an inhibitor of CUL1-SKP1 binding and SCF ligases. *Molecular Cell*, 10(6), pp.1511–1518.

Longtine, M.S. & Bi, E., 2003. Regulation of septin organization and function in yeast. *Trends in Cell Biology*, 13(8), pp.403–409.

Longva, K.E. et al., 2002. Ubiquitination and proteasomal activity is required for transport of the EGF receptor to inner membranes of multivesicular bodies. *Journal of Cell Biology*, 156(5), pp.843–854.

Low, C. & Macara, I.G., 2006. Structural analysis of septin 2, 6, and 7 complexes. *The Journal of biological chemistry*, 281(41), pp.30697–706.

Lowenstein, E.J. et al., 1992. The SH2 and SH3 domain-containing protein GRB2 links receptor tyrosine kinases to ras signaling. *Cell*, 70(3), pp.431–442.

Lu, Q. et al., 2003. TSG101 interaction with HRS mediates endosomal trafficking and receptor down-regulation. *Proceedings of the National Academy of Sciences of the United States of America*, 100(13), pp.7626–7631.

Luhtala, N. & Odorizzi, G., 2004. Bro1 coordinates deubiquitination in the multivesicular body pathway by recruiting Doa4 to endosomes. *Journal of Cell Biology*, 166(5), pp.717–729.

Lund, K.A. et al., 1990. Quantitative analysis of the endocytic system involved in hormone-induced receptor internalization. *Journal of Biological Chemistry*, 265(26), pp.15713–15723.

Lurje, G. & Lenz, H.-J., 2009. EGFR signaling and drug discovery. *Oncology*, 77(6), pp.400–410.

Lutz-Nicoladoni, C., Wolf, D. & Sopper, S., 2015. Modulation of Immune Cell Functions by the E3 Ligase Cbl-b. *Frontiers in Oncology*, 5(March), pp.1–14.

Maffucci, T. et al., 2003. Insulin induces phosphatidylinositol-3-phosphate formation through TC10 activation. *EMBO Journal*, 22(16), pp.4178–4189.

Magnifico, A. et al., 2003. WW Domain HECT E3s Target Cbl RING Finger E3s for Proteasomal Degradation. *Journal of Biological Chemistry*, 278(44), pp.43169–43177.

Mariotti, A. et al., 2001. EGF-R signaling through Fyn kinase disrupts the function of integrin ??6??4 at hemidesmosomes: Role in epithelial cell migration and carcinoma invasion. *Journal of Cell Biology*, 155(4), pp.447–457.

Massol, R.H. et al., 2006. A burst of auxilin recruitment determines the onset of clathrin-coated vesicle uncoating. *Proceedings of the National Academy of Sciences of the United States of America*, 103(27), pp.10265–10270.

Matsuda, S. et al., 1992. Xenopus MAP kinase activator: identification and function as a key intermediate in the phosphorylation cascade. *The EMBO journal*, 11(3), pp.973–982.

Mayevska, O. et al., 2006. Expression of adaptor protein Ruk/CIN85 isoforms in cell lines of various tissue origins and human melanoma. *Experimental oncology*, 28(4), pp.275–81.

McDonald, B. & Martin-Serrano, J., 2008. Regulation of Tsg101 Expression by the Steadiness Box: A Role of Tsg101-associated Ligase. *Molecular biology of the cell*, 19(1), pp.754–763.

McEwan, D.G. & Dikic, I., 2014. Cullins Keep Autophagy under Control. *Developmental Cell*, 31(6), pp.675–676.

McMahon, H.T. & Boucrot, E., 2011. Molecular mechanism and physiological functions of clathrin-mediated endocytosis. *Nature reviews. Molecular cell biology*, 12(8), pp.517–33.

McMurray, M. a & Thorner, J., 2009. Septins: molecular partitioning and the generation of cellular asymmetry. *Cell division*, 4, p.18.

Meijer, I.M.J. et al., 2013. Cbl and Itch binding sites in ERBB4 CYT-1 and CYT-2 mediate K48- and K63-polyubiquitination, respectively. *Cellular Signalling*, 25(2), pp.470–478.

Melikova, M.S., Kondratov, K. a. & Kornilova, E.S., 2006. Two different stages of epidermal growth factor (EGF) receptor endocytosis are sensitive to free ubiquitin depletion produced by proteasome inhibitor MG132. *Cell Biology International*, 30(1), pp.31–43.

Menon, M.B. et al., 2014. Genetic Deletion of SEPT7 Reveals a Cell Type-Specific Role of Septins in Microtubule Destabilization for the Completion of Cytokinesis. *PLoS Genetics*, 10(8), p.e1004558.

Merrifield, C.J. et al., 2002. Imaging actin and dynamin recruitment during invagination of single clathrin-coated pits. *Nature cell biology*, 4(September 2002), pp.691–698.

Mettlen, M. et al., 2009. Dissecting dynamin's role in clathrin-mediated endocytosis. *Biochemical Society transactions*, 37(Pt 5), pp.1022–1026.

Meyer, C. et al., 2009. New insights to the MLL recombinome of acute leukemias. *Leukemia : official journal of the Leukemia Society of America, Leukemia Research Fund, U.K*, 23, pp.1490–1499.

Miller, K. et al., 1986. Localization of the epidermal growth factor (EGF) receptor within the endosome of EGF-stimulated epidermoid carcinoma (A431) cells. *The Journal of cell biology*, 102(2), pp.500–509.

Mills, I.G., Urbé, S. & Clague, M.J., 2001. Relationships between EEA1 binding partners and their role in endosome fusion. *Journal of cell science*, 114(Pt 10), pp.1959–1965.

Minckwitz, G. et al., 2005. A multicentre phase II study on gefitinib in taxane- and anthracycline-pretreated metastatic breast cancer. *Breast Cancer Research and Treatment*, 89(2), pp.165–172.

Minegishi, Y. et al., 2013. Adaptor protein complex of FRS2β and CIN85/CD2AP provides a novel mechanism for ErbB2/HER2 protein downregulation. *Cancer Science*, 104(3), pp.345–352.

Mitchell, L. et al., 2011. Regulation of septin dynamics by the Saccharomyces cerevisiae lysine acetyltransferase NuA4. *PloS one*, 6(10), p.e25336.

Miura-Shimura, Y. et al., 2003. Cbl-mediated ubiquitinylation and negative regulation of Vav. *Journal of Biological Chemistry*, 278(40), pp.38495–38504.

Miyake, S. et al., 1999. Cbl-mediated Negative Regulation of Platelet-derived Growth Factor Receptor-dependent Cell Proliferation. , 274(23), pp.16619–16628.

Monzo, P. et al., 2005. Clues to CD2-associated protein involvement in cytokinesis. *Molecular biology of the cell*, 16(6), pp.2891–2902.

Morita, E. et al., 2007. Human ESCRT and ALIX proteins interact with proteins of the midbody and function in cytokinesis. *The EMBO journal*, 26(19), pp.4215–27.

Moro, L. et al., 2002. Integrin-induced epidermal growth factor (EGF) receptor activation requires c-Src and p130Cas and leads to phosphorylation of specific EGF receptor tyrosines. *Journal of Biological Chemistry*, 277(11), pp.9405–9414.

Mostowy, S. et al., 2009. Septins regulate bacterial entry into host cells. *PloS one*, 4(1), p.e4196.

Mostowy, S. & Cossart, P., 2011a. Autophagy and the cytoskeleton. *Autophagy*, 7(July), pp.1–3.

Mostowy, S. & Cossart, P., 2011b. Autophagy and the cytoskeleton. *Autophagy*, 7(7), pp.780–782.

Mostowy, S. & Cossart, P., 2011c. Septins as key regulators of actin based processes in bacterial infection. *Biological chemistry*, 392(8-9), pp.831–5.

Mostowy, S. & Cossart, P., 2012. Septins: the fourth component of the cytoskeleton. *Nature reviews. Molecular cell biology*, 13(3), pp.183–94.

Motley, A. et al., 2003. Clathrin-mediated endocytosis in AP-2-depleted cells. *Journal of Cell Biology*, 162(5), pp.909–918.

Mundy, D.I. et al., 2002. Dual control of caveolar membrane traffic by microtubules and the actin cytoskeleton. *Journal of cell science*, 115(Pt 22), pp.4327–4339.

Muriel, O. et al., 2011. Phosphorylated filamin A regulates actin-linked caveolae dynamics. *Journal of cell science*, 124(Pt 16), pp.2763–2776.

Muzioł, T. et al., 2006. Structural Basis for Budding by the ESCRT-III Factor CHMP3. *Developmental Cell*, 10(6), pp.821–830.

Nagata, K. et al., 2004. Biochemical and cell biological analyses of a mammalian septin complex, Sept7/9b/11. *The Journal of biological chemistry*, 279(53), pp.55895–904.

Nagata, K.-I. & Inagaki, M., 2005. Cytoskeletal modification of Rho guanine nucleotide exchange factor activity: identification of a Rho guanine nucleotide exchange factor as a binding partner for Sept9b, a mammalian septin. *Oncogene*, 24(1), pp.65–76.

Nam, J.-M. et al., 2007. CIN85, a Cbl-interacting protein, is a component of AMAP1-mediated breast cancer invasion machinery. *The EMBO journal*, 26(3), pp.647–656.

Näthke, I.S. et al., 1992. Folding and trimerization of clathrin subunits at the triskelion hub. *Cell*, 68(5), pp.899–910.

Nikolaienko, O. et al., 2009. Intersectin 1 forms a complex with adaptor protein Ruk/CIN85 in vivo independently of epidermal growth factor stimulation. *Cellular signalling*, 21(5), pp.753–9.

Nojima, H. et al., 2003. The mammalian target of rapamycin (mTOR) partner, raptor, binds the mTOR substrates p70 S6 kinase and 4E-BP1 through their TOR signaling (TOS) motif. *Journal of Biological Chemistry*, 278(18), pp.15461–15464.

Normanno, N. et al., 2006. Epidermal growth factor receptor (EGFR) signaling in cancer. *Gene*, 366, pp.2–16.

Oh, Y. & Bi, E., 2011. Septin structure and function in yeast and beyond. *Trends in Cell Biology*, 21(3), pp.141–148.

Ohashi, E. et al., 2011. Receptor Sorting within Endosomal Trafficking Pathway is Facilitated by Dynamic Actin Filaments. *PLoS ONE*, 6(5).

Oksvold, M.P. et al., 2001. Re-localization of activated EGF receptor and its signal transducers to multivesicular compartments downstream of early endosomes in response to EGF. *European journal of cell biology*, 80(4), pp.285–294.

Olayioye, M. a et al., 2000. The ErbB signaling network: receptor heterodimerization in development and cancer. *The EMBO journal*, 19(13), pp.3159–3167.

Orth, J.D. & McNiven, M. a., 2006a. Get off my back! Rapid receptor internalization through circular dorsal ruffles. *Cancer Research*, 66(23), pp.11094–11096.

Orth, J.D. & McNiven, M. a., 2006b. Get off my back! Rapid receptor internalization through circular dorsal ruffles. *Cancer Research*, 66(9), pp.11094–11096.

Paavola, P. et al., 1999. Characterization of a novel gene, PNUTL2, on human chromosome 17q22-q23 and its exclusion as the Meckel syndrome gene. *Genomics*, 55(1), pp.122–125.

Pankiv, S. et al., 2007. p62/SQSTM1 binds directly to Atg8/LC3 to facilitate degradation of ubiquitinated protein aggregates by autophagy*[S]. *Journal of Biological Chemistry*, 282(33), pp.24131–24145.

Di Paolo, G. & De Camilli, P., 2006. Phosphoinositides in cell regulation and membrane dynamics. *Nature*, 443(7112), pp.651–657.

Pasqualato, S. et al., 2004. The Structural GDP/GTP Cycle of Rab11 Reveals a Novel Interface Involved in the Dynamics of Recycling Endosomes. *Journal of Biological Chemistry*, 279(12), pp.11480–11488.

Peden, A. a. et al., 2004. Localization of the AP-3 adaptor complex defines a novel endosomal exit site for lysosomal membrane proteins. *Journal of Cell Biology*, 164(7), pp.1065–1076.

Penengo, L. et al., 2003. c-Cbl is a critical modulator of the Ron tyrosine kinase receptor. *Oncogene*, 22(24), pp.3669–3679.

Pennock, S. & Wang, Z., 2008. A tale of two Cbls: interplay of c-Cbl and Cbl-b in epidermal growth factor receptor downregulation. *Molecular and cellular biology*, 28(9), pp.3020–37.

Peterson, E.A. et al., 2011. SEPT9 _ i1 and Genomic Instability : Mechanistic Insights and Relevance to Tumorigenesis. *Genes, Chromosomes & Cancer*, 949(July), pp.940–949.

Petiot, A. et al., 2003. PI3P signaling regulates receptor sorting but not transport in the endosomal pathway. *Journal of Cell Biology*, 162(6), pp.971–979.

Petrelli, A. et al., 2002. The endophilin-CIN85-Cbl complex mediates ligand-dependent downregulation of c-Met. *Nature*, 416(6877), pp.187–90.

Poirier, M.G., Eroglu, S. & Marko, J.F., 2002. The bending rigidity of mitotic chromosomes. *Molecular biology of the cell*, 13(6), pp.2170–2179.

Pol, A. et al., 2000. Epidermal growth factor-mediated caveolin recruitment to early endosomes and MAPK activation. Role of cholesterol and actin cytoskeleton. *Journal of Biological Chemistry*, 275(39), pp.30566–30572.

Posor, Y. et al., 2013. Spatiotemporal control of endocytosis by phosphatidylinositol-3,4-bisphosphate. *Nature*, 499(7457), pp.233–7.

Potter, N.T. et al., 2014. Validation of a Real-Time PCR-Based Qualitative Assay for the Detection of Methylated SEPT9 DNA in Human Plasma. *Clinical Chemistry*, 000, pp.1–9.

Prekeris, R. et al., 1998. Syntaxin 13 mediates cycling of plasma membrane proteins via tubulovesicular recycling endosomes. *Journal of Cell Biology*, 143(4), pp.957–971.

Price, J.T. et al., 1999. Epidermal Growth Factor Promotes MDA-MB-231 Breast Cancer Cell Migration through a Phosphatidylinositol 3 ′ -Kinase and Phospholipase C-dependent Mechanism Advances in Brief Epidermal Growth Factor Promotes MDA-MB-231 Breast Cancer Cell Migration through . , pp.5475–5478.

Puthenveedu, M. a. et al., 2010. Sequence-dependent sorting of recycling proteins by actin-stabilized endosomal microdomains. *Cell*, 143(5), pp.761–773.

Rabinovitz, I. et al., 2004. Protein Kinase C-␣ Phosphorylation of Speci c Serines in the Connecting Segment of the 4 Integrin Regulates the Dynamics of Type II Hemidesmosomes. *Society*, 24(10), pp.4351–4360.

Rabinovitz, I., Toker, A. & Mercurio, A.M., 1999. Protein kinase C-dependent mobilization of the ??6??4 integrin from hemidesmosomes and its association with actin-rich cell protrusions drive the chemotactic migration of carcinoma cells. *Journal of Cell Biology*, 146(5), pp.1147–1159.

Radisky, D.C., 2005. Epithelial-mesenchymal transition. *Journal of cell science*, 118(Pt 19), pp.4325–4326.

Raiborg, C. et al., 2002. Hrs sorts ubiquitinated proteins into clathrin-coated microdomains of early endosomes. *Nature cell biology*, 4(5), pp.394–398.

Reinstein, E. et al., 2000. Degradation of the E7 human papillomavirus oncoprotein by the ubiquitin-proteasome system: targeting via ubiquitination of the N-terminal residue. *Oncogene*, 19(51), pp.5944–5950.

Ren, M. et al., 1998. Hydrolysis of GTP on rab11 is required for the direct delivery of transferrin from the pericentriolar recycling compartment to the cell surface but not from sorting endosomes. *Proceedings of the National Academy of Sciences of the United States of America*, 95(11), pp.6187–6192.

Ren, X. & Hurley, J.H., 2010. VHS domains of ESCRT-0 cooperate in high-avidity binding to polyubiquitinated cargo. *The EMBO journal*, 29(6), pp.1045–1054.

Renshaw, M.J. et al., 2014. Anillin-dependent organization of septin filaments promotes intercellular bridge elongation and Chmp4B targeting to the abscission site. *Open biology*, 4, p.130190.

Reusch, U. et al., 2002. AP-1A and AP-3A lysosomal sorting functions. *Traffic (Copenhagen, Denmark)*, 3(10), pp.752–761.

Richards, R.C. et al., 1983. Epidermal growth factor receptors on isolated human placental syncytiotrophoblast plasma membrane. *Placenta*, 4(2), pp.133–138.

Rink, J. et al., 2005. Rab conversion as a mechanism of progression from early to late endosomes. *Cell*, 122(5), pp.735–749.

Robertson, C. et al., 2004. Properties of SEPT9 isoforms and the requirement for GTP binding. *Journal of Pathology*, 203(1), pp.519–527.

Rohde, G., Wenzel, D. & Haucke, V., 2002. A phosphatidylinositol (4,5)-bisphosphate binding site within mu2-adaptin regulates clathrin-mediated endocytosis. *Journal of Cell Biology*, 158(2), pp.209–214.

Rønning, S.B. et al., 2011. CIN85 regulates ubiquitination and degradative endosomal sorting of the EGF receptor. *Experimental cell research*, 317(13), pp.1804–16.

Rubin, E.J. et al., 1988. Functional modification of a 21-kilodalton G protein when ADP-ribosylated by exoenzyme C3 of Clostridium botulinum. *Molecular and cellular biology*, 8(1), pp.418–426.

Rubino, M. et al., 2000. Selective membrane recruitment of EEA1 suggests a role in directional transport of clathrin-coated vesicles to early endosomes. *Journal of Biological Chemistry*, 275(6), pp.3745–3748.

Sadian, Y. et al., 2013. The role of Cdc42 and Gic1 in the regulation of septin filament formation and dissociation. *eLife*, 2, p.e01085.

Sahai, E. & Marshall, C.J., 2003. Differing modes of tumour cell invasion have distinct requirements for Rho/ROCK signalling and extracellular proteolysis. *Nature cell biology*, 5(8), pp.711–719.

Saiki, R.K. et al., 1988. Primer-Directed Enzymatic Amplification of DNA with a Thermostable DNA Polymerase. *Science*, 239(4839), pp.487–91.

Salani, B. et al., 2010. Igf-ir internalizes with caveolin-1 and ptrf/cavin in hacat cells. *PLoS ONE*, 5(11), pp.1–9.

Samoylenko, A.. et al., 2012. Increased levels of the HER1 adaptor protein Rukl/CIN85 contribute to breast cancer malignancy. *Carcinogenesis*.

Sanjay, A. et al., 2001. Cbl associates with Pyk2 and Src to regulate Src kinase activity, αvβ3 integrin-mediated signaling, cell adhesion, and osteoclast motility. *Journal of Cell Biology*, 152(1), pp.181–195.

Sarbassov, D.D. et al., 2005. Phosphorylation and regulation of Akt/PKB by the rictor-mTOR complex. *Science (New York, N.Y.)*, 307(5712), pp.1098–1101.

Sato, M. et al., 2008. Regulation of endocytic recycling by C. elegans Rab35 and its regulator RME-4, a coated-pit protein. *The EMBO journal*, 27(8), pp.1183–1196.

Schaik, M. Van, Hospital, A. & Kingdom, U., 1989. Reconstitution of an Endosome-Lysosome Interaction in a Cell-free System. , 108(June), pp.2093–2099.

Schmid, S.L. et al., 1984. A role for clathrin light chains in the recognition of clathrin cages by “uncoating ATPase”. *Nature*, 311(5983), pp.228–231.

Schmidt, M.H.H. et al., 2004. Alix / AIP1 Antagonizes Epidermal Growth Factor Receptor Downregulation by the Cbl-SETA / CIN85 Complex. , 24(20), pp.8981–8993.

Schmidt, M.H.H. et al., 2003. SETA/CIN85/Ruk and its binding partner AIP1 associate with diverse cytoskeletal elements, including FAKs, and modulate cell adhesion. *Journal of cell science*, 116(Pt 14), pp.2845–55.

Schmidt, M.H.H. & Dikic, I., 2005. The Cbl interactome and its functions. *Nature reviews. Molecular cell biology*, 6(12), pp.907–18.

Schmitz, a a et al., 2000. Rho GTPases: signaling, migration, and invasion. *Experimental cell research*, 261(1), pp.1–12.

Schmutz, C. et al., 2013. Systems-level overview of host protein phosphorylation during Shigella flexneri infection revealed by phosphoproteomics. *Molecular & cellular proteomics : MCP*, 12(10), pp.2952–2968.

Schneider, C. a, Rasband, W.S. & Eliceiri, K.W., 2012. NIH Image to ImageJ: 25 years of image analysis. *Nature Methods*, 9(7), pp.671–675.

Schroeder, B. et al., 2010a. A Dyn2-CIN85 complex mediates degradative traffic of the EGFR by regulation of late endosomal budding. *The EMBO journal*, 29(18), pp.3039–53.

Schroeder, B. et al., 2010b. A Dyn2-CIN85 complex mediates degradative traffic of the EGFR by regulation of late endosomal budding. *The EMBO journal*, 29(18), pp.3039–53.

Schroeder, B. et al., 2012. CIN85 phosphorylation is essential for EGFR ubiquitination and sorting into multivesicular bodies. *Molecular biology of the cell*, 23, pp.3602–3611.

Schulman, B. a & Harper, J.W., 2009. Ubiquitin-like protein activation by E1 enzymes: the apex for downstream signalling pathways. *Nature reviews. Molecular cell biology*, 10(5), pp.319–331.

Scott, M. et al., 2005. Multimodality expression profiling shows SEPT9 to be overexpressed in a wide range of human tumours. *Oncogene*, 24(29), pp.4688–700.

Seger, R. et al., 1992. Purification and characterization of mitogen-activated protein kinase activator(s) from epidermal growth factor-stimulated A431 cells. *The Journal of biological chemistry*, 267(20), pp.14373–14381.

Sehat, B. et al., 2008. Identification of c-Cbl as a new ligase for insulin-like growth factor-I receptor with distinct roles from Mdm2 in receptor ubiquitination and endocytosis. *Cancer Research*, 68(14), pp.5669–5677.

Sellin, M.E. et al., 2011. Deciphering the rules governing assembly order of mammalian septin complexes. *Molecular biology of the cell*, 22(17), pp.3152–64.

Semerdjieva, S. et al., 2008. Coordinated regulation of AP2 uncoating from clathrin-coated vesicles by rab5 and hRME-6. *Journal of Cell Biology*, 183(3), pp.499–511.

Sharma, S. V et al., 2007. Epidermal growth factor receptor mutations in lung cancer. *Nature reviews. Cancer*, 7(3), pp.169–181.

She, Y.-M. et al., 2004. Septin 2 phosphorylation: theoretical and mass spectrometric evidence for the existence of a single phosphorylation site in vivo. *Rapid communications in mass spectrometry : RCM*, 18(10), pp.1123–30.

Sheffield, P.J. et al., 2003a. Borg/Septin interactions and the assembly of mammalian septin heterodimers, trimers, and filaments. *Journal of Biological Chemistry*, 278, pp.3483–3488.

Sheffield, P.J. et al., 2003b. Borg/Septin interactions and the assembly of mammalian septin heterodimers, trimers, and filaments. *Journal of Biological Chemistry*, 278(5), pp.3483–3488.

El Sheikh, S.S. et al., 2003. Topographical expression of class IA and class II phosphoinositide 3-kinase enzymes in normal human tissues is consistent with a role in differentiation. *BMC clinical pathology*, 3, p.4.

Shimokawa, N. et al., 2010. CIN85 regulates dopamine receptor endocytosis and governs behaviour in mice. *The EMBO journal*, 29(14), pp.2421–32.

Shin, H.W. et al., 2005. An enzymatic cascade of Rab5 effectors regulates phosphoinositide turnover in the endocytic pathway. *Journal of Cell Biology*, 170(4), pp.607–618.

Shinoda, T. et al., 2010. Septin 14 is involved in cortical neuronal migration via interaction with Septin 4. *Molecular biology of the cell*, 21(8), pp.1324–1334.

Sigismund, S. et al., 2005. Clathrin-independent endocytosis of ubiquitinated cargos. *Proceedings of the National Academy of Sciences of the United States of America*, 102(8), pp.2760–5.

Sigismund, S. et al., 2008. Clathrin-mediated internalization is essential for sustained EGFR signaling but dispensable for degradation. *Developmental cell*, 15(2), pp.209–19.

Sigismund, S. et al., 2013. Threshold-controlled ubiquitination of the EGFR directs receptor fate. *The EMBO journal*, 32(15), pp.2140–57.

Sirajuddin, M. et al., 2009. GTP-induced conformational changes in septins and implications for function. *Proceedings of the National Academy of Sciences of the United States of America*, 106(39), pp.16592–16597.

Sirajuddin, M. et al., 2007. Structural insight into filament formation by mammalian septins. *Nature*, 449(7160), pp.311–5.

Sitz, J.H. et al., 2008. The Down syndrome candidate dual-specificity tyrosine phosphorylation-regulated kinase 1A phosphorylates the neurodegeneration-related septin 4. *Neuroscience*, 157(3), pp.596–605.

Van der Sluijs, P. et al., 1992. The small GTP-binding protein rab4 controls an early sorting event on the endocytic pathway. *Cell*, 70(5), pp.729–740.

Soldati, T. & Schliwa, M., 2006. Powering membrane traffic in endocytosis and recycling. *Nature reviews. Molecular cell biology*, 7(December), pp.897–908.

Soltoff, S.P. et al., 1994. ErbB3 is involved in activation of phosphatidylinositol 3-kinase by epidermal growth factor. *Molecular and cellular biology*, 14(6), pp.3550–3558.

Sorkin, a D., Teslenko, L. V & Nikolsky, N.N., 1988. The endocytosis of epidermal growth factor in A431 cells: a pH of microenvironment and the dynamics of receptor complex dissociation. *Experimental cell research*, 175(1), pp.192–205.

Sorkin, A. et al., 1996. Epidermal growth factor receptor interaction with clathrin adaptors is mediated by the Tyr974-containing internalization motif. *Journal of Biological Chemistry*, 271(23), pp.13377–13384.

Sparatore, B. et al., 2005. Activation of A431 human carcinoma cell motility by extracellular high-mobility group box 1 protein and epidermal growth factor stimuli. *The Biochemical journal*, 389(Pt 1), pp.215–221.

Spiliotis, E.T. & Gladfelter, A.S., 2012. Spatial Guidance of Cell Asymmetry: Septin GTPases Show the Way. *Traffic*, 13(2), pp.195–203.

Spiliotis, E.T., Kinoshita, M. & Nelson, W.J., 2005. A mitotic septin scaffold required for Mammalian chromosome congression and segregation. *Science (New York, N.Y.)*, 307(5716), pp.1781–5.

Stanbery, L. & Petty, E.M., 2012. Steps solidifying a role for SEPT9 in breast cancer suggest that greater strides are needed. *Breast cancer research : BCR*, 14(1), p.101.

Stasyk, T. et al., 2007. Identification of endosomal epidermal growth factor receptor signaling targets by functional organelle proteomics. *Molecular & cellular proteomics : MCP*, 6(5), pp.908–22.

Stokoe, D. et al., 1997. Dual role of phosphatidylinositol-3,4,5-trisphosphate in the activation of protein kinase B. *Science (New York, N.Y.)*, 277(5325), pp.567–570.

Stuchell-Brereton, M.D. et al., 2007. ESCRT-III recognition by VPS4 ATPases. *Nature*, 449(7163), pp.740–744.

Sudo, K. et al., 2007. SEPT9 Sequence Alternations Causing Hereditary Neuralgic Amyotrophy Are Associated With Altered Interactions With SEPT4 / SEPT11 and Resistance to Rho / Rhotekin-Signaling. , 28(June), pp.1005–1013.

Surka, M.C., Tsang, C.W. & Trimble, W.S., 2002. The Mammalian Septin MSF Localizes with Microtubules and Is Required for Completion of Cytokinesis. , 13(October), pp.3532–3545.

Szymkiewicz, I. et al., 2002. CIN85 participates in Cbl-b-mediated down-regulation of receptor tyrosine kinases. *The Journal of biological chemistry*, 277(42), pp.39666–72.

Tada, T. et al., 2007. Role of Septin Cytoskeleton in Spine Morphogenesis and Dendrite Development in Neurons. *Current Biology*, 17(20), pp.1752–1758.

Takahashi, S. et al., 2012. Rab11 regulates exocytosis of recycling vesicles at the plasma membrane. *Journal of Cell Science*, 125(17), pp.4049–4057.

Take, H. et al., 2000. Cloning and characterization of a novel adaptor protein, CIN85, that interacts with c-Cbl. *Biochemical and biophysical research communications*, 268(2), pp.321–328.

Tan, E.Y.M. et al., 2007. Development of a cell transducible RhoA inhibitor TAT-C3 transferase and its encapsulation in biocompatible microspheres to promote survival and enhance regeneration of severed neurons. *Pharmaceutical Research*, 24(12), pp.2297–2308.

Tanaka-Takiguchi, Y., Kinoshita, M. & Takiguchi, K., 2009. Septin-Mediated Uniform Bracing of Phospholipid Membranes. *Current Biology*, 19(2), pp.140–145.

Thalappilly, S. et al., 2010. VAV2 regulates epidermal growth factor receptor endocytosis and degradation. *Oncogene*, 29(17), pp.2528–2539.

Thien, C.B. & Langdon, W.Y., 2001. Cbl: many adaptations to regulate protein tyrosine kinases. *Nature reviews. Molecular cell biology*, 2(April), pp.294–307.

Thiery, J.P., 2002. Epithelial-mesenchymal transitions in tumour progression. *Nature reviews. Cancer*, 2(6), pp.442–454.

Tokhtaeva, E. et al., 2015. Septin dynamics are essential for exocytosis. *Journal of Biological Chemistry*, 290(9), p.jbc.M114.616201.

Tong, J., Taylor, P. & Moran, M.F., 2014. Proteomic Analysis of the Epidermal Growth Factor Receptor (EGFR) Interactome and Post-translational Modifications Associated with Receptor Endocytosis in Response to EGF and Stress. *Molecular & cellular proteomics : MCP*, 13(7), pp.1644–58.

Tooley, A.J. et al., 2009. Amoeboid T lymphocytes require the septin cytoskeleton for cortical integrity and persistent motility. *Nature cell biology*, 11(1), pp.17–26.

Tóth, K. et al., 2014. Detection of Methylated Septin 9 in Tissue and Plasma of Colorectal Patients with Neoplasia and the Relationship to the Amount of Circulating Cell-Free DNA. *PLoS ONE*, 9(12), p.e115415.

Tóth, K. et al., 2011. The influence of methylated septin 9 gene on RNA and protein level in colorectal cancer. *Pathology oncology research : POR*, 17(3), pp.503–9.

Toure, A. et al., 2011. Septins at the annulus of mammalian sperm. *Biological Chemistry*, 392, pp.799–803.

Traikov, S. et al., 2014. Septin6 and Septin7 GTP binding proteins regulate AP-3- and ESCRT-dependent multivesicular body biogenesis. *PloS one*, 9(11), p.e109372.

Uddin, S. et al., 1996. Interaction of the c-cbl proto-oncogene product with the Tyk-2 protein tyrosine kinase. *Biochemical and biophysical research communications*, 225(3), pp.833–838.

Ueda, M. et al., 2010. Phenotypic spectrum of hereditary neuralgic amyotrophy caused by the SEPT9 R88W mutation. *Journal of neurology, neurosurgery, and psychiatry*, 81(1), pp.94–6.

Ueki, K. et al., 2000. Positive and negative regulation of phosphoinositide 3-kinase-dependent signaling pathways by three different gene products of the p85alpha regulatory subunit. *Molecular and cellular biology*, 20(21), pp.8035–8046.

Ullrich, O. et al., 1996. Rab11 regulates recycling through the pericentriolar recycling endosome. *Journal of Cell Biology*, 135(4), pp.913–924.

Urbé, S. et al., 2003. The UIM domain of Hrs couples receptor sorting to vesicle formation. *Journal of cell science*, 116(Pt 20), pp.4169–4179.

Valdez, G. et al., 2007. Trk-signaling endosomes are generated by Rac-dependent macroendocytosis. *Proceedings of the National Academy of Sciences of the United States of America*, 104(30), pp.12270–12275.

Vanhaesebroeck, B. et al., 1997. Phosphoinositide 3-kinases: A conserved family of signal transducers. *Trends in Biochemical Sciences*, 22(7), pp.267–272.

Vanhaesebroeck, B. et al., 2010. The emerging mechanisms of isoform-specific PI3K signalling. *Nature reviews. Molecular cell biology*, 11(May), pp.329–341.

Varadan, R. et al., 2004. Solution Conformation of Lys63-linked Di-ubiquitin Chain Provides Clues to Functional Diversity of Polyubiquitin Signaling. *Journal of Biological Chemistry*, 279(8), pp.7055–7063.

Vega, I.E. & Hsu, S.C., 2003. The septin protein Nedd5 associates with both the exocyst complex and microtubules and disruption of its GTPase activity promotes aberrant neurite sprouting in PC12 cells. *Molecular Neuroscience*, 14(1), pp.1–7.

Veiga, E. & Cossart, P., 2005. Listeria hijacks the clathrin-dependent endocytic machinery to invade mammalian cells. *Nature cell biology*, 7(9), pp.894–900.

Verdier, F. et al., 2002. Ruk is ubiquitinated but not degraded by the proteasome. *European Journal of Biochemistry*, 269(14), pp.3402–3408.

Vieira, a V, Lamaze, C. & Schmid, S.L., 1996. Control of EGF receptor signaling by clathrin-mediated endocytosis. *Science (New York, N.Y.)*, 274(5295), pp.2086–2089.

Virbasius, J. V, Guilherme, a & Czech, M.P., 1996. Mouse p170 is a novel phosphatidylinositol 3-kinase containing a C2 domain. *The Journal of biological chemistry*, 271(23), pp.13304–13307.

Vojtek, a B., Hollenberg, S.M. & Cooper, J. a, 1993. Mammalian Ras interacts directly with the serine/threonine kinase Raf. *Cell*, 74(1), pp.205–214.

Volinia, S. et al., 1995. A human phosphatidylinositol 3-kinase complex related to the yeast Vps34p-Vps15p protein sorting system. *The EMBO journal*, 14(14), pp.3339–3348.

Wakasaki, T. et al., 2010. A critical role of c-Cbl-interacting protein of 85 kDa in the development and progression of head and neck squamous cell carcinomas through the ras-ERK pathway. *Neoplasia (New York, N.Y.)*, 12(10), pp.789–796.

Wang, F. et al., 1998. Reciprocal interactions between beta1-integrin and epidermal growth factor receptor in three-dimensional basement membrane breast cultures: a different perspective in epithelial biology. *Proceedings of the National Academy of Sciences of the United States of America*, 95(25), pp.14821–14826.

Wang Ip, C. et al., 2006. Role of immune cells in animal models for inherited peripheral neuropathies. *Neuromolecular medicine*, 8(1-2), pp.175–190.

Ward, E.S. et al., 2005. From sorting endosomes to exocytosis: association of Rab4 and Rab11 GTPases with the Fc receptor, FcRn, during recycling. *Molecular biology of the cell*, 16(4), pp.2028–2038.

Ware, M.F., Wells, a & Lauffenburger, D. a, 1998. Epidermal growth factor alters fibroblast migration speed and directional persistence reciprocally and in a matrix-dependent manner. *Journal of cell science*, 111 ( Pt 1, pp.2423–2432.

Warren, J.D. et al., 2011. Septin 9 methylated DNA is a sensitive and specific blood test for colorectal cancer. *BMC medicine*, 9, p.133.

Warren, R. a, Green, F. a & Enns, C. a, 1997. Saturation of the endocytic pathway for the transferrin receptor does not affect the endocytosis of the epidermal growth factor receptor. *The Journal of biological chemistry*, 272(4), pp.2116–2121.

Wasik, a. a. et al., 2012. Septin 7 forms a complex with CD2AP and nephrin and regulates glucose transporter trafficking. *Molecular Biology of the Cell*, 23(17), pp.3370–3379.

Watanabe, S. et al., 2000. Characterization of the CIN85 adaptor protein and identification of components involved in CIN85 complexes. *Biochemical and biophysical research communications*, 278(1), pp.167–174.

Wegner, C.S. et al., 2010. Ultrastructural characterization of giant endosomes induced by GTPase-deficient Rab5. *Histochemistry and cell biology*, 133(1), pp.41–55.

Weirich, C.S., Erzberger, J.P. & Barral, Y., 2008. The septin family of GTPases: architecture and dynamics. *Nature reviews. Molecular cell biology*, 9(6), pp.478–89.

Wells, A. et al., 2002. Growth factor-induced cell motility in tumor invasion. *Acta oncologica (Stockholm, Sweden)*, 41(2), pp.124–130.

Wesseling, H., Gottschalk, M.G. & Bahn, S., 2014. Targeted Multiplexed Selected Reaction Monitoring Analysis Evaluates Protein Expression Changes of Molecular Risk Factors for Major Psychiatric Disorders. *International Journal of Neuropsychopharmacology*, pp.1–13.

Wheeler, M. & Domin, J., 2001. Recruitment of the class II phosphoinositide 3-kinase C2beta to the epidermal growth factor receptor: role of Grb2. *Mol Cell Biol*, 21(19), pp.6660–7.

Wheeler, M. & Domin, J., 2006. The N-terminus of phosphoinositide 3-kinase-C2?? regulates lipid kinase activity and binding to clathrin. *Journal of Cellular Physiology*, 206(July 2005), pp.586–593.

Wightman, R. et al., 2004. In Candida albicans, the Nim1 kinases Gin4 and Hsl1 negatively regulate pseudohypha formation and Gin4 also controls septin organization. *Journal of Cell Biology*, 164(4), pp.581–591.

Wilhelmsen, K., Burkhalter, S. & van der Geer, P., 2002. C-Cbl binds the CSF-1 receptor at tyrosine 973, a novel phosphorylation site in the receptor's carboxy-terminus. *Oncogene*, 21(7), pp.1079–1089.

Wollert, T. et al., 2009. Membrane scission by the ESCRT-III complex. *Nature*, 458(7235), pp.172–177.

Xie, Y. et al., 2007. The GTP-Binding Protein Septin 7 Is Critical for Dendrite Branching and Dendritic-Spine Morphology. *Current Biology*, 17, pp.1746–1751.

Xu, P. et al., 2009. Quantitative Proteomics Reveals the Function of Unconventional Ubiquitin Chains in Proteasomal Degradation. *Cell*, 137(1), pp.133–145.

Xue, L. & Lucocq, J., 1998. ERK2 signalling from internalised epidermal growth factor receptor in broken A431 cells. *Cellular Signalling*, 10(5), pp.339–348.

Yamazaki, T. et al., 2002. Role of Grb2 in EGF-stimulated EGFR internalization. *Journal of cell science*, 115, pp.1791–1802.

Ybe, J. a et al., 1999. Clathrin self-assembly is mediated by a tandemly repeated superhelix. *Nature*, 399(6734), pp.371–375.

Ye, Y. & Rape, M., 2009. Building ubiquitin chains: E2 enzymes at work. *Nature reviews. Molecular cell biology*, 10(11), pp.755–764.

Yu, W. et al., 2009. The phosphorylation of SEPT2 on Ser218 by casein kinase 2 is important to hepatoma carcinoma cell proliferation. *Molecular and cellular biochemistry*, 325(1-2), pp.61–7.

Zeng, L. et al., 2000. Vav3 Mediates Receptor Protein Tyrosine Kinase Signaling , Regulates GTPase Activity , Modulates Cell Morphology , and Induces Cell Transformation Vav3 Mediates Receptor Protein Tyrosine Kinase Signaling , Regulates GTPase Activity , Modulates Cell Morpho. *Molecular and cellular biology*, 20, pp.9212–9224.

Zent, E. & Wittinghofer, A., 2014. Human septin isoforms and the GDP-GTP cycle. *Biological chemistry*, 395(2), pp.169–80.

Zerial, M. & McBride, H., 2001. Rab proteins as membrane organizers. *Nature reviews. Molecular cell biology*, 2(2), pp.107–117.

Zhang, J. et al., 2009. CIN85 associates with endosomal membrane and binds phosphatidic acid. *Cell research*, 19(6), pp.733–46.

Zhang, J. et al., 1999. Phosphatidylinositol polyphosphate binding to the mammalian septin H5 is modulated by GTP. *Current Biology*, 9, pp.1458–1467.

Zhang, Y. et al., 2000. Parkin functions as an E2-dependent ubiquitin- protein ligase and promotes the degradation of the synaptic vesicle-associated protein, CDCrel-1. *Proceedings of the National Academy of Sciences of the United States of America*, 97(24), pp.13354–13359.

Zheng, J. et al., 2002. CAND1 binds to unneddylated CUL1 and regulates the formation of SCF ubiquitin E3 ligase complex. *Molecular Cell*, 10(6), pp.1519–1526.

Zhu, M. et al., 2008. Septin 7 interacts with centromere-associated protein E and is required for its kinetochore localization. *Journal of Biological Chemistry*, 283(27), pp.18916–18925.

Zieger, B. et al., 2000. Characterization and expression analysis of two human septin genes, PNUTL1 and PNUTL2. *Gene*, 261(2), pp.197–203.

# 6 Appendix

**Appendix 1:** EGFR interactome upon loss of SEPT9. HeLa cells were kept in medium containing either heavy isotopes of arginine and lysine or light isotopes, respectively, for 8 days in total. Upon siRNA-treatment cells were surface-stimulated with 500 ng/ml EGF and subjected to affinity-purification of EGFR using specific antibodies. For the forward experiment (fw), eluates with equal amounts of EGFR from control cells containing heavy isotopes (H) and from SEPT9 knockdown cells containing light isotopes (L) were mixed and analyzed by MS/MS (performed in cooperation with Dr. Eberhard Krause; Leibniz Institute for Molecular Pharmacology, Berlin). The reverse (rv) experiment with SEPT9 knockdown cells being labeled was performed in parallel. The ratio L/H (or H/L for the reverse experiment) is shown as mean ± s.e.m from n = 2 experiments. Please note, that some proteins were not identified in all four experiments due to low abundance.

| | | | Unique peptides | | | | Ratio count | | | | Ratio normalized | | | | | |
|---|---|---|---|---|---|---|---|---|---|---|---|---|---|---|---|---|
| Protein name | Gene name | UniProt | fw 1 | rv 1 | fw 2 | rv 2 | fw 1 | rv1 | fw2 | rv2 | fw 1 (L/H) | rv 1 (H/L) | fw 2 (L/H) | rv 2 (H/L) | mean | SEM |
| **Epidermal growth factor receptor** | **EGFR** | **P00533** | **52** | **46** | **38** | **49** | **576** | **280** | **281** | **313** | **0,97** | **0,89** | **0,75** | **1,01** | **0,91** | **0,08** |
| Receptor tyrosine-protein kinase erbB-2 | ERBB2 | P04626 | 5 | 1 | | 3 | 11 | 4 | | 4 | 1,82 | 1,10 | | 1,80 | **1,54** | 0,32 |
| Guanine nucleotide exchange factor VAV3 | VAV3 | Q9UKW4 | 13 | 11 | 14 | 15 | 57 | 11 | 34 | 23 | 1,33 | 1,27 | 1,50 | 1,67 | **1,45** | 0,12 |
| E3 ubiquitin-protein ligase CBL-B | CBLB | E7ENW2 | 16 | 11 | 12 | 13 | 67 | 27 | 14 | 21 | 1,50 | 1,38 | 1,48 | 1,39 | **1,42** | 0,06 |
| Clathrin heavy chain 1 | CLTC | Q00610 | 12 | 2 | 22 | 26 | 19 | 2 | 34 | 31 | 1,93 | 1,01 | 1,34 | 1,42 | **1,41** | 0,28 |
| PI 4-phosphate 3-kinase C2 domain-containing subunit beta | PIK3C2B | F5GWN5 | 42 | 12 | 28 | 29 | 133 | 24 | 39 | 39 | 1,47 | 1,54 | 1,36 | 1,22 | **1,37** | 0,08 |
| Signal transducer and activator of transcription 3 | STAT3 | P40763 | 23 | 17 | 11 | 16 | 44 | 22 | 15 | 18 | 0,45 | 2,13 | 1,32 | 1,15 | **1,26** | 0,48 |
| ERBB receptor feedback inhibitor 1 | ERRFI1 | Q9UJM3 | 3 | 2 | 5 | 4 | 4 | 6 | 6 | 6 | 1,29 | 1,28 | 1,13 | 1,33 | **1,25** | 0,06 |
| Son of sevenless homolog 1 | SOS1 | Q07889 | 44 | 26 | 36 | 41 | 211 | 68 | 78 | 79 | 1,36 | 1,06 | 1,09 | 1,11 | **1,15** | 0,10 |
| Protein arginine N-methyltransferase 5 | PRMT5 | O14744 | 4 | 5 | | 2 | 4 | 4 | | 2 | 1,59 | 1,06 | | 0,85 | **1,15** | 0,27 |
| Grow th factor receptor-bound protein 2 | GRB2 | P62993 | 21 | 25 | 16 | 17 | 169 | 96 | 72 | 60 | 1,11 | 1,17 | 1,03 | 1,11 | **1,10** | 0,04 |
| SHC-transforming protein 1 | SHC1 | P29353 | 9 | 8 | 5 | 7 | 151 | 121 | 88 | 72 | 1,22 | 1,14 | 1,10 | 0,97 | **1,09** | 0,07 |
| Dynamin-2 | DNM2 | P50570 | 9 | 2 | | | 25 | 4 | | | 1,04 | 1,16 | | | **1,08** | 0,05 |
| PI 3,4,5-trisphosphate 5-phosphatase 2 | INPPL1 | O15357 | 19 | 6 | 13 | 10 | 37 | 11 | 12 | 10 | 0,96 | 1,13 | 1,15 | 1,13 | **1,07** | 0,06 |
| Rho guanine nucleotide exchange factor 5 | ARHGEF5 | Q12774 | 13 | 4 | | 2 | 53 | 12 | | 2 | 1,25 | 1,15 | | 0,92 | **1,06** | 0,12 |
| AP-2 complex subunit alpha-1 | AP2A1 | O95782 | 15 | 1 | | | 26 | 2 | | | 1,16 | 0,92 | | | **1,03** | 0,13 |
| Cytoskeleton-associated protein 4 | CKAP4 | Q07065 | 9 | 9 | 9 | 7 | 9 | 16 | 8 | 7 | 1,02 | 1,09 | 1,09 | 0,97 | **1,03** | 0,04 |
| PI 4,5-bisphosphate 3-kinase catalytic subunit beta isoform | PIK3CB | P42338 | 6 | 2 | 6 | 5 | 12 | 3 | 6 | 5 | 1,02 | 0,98 | 1,01 | 1,03 | **1,01** | 0,02 |
| AP-2 complex subunit mu | AP2M1 | C9JTK4 | 2 | 2 | | | 4 | 3 | | | 1,18 | 0,85 | | | **1,01** | 0,17 |
| AP-2 complex subunit beta | AP2B1 | P63010 | 7 | 2 | | | 18 | 2 | | | 1,14 | 0,83 | | | **0,96** | 0,18 |
| E3 ubiquitin-protein ligase CBL | CBL | P22681 | 26 | 19 | 17 | 18 | 113 | 35 | 37 | 31 | 1,10 | 0,83 | 1,05 | 0,86 | **0,94** | 0,12 |
| PI 3-kinase regulatory subunit beta | PIK3R2 | O00459 | 20 | 19 | 11 | 14 | 36 | 21 | 14 | 14 | 0,99 | 1,03 | 1,05 | 0,80 | **0,93** | 0,08 |
| Ubiquitin-associated and SH3 domain-containing protein B | UBASH3B | Q8TF42 | 23 | 25 | 19 | 20 | 157 | 117 | 73 | 82 | 0,98 | 0,88 | 0,79 | 0,78 | **0,84** | 0,06 |
| Guanine nucleotide exchange factor VAV2 | VAV2 | P52735 | 18 | 5 | 17 | 7 | 42 | 8 | 20 | 12 | 0,86 | 0,92 | 0,69 | 0,71 | **0,79** | 0,07 |
| Tyrosine-protein kinase CSK | CSK | P41240 | 7 | 7 | 6 | 6 | 14 | 13 | 7 | 6 | 0,80 | 0,68 | 0,68 | 0,60 | **0,70** | 0,06 |

**Appendix 2:** MS/MS analysis of the SEPT9_v3 interactome.

| Protein | Accession | Score | Mass | Quantif. of unique peptides | | |
|---|---|---|---|---|---|---|
| | | | | H/L | SD(geo) | # quantif. |
| **Septins** | | | | | | |
| Isoform 5 of Septin-9 OS=Homo sapiens GN=SEPT9 | Q9UHD8-5 | 9602 | 64641 | **0,48** | 1,06 | 2 |
| Septin-9 OS=Homo sapiens GN=SEPT9 PE=1 SV=2 | Q9UHD8 | 9679 | 65361 | **0,51** | 1,25 | 3 |
| Septin-8 OS=Homo sapiens GN=SEPT8 PE=2 SV=1 | A6NMH6 | 2278 | 49884 | **0,64** | 1,13 | 32 |
| Septin-11 OS=Homo sapiens GN=SEPT11 PE=2 SV=1 | D6RER5 | 3354 | 49777 | **0,68** | 1,21 | 42 |
| Septin-7 OS=Homo sapiens GN=SEPT7 PE=1 SV=2 | Q16181 | 5079 | 50648 | **0,71** | 1,06 | 94 |
| Septin-2 OS=Homo sapiens GN=SEPT2 PE=2 SV=1 | B5MCX3 | 3335 | 36917 | **0,75** | 1,03 | 2 |
| Septin 6, isoform CRA_b OS=Homo sapiens GN=SEPT6 PE=2 SV=1 | B1AMS2 | 2600 | 49272 | **0,75** | 1,14 | 18 |
| Septin 10, isoform CRA_c OS=Homo sapiens GN=SEPT10 PE=2 SV=2 | B5ME97 | 978 | 62905 | **0,84** | 1,05 | 17 |
| Septin-2 OS=Homo sapiens GN=SEPT2 PE=1 SV=1 | Q15019 | 3856 | 41461 | **0,86** | 1,15 | 5 |
| **Ubiquitylation** | | | | | | |
| Ubiquitin-like modifier-activating enzyme 1 OS=Homo sapiens GN=UBA1 PE=1 SV=3 | P22314 | 320 | 117774 | **0,09** | 1,13 | 7 |
| E3 UFM1-protein ligase 1 OS=Homo sapiens GN=UFL1 PE=1 SV=2 | O94874 | 212 | 89540 | **0,26** | 1,13 | 2 |
| Transcription intermediary factor 1-beta OS=Homo sapiens GN=TRIM28 PE=1 SV=5 | Q13263 | 1205 | 88493 | **0,28** | 1,15 | 31 |
| E3 ubiquitin-protein ligase Itchy homolog OS=Homo sapiens GN=ITCH PE=1 SV=2 | Q96J02 | 454 | 102738 | **0,29** | 1,08 | 2 |
| E3 ubiquitin-protein ligase MIB2 OS=Homo sapiens GN=MIB2 PE=2 SV=1 | F8WA73 | 492 | 115788 | **0,31** | 1,17 | 9 |
| E3 ubiquitin-protein ligase CHIP OS=Homo sapiens GN=STUB1 PE=1 SV=2 | Q9UNE7 | 124 | 34834 | **0,49** | 1,18 | 2 |
| Cullin-1 OS=Homo sapiens GN=CUL1 PE=1 SV=2 | Q13616 | 365 | 89622 | **0,59** | 1,44 | 3 |
| E3 ubiquitin-protein ligase TRIM21 OS=Homo sapiens GN=TRIM21 PE=2 SV=1 | F5H012 | 984 | 54047 | **0,62** | 1,08 | 39 |
| Probable ubiquitin carboxyl-terminal hydrolase FAF-X OS=Homo sapiens GN=USP9X PE=1 SV=3 | Q93008 | 3880 | 292094 | **0,63** | 1,15 | 69 |
| E3 ubiquitin-protein ligase TRIM11 OS=Homo sapiens GN=TRIM11 PE=1 SV=2 | Q96F44 | 476 | 52741 | **0,63** | 1,14 | 9 |
| Cullin-associated NEDD8-dissociated protein 1 OS=Homo sapiens GN=CAND1 PE=1 SV=2 | Q86VP6 | 1359 | 136289 | **0,65** | 1,14 | 14 |
| E3 ubiquitin-protein ligase DTX3L OS=Homo sapiens GN=DTX3L PE=1 SV=1 | Q8TDB6 | 395 | 83501 | **0,69** | 1,35 | 4 |
| Ubiquitin (Fragment) OS=Homo sapiens GN=UBB PE=4 SV=1 | J3QS39 | 1162 | 10463 | **0,78** | 1,12 | 41 |
| **Endocytosis** | | | | | | |
| AP-2 complex subunit alpha-2 OS=Homo sapiens GN=AP2A2 PE=1 SV=2 | O94973 | 493 | 103895 | **0,19** | 1,04 | 2 |
| Dynamin-2 OS=Homo sapiens GN=DNM2 PE=3 SV=1 | K7ESI9 | 266 | 97916 | **0,28** | 1,13 | 4 |
| Calmodulin OS=Homo sapiens GN=CALM1 PE=1 SV=2 | P62158 | 182 | 16827 | **0,30** | 1,12 | 2 |
| Cytoskeleton-associated protein 4 OS=Homo sapiens GN=CKAP4 PE=1 SV=2 | Q07065 | 1013 | 65983 | **0,46** | 1,07 | 12 |
| Isoform Non-brain of Clathrin light chain B OS=Homo sapiens GN=CLTB | P09497-2 | 342 | 23167 | **0,56** | 1,15 | 16 |
| Transferrin receptor protein 1 OS=Homo sapiens GN=TFRC PE=1 SV=2 | P02786 | 640 | 84818 | **0,57** | 1,19 | 5 |
| TNF receptor-associated factor 3 OS=Homo sapiens GN=TRAF3 PE=2 SV=1 | A6NHG8 | 523 | 61720 | **0,57** | 1,17 | 6 |
| Tumor susceptibility gene 101 protein OS=Homo sapiens GN=TSG101 PE=2 SV=1 | F5H442 | 118 | 40892 | **0,60** | 1,14 | 2 |
| SH3KBP1 binding protein 1, isoform CRA_c OS=Homo sapiens GN=SHKBP1 PE=4 SV=1 | M0R2P6 | 2189 | 73661 | **0,62** | 1,52 | 5 |
| Endophilin-B2 OS=Homo sapiens GN=SH3GLB2 PE=2 SV=1 | B7ZC38 | 404 | 44334 | **0,63** | 1,09 | 9 |
| Sorting nexin-9 OS=Homo sapiens GN=SNX9 PE=1 SV=1 | Q9Y5X1 | 1255 | 66550 | **0,78** | 1,17 | 25 |
| Clathrin heavy chain 2 OS=Homo sapiens GN=CLTCL1 PE=1 SV=2 | P53675 | 8546 | 186910 | **0,86** | 1,21 | 8 |

| Protein | Accession | Score | Mass | Quantif. of unique peptides | | |
|---|---|---|---|---|---|---|
| | | | | H/L | SD(geo) | # quantif. |
| **Cytoskeleton** | | | | | | |
| Gamma-tubulin complex component 4 OS=Homo sapiens GN=TUBGCP4 PE=1 SV=1 | Q9UGJ1 | 271 | 76041 | **0,08** | 5,59 | 2 |
| Vimentin OS=Homo sapiens GN=VIM PE=2 SV=1 | B0YJC4 | 1534 | 49623 | **0,22** | 1,07 | 21 |
| Kinesin-1 heavy chain OS=Homo sapiens GN=KIF5B PE=1 SV=1 | P33176 | 535 | 109617 | **0,23** | 1,07 | 2 |
| Alpha-actinin-4 OS=Homo sapiens GN=ACTN4 PE=1 SV=2 | O43707 | 1839 | 104788 | **0,24** | 1,10 | 18 |
| Alpha-actinin-1 OS=Homo sapiens GN=ACTN1 PE=1 SV=2 | P12814 | 1203 | 102993 | **0,25** | 1,14 | 5 |
| Isoform 2 of Nck-associated protein 1 OS=Homo sapiens GN=NCKAP1 | Q9Y2A7-2 | 442 | 129433 | **0,31** | 1,20 | 7 |
| Unconventional myosin-Ie OS=Homo sapiens GN=MYO1E PE=1 SV=2 | Q12965 | 393 | 126982 | **0,35** | 1,35 | 2 |
| Kinesin-like protein KIF27 OS=Homo sapiens GN=KIF27 PE=2 SV=1 | Q86VH2 | 34 | 160184 | **0,46** | 1,12 | 2 |
| Keratin, type II cuticular Hb4 OS=Homo sapiens GN=KRT84 PE=2 SV=2 | Q9NSB2 | 400 | 64801 | **0,47** | 1,79 | 3 |
| Gamma-tubulin complex component 3 OS=Homo sapiens GN=TUBGCP3 PE=1 SV=2 | Q96CW5 | 483 | 103506 | **0,50** | 1,13 | 7 |
| MAP/microtubule affinity-regulating kinase 3 OS=Homo sapiens GN=MARK3 PE=4 SV=1 | J3KNR0 | 261 | 86950 | **0,54** | 1,28 | 3 |
| Protein Shroom3 OS=Homo sapiens GN=SHROOM3 PE=1 SV=2 | Q8TF72 | 244 | 216724 | **0,55** | 1,22 | 16 |
| Spectrin alpha chain, non-erythrocytic 1 OS=Homo sapiens GN=SPTAN1 PE=2 SV=2 | A6NG51 | 1930 | 284772 | **0,55** | 1,03 | 47 |
| Spectrin beta chain, non-erythrocytic 1 OS=Homo sapiens GN=SPTBN1 PE=1 SV=2 | Q01082 | 2039 | 274439 | **0,58** | 1,05 | 26 |
| Gamma-tubulin complex component 2 OS=Homo sapiens GN=TUBGCP2 PE=1 SV=2 | Q9BSJ2 | 769 | 102469 | **0,64** | 1,06 | 18 |
| Actin, cytoplasmic 1 OS=Homo sapiens GN=ACTB PE=1 SV=1 | P60709 | 3305 | 41710 | **0,71** | 1,18 | 75 |
| Myosin-9 OS=Homo sapiens GN=MYH9 PE=1 SV=4 | P35579 | 1465 | 226392 | **0,71** | 1,09 | 22 |
| Myosin-10 OS=Homo sapiens GN=MYH10 PE=2 SV=1 | F8W6L6 | 1606 | 230635 | **0,74** | 1,08 | 19 |
| Tubulin alpha-1C chain OS=Homo sapiens GN=TUBA1C PE=2 SV=1 | F5H5D3 | 3588 | 57693 | **0,74** | 1,45 | 19 |
| **ER-Golgi transport** | | | | | | |
| Coatomer protein complex, subunit epsilon, isoform CRA_g OS=Homo sapiens GN=COPE PE=4 SV=1 | M0QXB4 | 56 | 36901 | **0,02** | 17,18 | 2 |
| Endoplasmin OS=Homo sapiens GN=HSP90B1 PE=1 SV=1 | P14625 | 1030 | 92411 | **0,14** | 1,27 | 7 |
| Coatomer subunit gamma-1 OS=Homo sapiens GN=COPG1 PE=1 SV=1 | Q9Y678 | 472 | 97655 | **0,21** | 4,42 | 2 |
| Coatomer protein complex, subunit beta 2 (Beta prime), isoform CRA_b OS=Homo sapiens GN=COPB2 PE=2 SV=1 | B4DZI8 | 405 | 98984 | **0,28** | 1,05 | 5 |
| Vesicle-associated membrane protein-associated protein A OS=Homo sapiens GN=VAPA PE=1 SV=3 | Q9P0L0 | 82 | 27875 | **0,39** | 1,04 | 2 |
| Protein transport protein Sec31A (Fragment) OS=Homo sapiens GN=SEC31A PE=4 SV=1 | H0YAB3 | 4938 | 48952 | **0,49** | 2,15 | 2 |
| Protein transport protein Sec24C OS=Homo sapiens GN=SEC24C PE=1 SV=3 | P53992 | 4847 | 118249 | **0,56** | 1,07 | 158 |
| Protein SEC13 homolog OS=Homo sapiens GN=SEC13 PE=1 SV=3 | P55735 | 1090 | 35518 | **0,56** | 1,34 | 23 |
| Protein transport protein Sec31A OS=Homo sapiens GN=SEC31A PE=2 SV=1 | D6REX3 | 8663 | 136141 | **0,62** | 1,12 | 108 |
| SEC23-interacting protein OS=Homo sapiens GN=SEC23IP PE=2 SV=1 | F5H0L8 | 2607 | 89610 | **0,70** | 1,17 | 79 |
| Protein transport protein Sec24B OS=Homo sapiens GN=SEC24B PE=2 SV=1 | B7ZKM8 | 3654 | 140333 | **0,77** | 1,12 | 76 |
| Protein transport protein Sec23A OS=Homo sapiens GN=SEC23A PE=2 SV=1 | F5H365 | 6367 | 82916 | **0,82** | 1,05 | 87 |
| Protein transport protein Sec23B OS=Homo sapiens GN=SEC23B PE=1 SV=2 | Q15437 | 4874 | 86424 | **0,84** | 1,04 | 67 |

| Protein | Accession | Score | Mass | Quantif. of unique peptides | | |
|---|---|---|---|---|---|---|
| | | | | H/L | SD(geo) | # quantif. |
| **small GTPase-associated proteins** | | | | | | |
| TBC1 domain family member 2B OS=Homo sapiens GN=TBC1D2B PE=1 SV=2 | Q9UPU7 | 275 | 109812 | **0,07** | 1,09 | 3 |
| Rab GTPase-binding effector protein 2 OS=Homo sapiens GN=RABEP2 PE=2 SV=1 | B4DHR0 | 386 | 56078 | **0,15** | 1,16 | 9 |
| Rho guanine nucleotide exchange factor 2 OS=Homo sapiens GN=ARHGEF2 PE=2 SV=1 | Q5VY93 | 613 | 111423 | **0,32** | 1,67 | 3 |
| Ras-related protein Rab-5C OS=Homo sapiens GN=RAB5C PE=1 SV=2 | P51148 | 94 | 23468 | **0,37** | 1,10 | 2 |
| **Nuclear Transport** | | | | | | |
| Exportin-2 OS=Homo sapiens GN=CSE1L PE=1 SV=3 | P55060 | 300 | 110346 | **0,07** | 2,01 | 4 |
| Leucine-rich repeat-containing protein 59 OS=Homo sapiens GN=LRRC59 PE=1 SV=1 | Q96AG4 | 40 | 34909 | **0,13** | 1,60 | 2 |
| Exportin-1 OS=Homo sapiens GN=XPO1 PE=1 SV=1 | O14980 | 294 | 123306 | **0,18** | 1,24 | 5 |
| Importin-8 OS=Homo sapiens GN=IPO8 PE=1 SV=2 | O15397 | 277 | 119861 | **0,19** | 1,60 | 4 |
| Importin-11 OS=Homo sapiens GN=IPO11 PE=1 SV=1 | Q9UI26 | 333 | 112463 | **0,21** | 1,24 | 7 |
| Importin-5 (Fragment) OS=Homo sapiens GN=IPO5 PE=4 SV=1 | H0Y8C6 | 235 | 123779 | **0,24** | 1,11 | 5 |
| GTP-binding nuclear protein Ran OS=Homo sapiens GN=RAN PE=2 SV=1 | B5MDF5 | 65 | 26207 | **0,27** | 1,04 | 2 |
| Nuclear pore complex protein Nup98-Nup96 OS=Homo sapiens GN=NUP98 PE=1 SV=4 | P52948 | 279 | 197457 | **0,45** | 1,28 | 3 |
| Nuclear pore complex protein Nup214 OS=Homo sapiens GN=NUP214 PE=1 SV=2 | P35658 | 727 | 213488 | **0,50** | 1,09 | 7 |
| Importin subunit alpha-3 OS=Homo sapiens GN=KPNA3 PE=1 SV=2 | O00505 | 435 | 57775 | **0,52** | 1,08 | 8 |
| Importin subunit alpha OS=Homo sapiens GN=KPNA6 PE=2 SV=1 | F5GYL8 | 308 | 60556 | **0,53** | 1,16 | 3 |
| Nuclear pore complex protein Nup85 OS=Homo sapiens GN=NUP85 PE=2 SV=1 | B4DPW1 | 223 | 52565 | **0,54** | 1,15 | 3 |
| mRNA export factor OS=Homo sapiens GN=RAE1 PE=1 SV=1 | P78406 | 194 | 40942 | **0,58** | 1,22 | 5 |
| Importin subunit beta-1 OS=Homo sapiens GN=KPNB1 PE=1 SV=2 | Q14974 | 1163 | 97108 | **0,63** | 1,05 | 24 |
| Importin subunit alpha-2 OS=Homo sapiens GN=KPNA2 PE=1 SV=1 | P52292 | 1207 | 57826 | **0,63** | 1,09 | 28 |
| Importin subunit alpha-1 OS=Homo sapiens GN=KPNA1 PE=1 SV=3 | P52294 | 307 | 60184 | **0,64** | 1,20 | 3 |
| Transportin-1 OS=Homo sapiens GN=TNPO1 PE=1 SV=2 | Q92973 | 390 | 102289 | **0,64** | 1,06 | 4 |
| Transportin-3 OS=Homo sapiens GN=TNPO3 PE=2 SV=1 | C9J7E5 | 313 | 107978 | **0,67** | 1,06 | 5 |
| Importin subunit alpha-4 OS=Homo sapiens GN=KPNA4 PE=1 SV=1 | O00629 | 255 | 57851 | **0,72** | 1,12 | 6 |

**Appendix 3: A**bbreviations

| | |
|---|---|
| AF-647 | AlexaFluor 647 |
| AML | acute myeloid leukemia |
| AP-2 | Adaptor protein 2 |
| AR | amphiregulin |
| BL | Basal like |
| BTC | Beta-cellulin |
| Cbl | Casitas B-lineage lymphoma proto-oncogene |
| CC domain | Coiled coil domain |
| CCP | Clathrin-coated pit |
| CD2AP | CD2-interacting protein |
| CIE | Clathrin-independent endocytosis |
| CIN85 | Cbl-interacting protein of 85kDa |
| CME | Clathrin-mediated endocytosis |
| cond | conditional |
| DUB | Deubiquitylating enzymes |
| EE | Early endosome |
| EEA1 | Early endosome antigen-1 |
| EGF | Epidermal growth factor |
| EGFP | Enhanced green fluorescent protein |
| EGFR | Epidermal growth factor receptor |
| EMT | Epithelial-mesenchymal transition |
| Eph | Ephrin receptor |
| ER | Estrogen receptor |
| ERAD | Endoplasmic reticulum associated degradation |
| ERK | Extracellular regulated kinase |
| ESCRT | Endosomal sorting complex required for transport |
| F-actin | Filamentous actin |
| FCS | Fetal calf serum |
| FGFR | Fibroblast growth factor receptor |
| FL | Full-length |
| FRET | Förster resonance energy transfer |
| FYVE domain | Fab1, YOTB, Vac1, EEA1 |
| G-domain | GTP binding domain |
| GAP | GTPase activating protein |
| GDP | Guanosine diphosphate |
| GEF | Guanine nucleotide exchange factor |
| GPCR | G-protein coupled receptor |
| Grb2 | Growth factor receptor-bound protein 2 |
| GSDB | Goat serum dilution buffer |

| | |
|---|---|
| GST | Glutathione-S-transferase |
| GTP | Guanosine triphosphate |
| HA | Hemagglutinin |
| HECT | Homologous to the E6-AP Carboxyl Terminus |
| HER | Human epidermal growth factor receptors |
| HGFR | Hepatocyte growth factor receptor |
| HNA | Hereditary neuralgic amyotrophy |
| IF | immunofluorescence |
| ILV | Intraluminal vesicle |
| MAP | microtubule-associated protein |
| MAPK | Mitogen activated protein kinase |
| MEF | Mouse embryonic fibroblast |
| MLL | Mixed-lineage leukemia |
| MVB | Multi-vesicular body |
| NMR | Nuclear magnetic resonance |
| PBS | Phosphate buffered saline |
| PDGFR | Platelet derived growth factor receptor |
| PH domain | Pleckstrin homology domain |
| PI | Phosphatidyl-inositol |
| PI3K | Phosphatidylinositol-3 kinase |
| PKB | Protein kinase B (also known as AKT) |
| PLC-γ | Phospholipase C γ |
| PR | Progesterone receptor |
| PTB | Phosphotyrosine binding domain |
| REF | rat embryonic fibroblast |
| Rho | Ras homolog |
| RING | Really interesting new gene |
| RT | Room temperature |
| RTK | Receptor tyrosine kinase |
| sb | Surface-bound |
| SEPT | septin |
| SH2 domain | Src homology 2 domain |
| SH3 | Src homology 3 domain |
| SH3KBP1 | SH3 domain-containing kinase-binding protein 1 |
| SHP1 | Src-homology-2-containing phosphatase-1 |
| siRNA | Small interfering ribonucleic acid |
| SNARE | SNAP (soluble NSF attachment protein) receptor |
| SOS | Son of sevenless |
| SUE | Septin unique element |

| | |
|---|---|
| TAL | Tsg101-associated ligase |
| TBS | Tris buffered saline |
| TfR | Transferrin receptor |
| TGFα | Transforming growth factor alpha |
| TIRF | Total internal reflection fluorescence |
| TNBC | Triple-negative breast cancer |
| Ub | Ubiquitin |
| UBA domain | Ubiquitin associated domain |
| UIM | Ubiquitin interacting motif |
| WB | Western blot |
| wt | Wild-type |

**Appendix 4: List of figures**

## List of figures

Fig. 1.1: Structure of the HER family members HER1-4....10
Fig. 1.2: Major signaling pathways activated by EGF....11
Fig. 1.3: EGFR internalization....14
Fig. 1.4: Trafficking of RTKs. Taken from (Goh & Sorkin 2013)....16
Fig. 1.5: Domain structure and a selected interactome of CIN85....21
Fig. 1.6: CIN85 recruitment to activated EGFR in complex with Cbl....22
Fig. 1.7: Domain structure of septin GTPases....24
Fig. 1.8: Arrangement and filament assembly of the SEPT2/6/7/9 complex....25
Fig. 1.9: Septins in several biological processes....28
Fig. 1.10: Domain structure of human SEPT9 isoforms....31
Fig. 3.1: Verification of siRNAs and home-brew antibodies against SEPT9....69
Fig. 3.2: Depletion of SEPT9 decreases surface level of EGFR....71
Fig. 3.3: SEPT9 regulates EGFR sorting....72
Fig. 3.4: Cytoskeleton after knockdown of SEPT9....74
Fig. 3.5: Knockdown/Rescue experiment for downregulation of EGFR surface level....75
Fig. 3.6: SEPT9 forms a complex with the adaptor protein CIN85....76
Fig. 3.7: In silico analysis of the N-terminal region of SEPT9....77
Fig. 3.8: CIN85 binds to a PR-enriched motif in the N-terminus of SEPT9_v3....78
Fig. 3.9: CIN85 associates with septin complexes by binding to SEPT9....79
Fig. 3.10: Verification of siRNA and home-brew antibodies against CIN85....80
Fig. 3.11: Overexpression of mRFP-CIN85 recruits endogenous SEPT9....81
Fig. 3.12: SEPT9 and CIN85 colocalize at the plasma membrane with activated EGFR....82
Fig. 3.13: CIN85 recruits septin oligomers to the plasma membrane....83
Fig. 3.14: SEPT9 does not localize to internalized EGF....84
Fig. 3.15: SEPT9 is not localized on endosomes....86
Fig. 3.16: EGF stimulation induces translocation of septins to membrane....87
Fig. 3.17: Effect of SEPT9 depletion on downstream EGFR signaling....88
Fig. 3.18: SEPT9 and Cbl-b share the same binding pocket on CIN85....90
Fig. 3.19: SEPT9 regulates EGFR ubiquitylation....91
Fig. 3.20: Proteomic analysis of the EGFR-Interactome after loss of SEPT9....93
Fig. 3.21: Proteomic analysis of the SEPT9 interactome....96
Fig. 3.22: Loss of SEPT9 causes increased p62-level....97
Fig. 4.1: Hypothetical model for inactive CIN85 conformation....99
Fig. 4.2: Hypothetical model of SEPT9 function in stabilizing EGFR at the plasma membrane…106